Kathrin Herzog

Characterization of the molecular basis of *Klebsiella oxytoca* cytotoxicity

Masterarbeit

zur Erlangung des akademischen Grades

Master of Science
(MSc)

der Studienrichtung Molekulare Mikrobiologie

an der
Technischen Universität Graz

Unter der Betreuung von

Ao. Univ.-Prof. Dr. rer. nat. Ellen L. Zechner

durchgeführt am
Institut für molekulare Biowissenschaften
Karl-Franzens-Universität Graz

2012

Deutsche Fassung:
Beschluss der Curricula-Kommission für Bachelor-, Master- und Diplomstudien vom 10.11.2008
Genehmigung des Senates am 1.12.2008

EIDESSTATTLICHE ERKLÄRUNG

Ich erkläre an Eides statt, dass ich die vorliegende Arbeit selbstständig verfasst, andere als die angegebenen Quellen/Hilfsmittel nicht benutzt, und die den benutzten Quellen wörtlich und inhaltlich entnommene Stellen als solche kenntlich gemacht habe.

Graz, am …… ……..
(Unterschrift)

Englische Fassung:

STATUTORY DECLARATION

I declare that I have authored this thesis independently, that I have not used other than the declared sources / resources, and that I have explicitly marked all material which has been quoted either literally or by content from the used sources.

…… ……..
date (signature)

Acknowledgements

I am very greatful to **Ellen Zechner** for providing me with the great opportunity to perform my master‘s thesis in her lab, for encouraging me to think independently and for her supportive criticism.

Many thanks also to **Christoph Högenauer** for his valuable input in the form of new ideas and for his faith in my work.

I could have not survived this year without **Georg Schneditz**. He was always there to listen to my problems and had the right answers. He taught me to see the the big picture and to deal with the correct questions.
And most importantly, he made my thesis year fun.

I would also like to thank the other Zechner **lab members** for providing scientific advice and for creating an enjoyable work atmosphere.

Best thanks also to **Jana Rentner** and **Rolf Breinbauer**
of the Institute of Organic Chemistry (Graz University of Technology)
for their help in performing the HPLC/MS experiments and for patiently explaining and discussing the results.

I would also like to thank
NAWI Graz
for generously funding my masters research.

For a lot of cheerful and unforgettable moments and for enriching my life,
I want to thank my friends,
above all **Veronika Hamminger**.

All this would not have been possible without the love and support of my parents,
Gabriella and **Robert Herzog**.
They gave me roots and wings.
Their endless faith and encouragement made me strong.
I dedicate this work to them.

Special thanks to **Bernhard Obereder**.
For catching me when I was falling. For laughing with me. For sharing my dreams.
For octillions of love.

Content

1.Introduction 1

1.1. Antibiotic associated colitis (AAC) and its causative agents 1

1.1.1. Antibiotic associated diarrhea and AAC 1

1.1.2. AAHC and K. oxytoca 2

1.2. What defines Klebsiella sp. as pathogens? 5

1.2.1. Klebsiella sp. cause opportunistic infection 5

1.2.2. Main virulence factors expressed by Klebsiella sp. 6

1.3. Cytotoxicity of Klebsiella oxytoca 9

1.3.1. The beginnings: the cytotoxic phenotype 9

1.3.2. The toxin gene cluster of K. oxytoca - a comparison 12

1.3.3. The chemical nature of the K. oxytoca cytotoxin 19

2.Aims of this study 20

3.Materials & Methods 21

3.1. Media, buffers, solutions and chemicals 21

3.2. Bacterial strains and eukaryotic cell lines 22

3.2.1. Bacterial strains 22

3.2.2. Eukaryotic cell lines 23

3.2.3. Growth conditions 23

3.3. Plasmids and oligonucleotides 24

3.4. DNA methods 26

3.4.1. Polymerase Chain Reaction 26

3.4.2. Chromosomal DNA preparation 27

3.4.3. Plasmid DNA preparation 27

3.4.4. Restriction enzyme digestion 27

3.4.5. Ligation 27

3.4.6. Agarose gel electrophoresis 28
3.4.7. Agarose gel extraction 28
3.4.8. DNA sequencing 29
3.5. Transposon mutagenesis 29
3.5.1. Conjugational transfer of pRL27 29
3.5.2. Plasposon rescue 30
3.5.3. Mutant storage 30
3.6. Preparation of electro competent cells 30
3.7. Transformation 31
3.8. RNA methods 31
3.8.1. RNA extraction 31
3.8.2. Reverse transcription 32
3.8.3. Second strand synthesis 32
3.9. Protein methods 33
3.9.1. SDS Page 33
3.9.2. Western Blot 34
3.10.Evaluation of cytotoxic phenotype 34
3.10.1.Preparation of conditioned supernatant 34
3.10.2.MTT assay 35
3.10.3.Microscopy 35
3.11.French press cell lysis 35
3.12.HPLC analysis 36
3.12.1.Organic extraction 36
3.12.2.High performance liquid chromatography 36
3.12.3.Mass spectrometry 36
4.Results 37

4.1. Screen of Klebsiella sp. isolate collection for occurrence of cytotoxin synthesis genes 37

4.1.1. Selection of adequate PAI targets 37

4.1.2. K. oxytoca species specific target 38

4.1.3. A correlation between phenotype and genotype could be detected 38

4.2. Transposon mutagenesis continued 40

4.2.1. Transposon mutagenesis keeps on doing its job 40

4.2.2. Mutant 873 - an „old acquaintance“ 41

4.2.2.1. Loss of cytotoxicity screen 41

4.2.2.2. Two plasposons of different size could be isolated 42

4.2.2.3. Sequencing and identification of the disrupted gene of Mut873 43

4.2.3. Loss of cytotoxicity mutant 1145 44

4.2.3.1. Loss of cytotoxicity screen 44

4.2.3.2. Plasposon rescue of plasp1145A and plasp1145B 45

4.2.3.3. Loss of cytotoxicity is not due to altered growth of Mut1145 47

4.2.3.4. yncE is affected in Mut1145 48

4.2.3.5. Comparative HPLC/MS analysis of cell lysates 49

4.2.3.6. MTT assay of cell lysates 54

4.2.3.7. In trans complementation of the yncE mutation 55

4.2.3.8. RT-PCR to check the expression of yncE and its neighbors 58

4.2.3.9. Choosing the right targets 58

4.2.3.10. yncE is not expressed under replete conditions 58

5. Discussion 60

5.1. Genotype allows prediction of cytotoxic phenotype 60

5.1.1. Speculating about a possible diagnostic PCR 61

5.1.2. The quest for K. oxytoca species specific targets 62

5.2. Proof for the potential of transposon mutagenesis 64

5.2.1. The K. oxytoca toxin gene cluster as a horizontally acquired PAI 64

5.2.2. yncE and its disguised role for K. oxytoca cytotoxicity.....65

5.2.2.1. What E. coli tells us 65

5.2.2.2. What could yncE do in K. oxytoca? 67

6.Conclusion 70

7.References 71

8.Appendix 76

ABSTRACT

Klebsiella oxytoca is the causative agent of the severe disease antibiotic associated hemorrhagic colitis (AAHC). AAHC patients suffer from bloody diarrhea and severe abdominal cramping after penicillin treatment and often require hospitalization. Current models propose that overgrowth of toxin-producing, penicillin-resistant *K. oxytoca* results in severe damage to the mucosa. This cytotoxicity against epithelial cells was already observed in earlier studies and is studied in detail in this laboratory. The cytotoxic substance in the supernatant of *K. oxytoca* AHC-6, an AAHC isolate, was purified and analyzed chemically. This analysis revealed a low molecular weight pentacyclic pyrrolobenzodiazepine (PBD) structure. A general mutagenesis approach determined that this substance is generated by non-ribosomal peptide synthases (NRPSs). Random transposon mutagenesis also revealed that the NRPS are encoded on a 20 kb pathogenicity island (PAI) which thus appears to contribute to *K. oxytoca* virulence. The aim of this study was to identify additional genes involved in *K. oxytoca* cytotoxicity, mainly in the transport and the regulation of the cytotoxin. Additionally, the correlation between the occurrence of the PAI on the chromosome and the cytotoxic phenotype of *K. oxytoca* isolates was investigated. Transposon mutants of *K. oxytoca* AHC-6 were generated using *Escherichia coli* BW20767 as a conjugation donor strain for the miniTn5 delivery vector pRL27. Subsequently, the 800 generated *K. oxytoca* transposon mutants were screened for loss of cytotoxicity in cell culture. In one mutant the already characterized *npsA* gene on the PAI was interrupted by the transposon. The high occurrence of transposon insertions within the PAI (3 out of 6 mutants) identifies it most likely as a mutation-prone HGT acquired element. The second causative mutation affected the *yncE* gene which is known in *E. coli* to be negatively regulated by iron and might have a role in iron import. We performed HPLC-MS analysis with extracted supernatants and cell lysates and showed that the 333 Da cytotoxic PBD substance is located intra- and extracellularly in wild type *K. oxytoca*. In the *yncE* transposon mutant a 110 Da larger substance of similar polarity was found only intracellularly, which can neither be detected in the wild type cell lysate or supernatant nor in a *K. oxytoca* toxin synthesis mutant. RT-PCR analysis revealed that *yncE* in *K. oxytoca* was not expressed under non-restrictive conditions and in trans complementation could not be achieved, although YncE was expressed from the complementation plasmid. Therefore, the loss of cytotoxicity is probably not due to the *yncE* gene function itself but might have some in cis-acting causes, possibly related to export of the substance. Furthermore a PCR screen for two PAI genes in a collection of 100 *Klebsiella* strains showed 100% correlation between occurrence of the targets and cytotoxic phenotype. This result allows us to consider the development of a diagnostic multiplex PCR which could also help in the risk assessment of healthy *K. oxytoca* carriers.

1. Introduction

1.1. Antibiotic associated colitis (AAC) and its causative agents

1.1.1. Antibiotic associated diarrhea and AAC

Antibiotic associated diarrhea (AAD) and its more severe form, antibiotic associated colitis (AAC), are common adverse effects after and during antibiotic therapy. These clinical pictures are characterized by a sudden onset of (bloody) diarrhea, abdominal cramping, fever and dehydration. 5 - 25% of patients under antibiotic therapy suffer from AAD depending on the antibiotic in use. The underlying mechanisms are the reduction and alteration of the normal intestinal flora due to the selective pressure of the antibiotic as well as direct effects of the antibiotic on intestinal motility or the intestinal mucosa [1]. In 10 - 20% of AAD patients an infection with *Clostridium difficile* causes the disease. This pathogen can cause various enteric infections ranging from mild cases of diarrhea to life-threatening colitis. One of the severest forms of colitis caused by *C. difficile* is pseudomembranous colitis (PMC). In this case, antibiotic therapy changes the constitutive microbiota thereby allowing the overgrowth of toxin-producing *C. difficile* strains. After successful penetration of the intestinal mucus and initial colonization, genes of the *C. difficile* pathogenicity locus (PaLoc) are expressed leading to the production of toxin A (TcdA), an enterotoxin, and toxin B (TcdB), a cytotoxin. Non-toxigenic strains lack this PaLoc. Both the toxins are glycosyltransferases and affect the cytoskeleton of colonocytes, thus leading to cell death [2, 3]. Subsequently the mucosa gets damaged, inflammation of the colon occurs and the characteristic pseudomembranes are formed. They consist of inflammatory cells, necrotic cells, and fibrin and can lead to adynamia and broadening of the colon. In the most severe cases, the intestinal wall is disintegrated and *C. difficile* and other intestinal bacteria are able to spread systemically and cause sepsis [4]. In most non-severe cases discontinuation of antibiotic therapy is sufficient for recovery. More severe cases require metronidazole or vancomycin treatment as well as supportive care [5].

Apart from *C. difficile*, other pathogens can cause AAD. Among those are drug-resistant *Salmonella* sp, *Staphylococcus aureus*, as well as *Clostridium perfringens*. [1].

1.1.2. AAHC and *K. oxytoca*

Antibiotic associated hemorrhagic colitis is a *C. difficile*-independent form of AAC, first described in 1978 [6]. It occurs predominantly after treatment with penicillins but there are also reports of AAHC cases as a result of administration of quinolones and cephalosporins [7]. The symptoms start soon after start of antibiotic therapy (mean 4 days) and include acute bloody diarrhea and severe abdominal cramping which often requires hospitalization. The endoscopic features include segmental colitis with mucosal hemorrhage and edema, and in some cases erosions or ulcerations, mainly affecting the ascending colon and cecum. Pseudomembranes are not present. Histology of affected tissue shows epithelial alterations including loss of goblet cells, anisonucleosis, and elevated levels of apoptosis and mitosis. A mild inflammation is indicated by low levels of neutrophils and mucosal hemorrhage is also present on histology. These key findings resemble those of patients with toxin-induced forms of colitis caused by enterohemorrhagic *Escherichia coli* (EHEC) or *Shigella* species. Unlike *C. difficile* associated AAC, AAHC is self-limiting and resolves spontaneously after cessation of the antibiotic therapy [1, 7]. Characteristic for AAHC is the lack of *C. difficile* and other common intestinal pathogens like *Campylobacter, Salmonella, Shigella, Yersinia* and *E. coli* species. Microbial analysis of stool samples of AAHC patients reveals high levels of *Klebsiella oxytoca* of > 10^6 cfu/ml, which can be isolated almost as a pure culture [8]. Similar findings published earlier suggested a role of *K. oxytoca* in AAHC [9, 10], *K. oxytoca* can be isolated in low levels (< 10 cfu/g feces) from healthy carriers too (1,6% to 5% in Austria [7, 8]). *K. oxytoca* constitutively expresses β-lactamases, which confer resistance to amino- and carboxypenicillins, antibiotic classes that are often administered before the onset of AAHC. This suggests an overgrowth of resistant *K. oxytoca* due to alterations of the intestinal microbiota [8]. Recently it was shown that *K. oxytoca* is the causative agent of AAHC by the fulfillment of the postulates of Koch [7]. Rats with suppressed intestinal flora received a *K. oxytoca* strain isolated from an AAHC patient via an orogastric stomach probe. The resulting colonization and colitis phenotype resembled the picture seen in patients suffering from AAHC (Figure 1). In the absence of antibiotic treatment, the rats were not colonized by *K. oxytoca* nor were symptoms of colitis found. The administration of non-steroidal anti-inflammatory drugs (NSAIDs) in parallel to antibiotic treatment seemed to aggravate the colitis phenotype [7], a fact that is important regarding the frequent use of NSAIDs by AAHC patients before the onset of colitis.

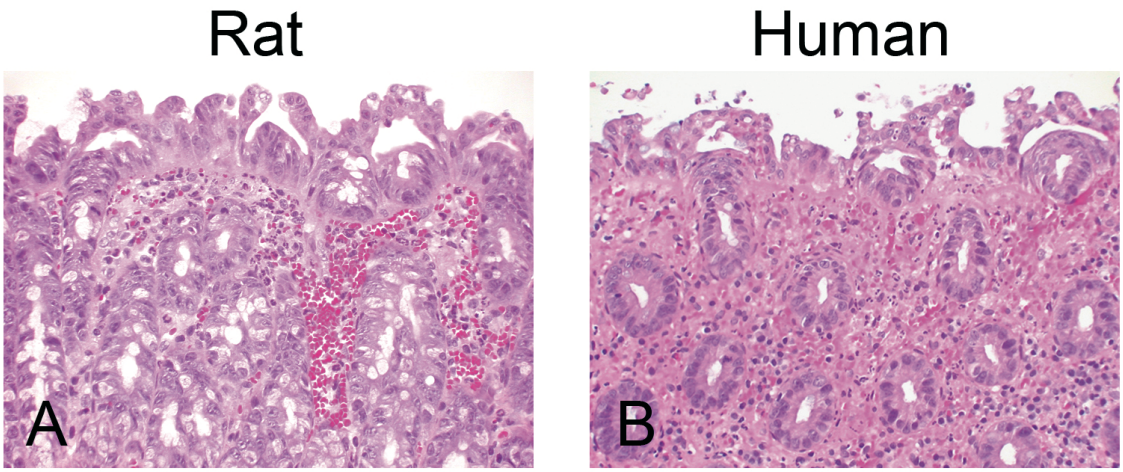

Figure 1: Histological picture of AAHC in the cecum mucosa of a rat (A) and a human AAHC patient (B).
Both specimens were stained with hematoxylin and eosin and show characteristic epithelial alteration (loss of goblet cells, anisonucleosis and elevated levels of mitosis and apoptosis), mucosal hemorrhage and mild inflammation. [7]

Already in the 1990s it was hypothesized that a unique cytotoxic substance produced by *K. oxytoca* AAHC isolates might be involved in the development of the disease, as this cytotoxin caused cell death in cultured mammalian cell lines and additionally led to mucosal damage in a rabbit intestinal loop model [11-14]. In contrast to clinical isolates, the cytotoxic effect was not seen in laboratory strains of *K. oxytoca*, supporting the role of the cytotoxin in AAHC [9, 13]. Compared to *K. oxytoca* isolates from other infections, AAHC *K. oxytoca* isolates exhibit the highest proportion of cytotoxicity producers, followed by diarrhea isolates (Figure 2). In the same study the co-isolation of cytotoxin-positive and -negative genetically distinct *K. oxytoca* strains in one single healthy subject or AAHC patient was observed [15] (Figure 3), which could explain why not all isolates of patients with AAHC were cytotoxin-positive. Therefore, more than one *K. oxytoca* isolate must be tested for cytotoxin production on the case of AAHC. These findings led to a pathogenic model of AAHC in which cytotoxin-producing *K. oxytoca* strains that are present in the colon of some healthy carriers, who receive antibiotic therapy, can overgrow the microbiota due to the selective pressure. This finally results in high concentrations of the cytotoxin including damage of the intestinal mucosa [7].

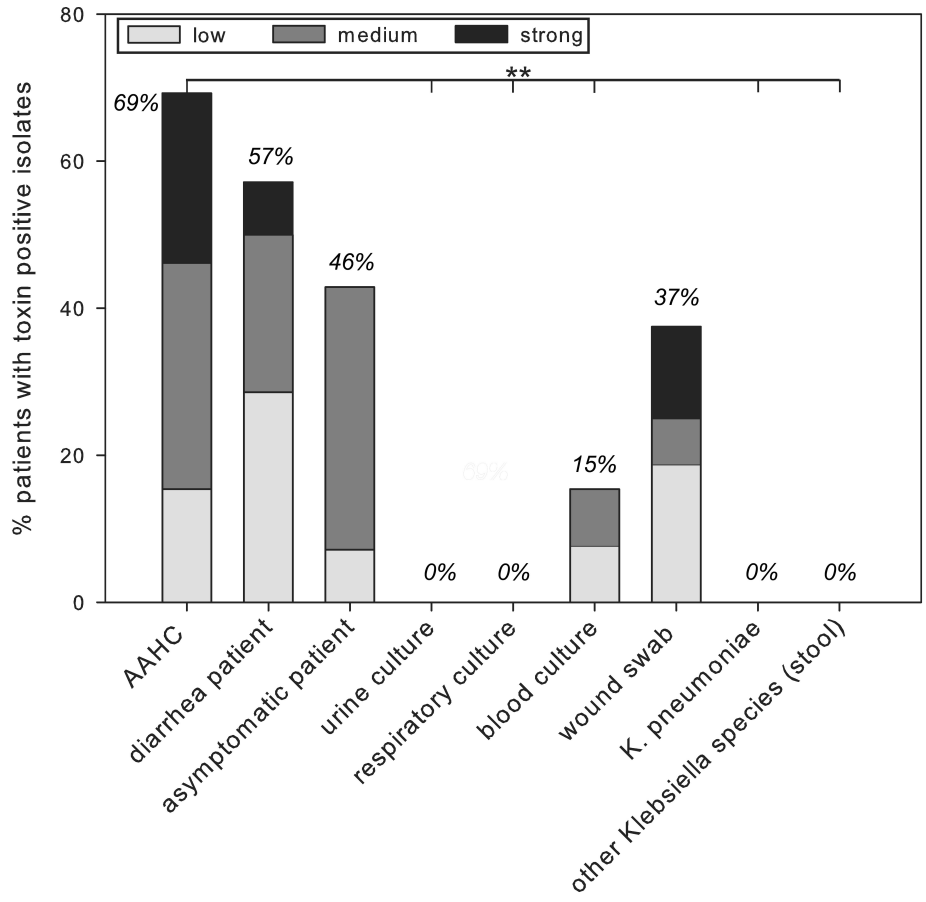

Figure 2: Proportion of toxin-positive *Klebsiella* isolates and degree of cytotoxin production.

Strains tested were *K. oxytoca* and the isolation source was stool unless otherwise indicated. Strains isolated from AAHC patients showed a significantly higher proportion of toxin producers compared to strains isolated from other body sites. Low indicates cytotoxic effect with dilution 1:3 of bacterial supernatant, medium with dilution 1:3 and 1:9 and strong up to dilution 1:27, respectively. [15]

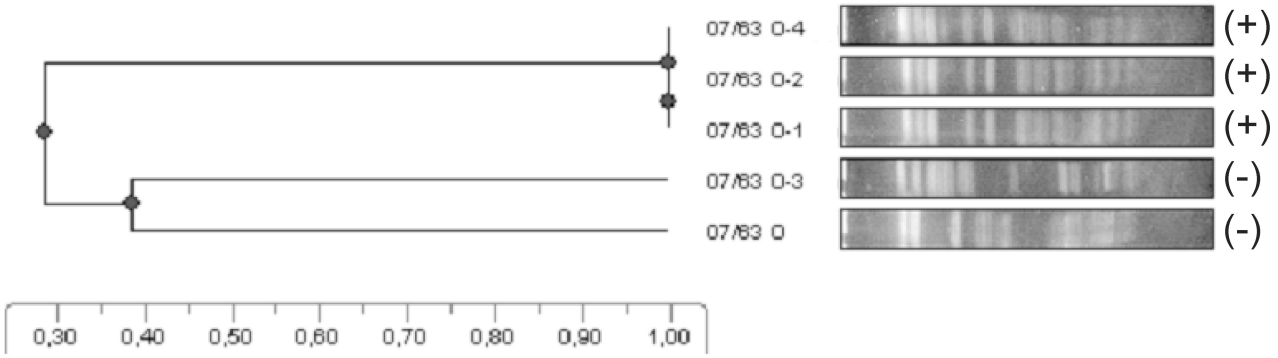

Figure 3: UPGMA dendrogramm (dice coefficient) of five *K. oxytoca* strains isolated from one AAHC patient

The relative genetic relatedness is shown on the scale bar at the bottom. + and - in parentheses indicate toxin-positive and -negative cell culture phenotypes respectively. UPGMA, Unweighted Pair Group Method with Arithmetic Mean. [15]

1.2. What defines *Klebsiella sp.* as pathogens?

1.2.1. *Klebsiella sp.* cause opportunistic infection

The genus *Klebsiella* is a member of the family *Enterobacteriaceae* and comprises seven species. They are gram-negative rods that are non-motile and usually encapsulated. *Klebsiella* sp. are facultative anaerobes and, under anoxic conditions, are able to ferment glucose to 2,3-butanendiol and CO_2. In contrast to other *Enterobacteriaceae, Klebsiella* sp. are capable of atmospheric nitrogen fixation under anoxic conditions [16, 17]. *Klebsiella* are ubiquitous in nature and can be found on the one hand in the environment where they live in water, sewage and soil. Their second natural habitat is the mucosa of mammals [18]. They are considered opportunistic pathogens of humans and account for 10 % of nosocomial infections [17]. Most of those infections are caused by *Klebsiella pneumoniae.* To a lesser degree *K. oxytoca* can be isolated from human clinical specimens. *Klebsiella* sp. carrier rates differ but studies showed that the intestinal carrier rates increased with the length of hospital stay to up to 77% in the stool [19]. Among the hospital-acquired infections caused by *Klebsiella*, urinary tract infections are the most prevalent, followed by pneumonia and septicemia [18]. Hospitalized patients with invasive medical devices like urinary catheters are at a higher risk of infection and *Klebsiella* biofilm formation on these devices makes treatment even more difficult [20]. Also immunocompromised patients are more likely to suffer from *Klebsiella* infections. Neonatal sepsis is caused by *Klebsiella oxytoca* in particular and nosocomial outbreaks in neonatal care wards are frequently associated with *Klebsiella* spp in general [21-23]. Of special concern is the occurrence of multiple resistant *Klebsiella* spp strains, especially extended-spectrum β-lactamase (ESBL) producing strains occurring in both *K. pneumoniae* and *K. oxytoca*. As these resistances are typically plasmid-mediated the rapid spread among *Enterobacteriaceae* is likely to result in more multi-resistant strains [18, 24].

1.2.2. Main virulence factors expressed by *Klebsiella* sp.

Klebsiella constitutively express low levels of class A β-lactamases which utilize a serine residue to attack the β-lactam ring of antibiotics conferring resistance to ampicillin, amoxicillin, carbenicillin and ticarcillin [25]. While in *K. pneumoniae* SHV-1 β-lactamases are present on the chromosome, *K. oxytoca* resistance is based on K1 type enzymes which are cefuroximases encoded by the bla_{OXY} genes. Hyperproduction of K1 β-lactamases can broaden the levels and spectra of β-lactam resistance [25]. In the United States around 10% of *Klebsiella* infections are caused by ESBL strains. Even higher numbers (up to 16%) have been reported for Europe. In the hospital environment the prevalence can reach 40% [18]. Usually ESBLs are plasmid encoded, which explains their fast and dangerous spread among bacteria. Adding to this problematic development is the fact that the plasmids mediating ESBLs are relatively stable inside the *Klebsiella* strains [18].

Another key pathogenicity factor found in most *K. pneumoniae* and *K. oxytoca* strains is the polysaccharide capsule which causes the mucoid appearance of colonies. *Klebsiella* have been classified into 77 serotypes according to the capsular subunits of four to six sugar residues and the uronic acids usually included [18]. As the capsular polysaccharides (CPS) form a thick layer around the bacterial surface, they protect the bacteria from phagocytosis by polymorphonuclear leucocytes (PMNL) [26]. Apart from this antiphagocytic function, it was shown that the K (capsule) antigens also confer protection from bactericidal serum factors. This mechanism probably works via inhibiting the activation of complement factors especially C3b (compare serum resistance section on page 7). It has been shown that CPS are essential for virulence and that the degree of virulence might be associated with the abundance of mannose and rhamnose in the CPS. These sugars trigger a special opsonin-independent form of phagocytosis, called lectinophagocytosis [27]. In contrast, strains lacking the specific mannose or rhamnose repeating sequences are not recognized by PMNL. Accordingly, K2 strains, which lack mannose residues in their CPS, are highly virulent [18].

A critical step during bacterial infection is the initial attachment and adherence of microorganisms to the host surfaces. In *Enterobacteriaceae* pili (fimbriae) are responsible for this step [18]. Fimbriae are non-flagellar, filamentous surface organelles that consist of protein subunits of pilin and are characterized by their ability to cause agglutination of human red blood cells (hRBC). *Klebsiellae* produce two predominant types of fimbriae. Type I fimbriae bind to mannosylated host glycoproteins mediated by the FimH adhesin.

Therefore attachment to the mucus or epithelium of the respiratory, intestinal and urogenital tract is enabled. Type I fimbriation has been correlated with virulence, especially regarding urinary tract infections (UTI) [28]. Binding to mannose-containing glycoproteins is not limited to host surfaces. Instead, type I fimbriae can also attach to soluble target proteins, e.g. in urine or saliva, explaining the colonization of the urogenital and respiratory tract [18, 29]. Expression of type I fimbriae can be switched off via a flip-flop-type control system leading to phase variation. After successful invasion, expression of type I fimbriae on the cell surface would make the bacteria more susceptible to lectinophagocytosis [28]. The second pilus form of *Klebsiella* is the type 3 fimbriation which can be found in many *Enterobacteriaceae.* They are characterized by the ability to cause agglutination of tannic acid-treated hRBC in vitro but can also bind to type V collagen. As the hemagglutination was first studied in *Klebsiella* it is often referred to as mannose-resistant *Klebsiella*-like hemagglutination (MR/HKA) [30]. Type 3 fimbriae are encoded by the *mrk* gene cluster containing among others MrkD and MrkA, the fimbrial adhesin and subunit, respectively [20]. The *mrkD* gene has been shown to be conserved in strains of *K. oxytoca* [31] and mediates binding to epithelial cells and extracellular matrix proteins [32].

Evading the first line of host defense, the bactericidal effect of serum, is known as serum resistance, which plays a major role during bacterial infection and has also been described for *K. oxytoca* [33]. The non-specific defense mechanisms in the host are mainly mediated by the complement system. This system is made up of a co-operative network of proteins which are activated in a cascade-like manner. The result of this activation is the formation of the membrane attack complex on the bacterial surface leading to lysis of the pathogen [17]. Serum resistance against this lysis is achieved via two mechanisms. First, CPS on the cell surface may mask the lipopolysaccharide (LPS) and therefore presents a non-complement activating cell surface. The second evasion mechanism works via initial activation of complement components like C3b, but as they are recruited to the far protruding O-chains of LPS, the membrane attack complex cannot form on the cell surface [18, 34]. Additionally it has been shown that smooth LPS only activates the alternative complement activation pathway leading to lower levels of recruited C3b and less bacterial cell damage [34].

Once inside the host tissue, *Klebsiella* have to face not only the host immune system but also the limited supply of free iron necessary as a redox catalyst for bacterial growth [18]. Iron in the host is almost totally sequestered by proteins like hemoglobin and ferritin intracellularly, and high-affinity iron-binding proteins like lactoferrin and transferrin extracellularly. For successful establishment of infection bacteria must find a way to obtain

iron from the host transport proteins. Therefore many bacteria secrete siderophores, low-molecular-weight high-affinity iron chelators. Their affinity is 10 orders of magnitude higher and therefore allows them to compete the iron off of transferrin or lactoferrin [35]. Subsequently, the siderophore-iron complexes are taken up via outer membrane receptors and translocated into the bacterial cell. *Klebsiellae* produce two types of siderophores: phenolate-type and hydroxamate-type siderophores. The most common siderophore in *Klebsiella* species is enterobactin (also called enterochelin), a phenolate-type siderophore. It is found in the majority of clinical *E. coli* and *Salmonella* isolates and has also been shown to be synthesized in almost all *Klebsiella* strains [36]. Enterobactin shows the highest iron affinity for a ferric iron chelator and its main source of iron is transferrin [18]. To a much lesser extent another phenolate-type siderophore, yersiniabactin, is found in *Klebsiella*. It was first observed in *Yersinia* species but has been introduced into other *Enterobacteriaceae* via horizontal gene transfer (HGT). Studies have shown an essential role for *Klebsiella* virulence [35]. Aerobactin, a hydroxamate-type siderophore, is also synthesized in *Klebsiella*. In contrast to enterobactin, aerobactin uses mainly host cells as iron sources and can be recycled and secreted again [18]. The expression of iron-acquisition systems is largely regulated by Fur (ferric uptake regulator), which has been ascribed the role of a global regulator in many Enterobacteriaceae including *Klebsiellae* [37, 38]. Under iron-saturated conditions the Fe^{2+}-Fur complex is known to bind to its consensus sequence called the Fur box. As a result, transcription of iron uptake systems is shut down to prevent intracellular iron accumulation leading to formation of reactive oxygen species [37]. Apart from siderophores, other virulence factors are regulated by the concentration of extracellular iron, among them hemolysins or bacterial toxins, e.g. the Shiga-like toxin (SLT) of *E. coli* [39]. In *Klebsiella* Fur also has a role in the regulation of CPS biosynthesis by repressing the expression of CPS genes under iron repletion [37].

The biosynthesis of toxins has been described several times for *Klebsiella* species, both enterotoxin and cytotoxin production. Their role for virulence and infection up to this date are not totally clear and are being investigated [15].

1.3. Cytotoxicity of *Klebsiella oxytoca*

1.3.1. The beginnings: the cytotoxic phenotype

The observation of a cytotoxic effect caused by the culture supernatant of *K. oxytoca* AAHC isolate was first made in 1989 [12]. After incubation with this supernatant tissue culture cells like HeLa, HEp-2, and Vero cells showed distinctive phenotypes such as cell rounding, detachment, and eventually cell death. Purification of the cytotoxin revealed its molecular mass of 217 Da and the chemical formula being $C_8H_{15}O_4N_3$. Furthermore, the cytotoxin seemed to be heat-labile and lead to inhibition of nucleic acid synthesis in cultured mammalian cells [13]. Injection of purified cytotoxin into rabbit intestinal loops caused accumulation of fluid in the loops, in the ileal loops the fluid was bloody. The same result was obtained after inoculation of cytotoxin-producing *K. oxytoca* into the intestinal loops. In contrast, inoculation with a non-cytotoxin-producing *K. oxytoca* strain did not cause any liquid accumulation. Histology of the affected tissue showed erosion and hemorrhage of the ileal loop after cytotoxin treatment, whereas the colonic loop only exhibited features of mild inflammation [11]. Although *K. oxytoca* was identified as the causative agent of AAHC in 2006, the causal link between cytotoxin production and pathogenicity remained to be determined [7]. A previous study of the Zechner group investigated a correlation between *K. oxytoca* cytotoxin production and AAHC and thereby clarifying the pathogenic role of the cytotoxin [15]. Comparison of different *K. oxytoca* isolates of AAHC patients, other infection sites and also other *Klebsiella* species showed that cytotoxin production was limited to *K. oxytoca*. Furthermore AAHC isolates showed the highest rate of toxin-producing strains followed by stool isolates and diarrhea isolates (Figure 2). Additionally, cytotoxin-positive and -negative strains could be isolated from one AAHC patient, probably explaining the negative toxin finding for the available isolates of some AAHC patients. Qualitative and quantitative assessment of cytotoxicity was achieved via a cell culture assay exhibiting similar toxin induced phenotypes as mentioned before (Figure 4) [12].

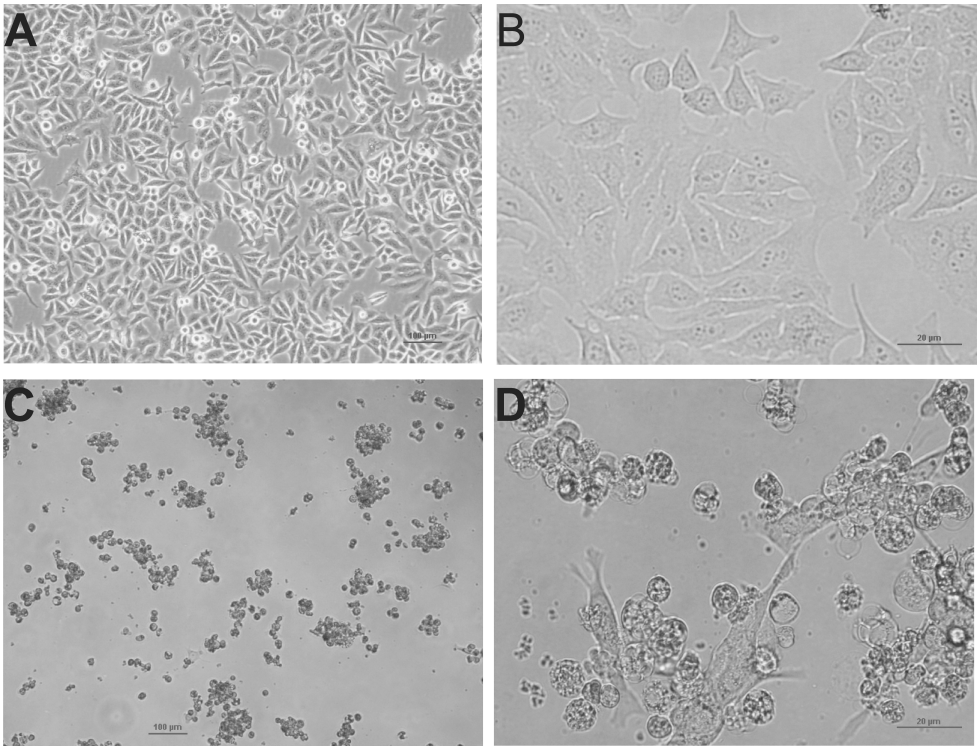

Figure 4: Phenotypic characteristics of the cytotoxic effect of bacterial supernatant on cultured human cells.

Pictures at the top show HEp-2 cells in medium supplemented with supernatant from a toxin-negative *K. oxytoca* strain at 100x (A) and 400x (B) magnification. Beneath, HEp-2 cells incubated with supernatant of a toxigenic AAHC *K. oxytoca* isolate are shown at 100x (C) and 400x (D) magnification. [15]

Comparison of cytotoxic effects produced as a function of bacterial culture time for a toxin-producing and a toxin-negative strain showed correlations between growth phase and cytotoxicity (Figure 5). Whereas with the toxin-negative strain no cytotoxicity was detected over the whole range of time (48 hours), cytotoxin production by the toxigenic strain started at late logarithmic phase and reached a maximum at early stationary phase (16 hours). About 30 hours later a drop in cytotoxic activity could be detected while bacterial viability stayed the same. This indicated that cytotoxicity was not a result of bacterial cell debris in the supernatant but more likely due to a secreted toxic substance that, after 46 hours, is no longer produced or loses activity [15].

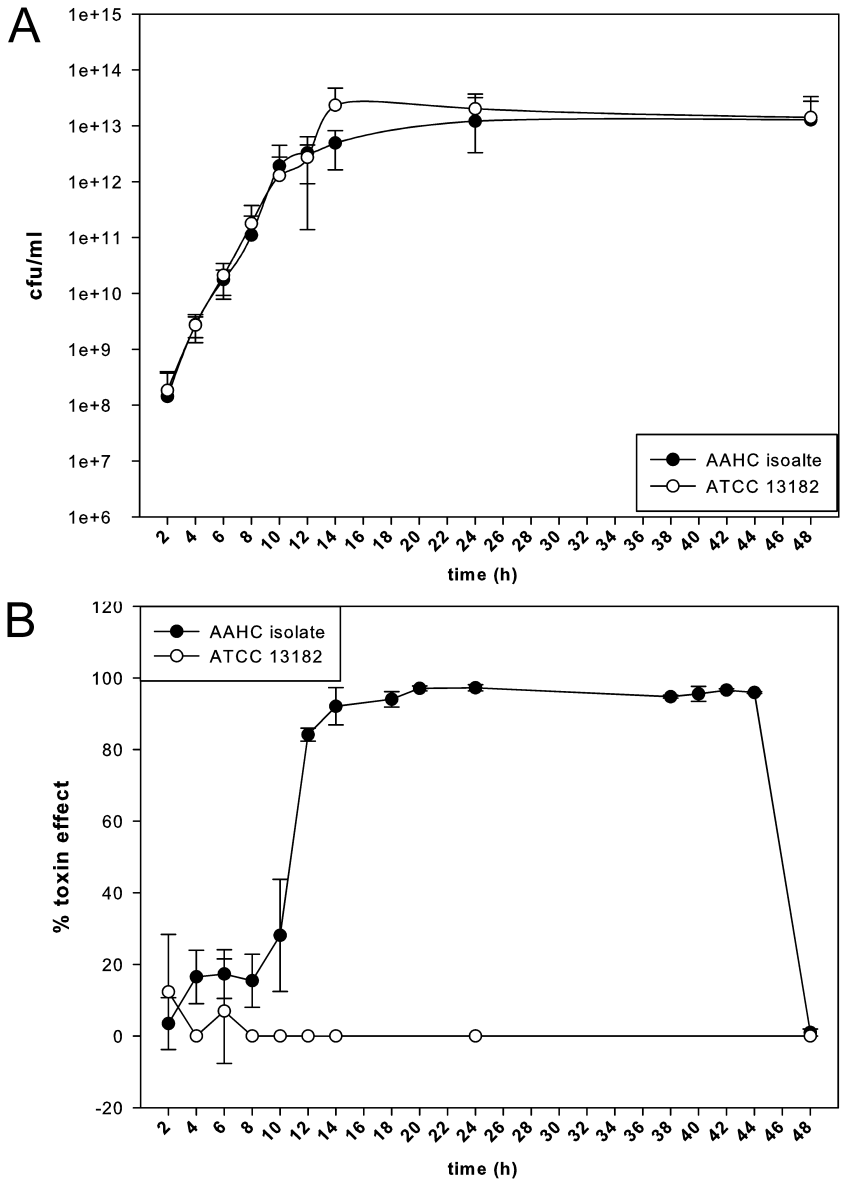

Figure 5: Cytotoxin production as a function of bacterial growth time of two *K. oxytoca* strains.

Growth curves of a toxigenic *K. oxytoca* AAHC isolate and the non-toxin producing *K. oxytoca* ATCC 13182 strain are shown in panel A and were determined by colony counts on agar plates. The same strains were tested for cytotoxicity in the cell culture assay. The percentage toxin effect (panel B) represents the fraction of HEp-2 cells killed after treatment with 48-fold dilutions of *K. oxytoca* supernatant compared to PBS treated cells. The data represent the mean values of three independent experiments ± SD. [15]

1.3.2. The toxin gene cluster of *K. oxytoca* - a comparison

The *K. oxytoca* toxin studied by the Minami laboratory was shown to have a low molecular mass [13]. This observation supported the hypothesis that production was less likely caused by a structural toxin gene but by a larger pathway leading to the production of a secondary metabolite. Although earlier studies tried to elucidate the toxin‘s chemical nature [13], little was known about its structure and biosynthesis. Identifying the underlying genetics therefore seemed promising to elucidate the cytotoxin‘s nature. Transposon mutagenesis, as a reverse genetics tool, was chosen to determine genes involved in the development of the cytotoxic phenotype. The applied miniTn5 based mutagenesis uses the randomness of transposon integration into the bacterial genome but also produces stable mutants because the transposase gene gets lost at integration [40]. The chosen miniTn5 suicide plasmid pRL27 [41] can be delivered to the target organism by conjugation facilitated by the oriT sequence from plasmid RP4 (Figure 6).

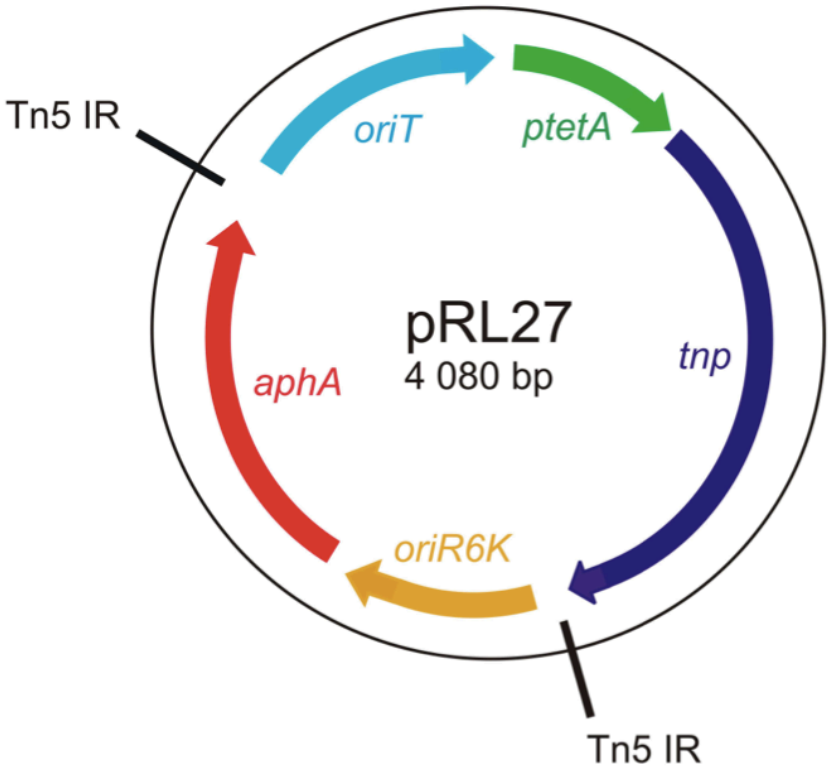

Figure 6: Plasmid map of MiniTn5 derived vector pRL27 used for random transposon mutagenesis.
Depicted features: origin of transfer (oriT); *tetA* promoter (ptetA); hyperactive transposase (*tnp*); pir protein dependent origin of replication (*oriR6K*); kanamycin resistance marker (*aphA*), internal repeats (Tn5 IR) flanking the insertion cassette. [42]

The insertion cassette contains the *aphA* kanamycin (Km) resistance marker allowing for selection of mutants as well as the origin of replication from the plasmid R6K (*ori*R6K). As this origin requires the π protein (*pir*) for replication it restricts replication in target cells lacking *pir*.

In the first phase of transposon mutagenesis about 700 mutants were generated by conjugation of the donor strain *E. coli* BW20767 λpir with the cytotoxin producing AAHC *K. oxytoca* isolate AHC-6 [42] (see 3.5). The generated mutants were then analyzed for loss of cytotoxicity in cell culture via the MTT assay (3.10.2). Additionally, Southern Blot analysis was used to guarantee single site insertion and to rule out co-integration of pRL27 backbone sequences. The plasposon rescue (3.5.2) allowed the recovery of the insertion cassettes and adjacent chromosomal DNA of *K. oxytoca* AHC-6. After amplification of the plasposons in a λpir host (*E. coli* BW20767), only transformants with plasposons carrying the *aphA* and *ori6K* sequences survive kanamycin selection. After amplification of those plasposons they were sequenced using primers ori6k_rev and claude-fwd (Table 5). They bind in the insertion cassette and allow sequencing of both upstream and downstream *K. oxytoca* sequence. After correct trimming of the obtained sequence data, a BLAST homology search (blastx) was carried out. To rule out growth deficiency as the reason for loss of cytotoxicity, growth curves of obtained mutants were compared to *K. oxytoca* AHC-6 (wild type). The detected slight growth differences were considered standard bacterial growth variations and therefore loss of cytotoxicity could be correlated with the gene mutations.

After screening about 700 mutants, four loss of cytotoxicity mutants were obtained. For mutant 2 (Mut2) blastx homology search revealed the 3-deoxy-D-arabino-heptulosonic acid 7-phosphate synthase (DAHP synthase) of *Streptomyces cinnamonensis* to be the most homologous gene. This enzyme catalyzes the first step in the shikimate pathway that leads to the biosynthesis of chorismate. The shikimate pathway and its product chorismate are prerequisites for aromatic amino acids, p-aminobenzoate, p-hydroxybenzoate and various secondary metabolites. Interestingly, the disrupted gene of mutant 614 was also found in the shikimate pathway as its homologue was identified as the 3-dehydroquinate synthase of *K. pneumoniae*. Disruption of this gene was lethal under amino acid limiting conditions.The disrupted gene of mutant 89 (Mut89) was identified as a homologue of the putative non-ribosomal peptide synthase (NRPS) TomB of *Streptomyces achromogenes*.

NRPSs lead to the production of peptides by ways independent of mRNA and ribosomes. The products of NRPS pathways are diverse and include antibiotics as well as cytostatics, siderophores (e.g. enterobactin), and toxins (e.g. microcystins, syringomycin) [43]. These non-ribosomal peptides (NRPs) often contain non-proteinogenic amino acids and form macrocyclic structures composed of identical multimers. NRPS are large modular enzyme complexes with each module responsible for the incorporation of one amino acid in the growing peptide chain. Each module is made up of at least the following three domains: (1) The adenylation domain (A-domain) is responsible for substrate recognition and activation as aminoacyl adenylates via ATP hydrolysis. The substrate is then transferred to the (2) peptidyl carrier protein (PCP-domain) for elongation. Peptide bond formation of the substrates bound to PCP domains is catalyzed by the (3) condensation domain (C-domain) [44, 45]. The last module also contains a thioesterase domain catalyzing the release of the peptide from the NRPS, often via cyclization.

The fourth loss of cytotoxicity mutant (Mut404) was affected in a gene homologue to the transcriptional regulator PhoU of *K. pneumoniae*. PhoU serves as a regulator of phosphate transport and stationary phase metabolism on the transcriptional level. Thus its role in the cytotoxic phenotype of *K. oxytoca* might be on an indirect, regulatory level [42].

Mapping of the obtained sequences provided a 20 kb genomic DNA sequence in which both the affected gene of Mut2 and Mut89 are located. Mut404 and Mut614 are located outside of this sequence. Homology search of this sequence gave rise to a whole toxin gene cluster on the K. oxytoca chromosome (Figure 7, Table 1). [46]

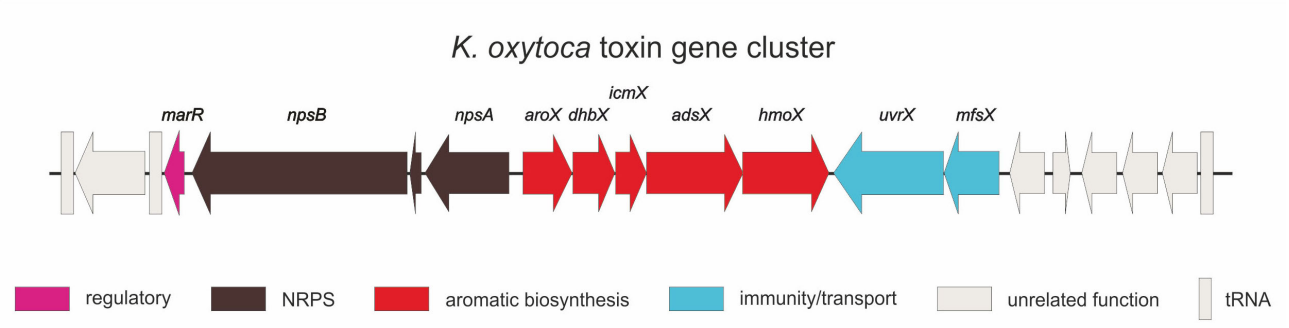

Figure 7: Toxin gene cluster of *K. oxytoca* AHC-6.
Gene names are based on the assigned gene functions according to BLAST homology search. The cluster spans in total about 20 kb on the *K. oxytoca* genome. [46]

Table 1: Genes and their annotated functions on the toxin gene cluster of *K. oxytoca* AHC-6.
Organization on the cluster is shown in Figure 7.

Gene	Annotated function
marR	MarR family transcriptional regulator
npsB	Non-ribosomal peptide synthase
npsA	Non-ribosomal peptide synthase
aroX	3-deoxy-7-phosphoheptulonate synthase (putative 3-deoxy-D-arabinose-heptulosonic-7-phosphate synthase)
dhbX	2,3-dihydro-2,3-dihydrobenzoate dehydrogenase
icmX	isochorismatase
adsX	putative phenazine biosynthesis protein PhzE
hmoX	4-hydroxyphenylacetate 3-monooxygenase oxygenase
uvrX	putative excinuclease ABC, subunit A
mfsX	drug resistance efflux protein

Downstream of the NRPS disrupted by Mut89, a homologue to *S. achromogenes* TomA was identified. In this organism *tomA* and *tomB* lead to the biosynthesis of tomaymycin, a pyrrolobenzodiazepine (PBD) discovered in the 1970s by its antimicrobial activity against Gram-positive bacteria [47, 48]. PBDs are sequence specific DNA alkylating agents which result in inhibition of DNA replication and transcription in eukaryotic cells giving them a cytostatic effect in cancer cells [49]. Other prominent members of PBDs are anthramycin and sibiromycin, which are also produced by *Actinomycetales.* These PBDs share the effect of cytotoxicity in vitro [50]. Comparison of these PBD clusters with the toxin gene cluster found in *K. oxytoca* revealed high similarities suggesting a PBD-producing gene cluster in *K. oxytoca* (Figure 8). Comparison of the NRPSs, encoded in the toxin gene cluster, with other PBD clusters and the characteristic sequence order of catalytic domains, suggested a bimodular assembly of the cytotoxic substance of *K. oxytoca* with the termination domain in NpsB.

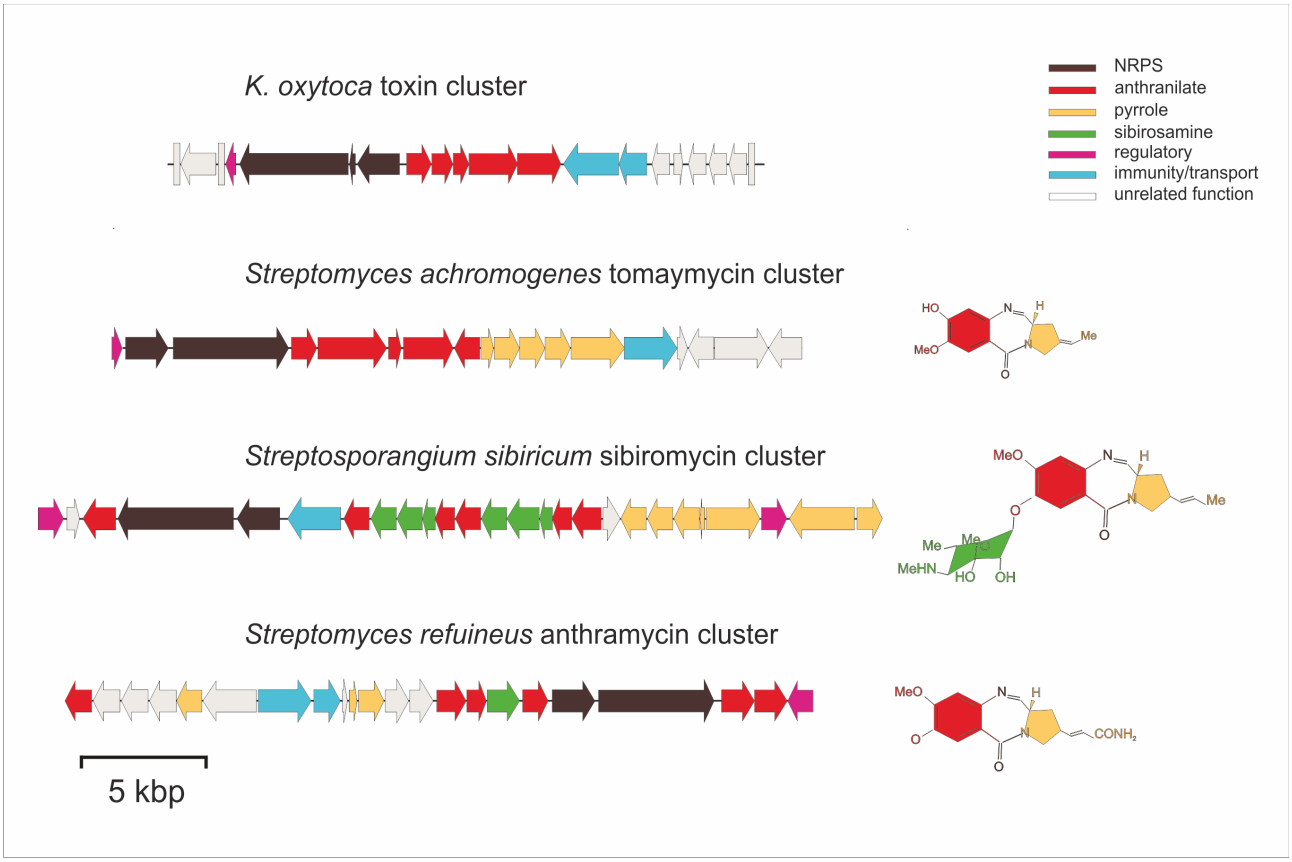

Figure 8: Toxin cluster of *K. oxytoca* AHC-6 and related PBD biosynthesis cluster. Tomaymycin, sibiromycin and anthramycin are antitumor antibiotics and share a common PBD ring system. Genes shown in red code for the anthranilate part of the PBD and are also involved in the shikimate pathway. The NRPS modules are shown in black. Autoimmunity of these DNA alkylating compounds is likely to be achieved by a UvrA homologue present in each cluster. [46]

Additionally, the sequencing and annotation of the *K. oxytoca* strain AHC-6 done by the Zechner group allowed us to identify the position of the cluster on the chromosome (Figure 7). tRNAs at the borders, flanked by conserved core genome regions, suggested the presence of a pathogenicity island (PAI) characterized by toxin and pathogenicity genes in close vicinity. As the toxin gene cluster in *K. oxytoca* shows these characteristics it can be regarded as a PAI.

The concept of PAIs was founded by Jörg Hacker and colleagues in the 1980s while investigating the virulence of uropathogenic *E. coli* (UPEC) strains. They could show that strains deleted of a certain chromosomal region, the PAI, exhibited a nonpathogenic phenotype [51]. The acquisition of genomic islands via horizontal gene transfer (HGT) represents quantum leaps in genome evolution and mainly occurs to guarantee adaption to novel environments and hence increase to the in vivo fitness [52]. Depending on the bacterial species or strains involved this transfer could work via natural transformation, plasmids or bacteriophage transduction. For pathogenic bacteria increased fitness is mainly characterized by better survival and transmission to new hosts [53]. Apart from *E. coli*, PAIs have been found in many other pathogens but they always share certain features characteristic for PAIs. They are defined by the presence of virulence genes and are specific to pathogenic representatives of a species. Their size varies from 10 to 200 kb and they show different base composition (G+C content) than the core genome. PAIs are usually located adjacent to tRNA genes which might serve as anchor points facilitating the integration of foreign DNA due to their high degree of conservation. Furthermore PAIs are often associated with mobile genetic elements like flanking direct repeats, integrase or transposase genes, or IS elements. They are also considered unstable genetic elements which are affected by mutations at a higher rate than the core genome, most of the time meaning the loss of parts or the whole PAI [54]. Virulence genes encoded by PAIs include iron uptake systems, adhesins, pore-forming toxins, superantigens, secreted lipases and proteases, O antigens, type I to V secretion systems, and their cargo as well as antibiotic resistances [53]. Some PAIs also encode their own regulators, for example the HilA/C/D transcriptional regulators of the SPI-1 PAI of *Salmonella enterica,* but it is also common that the PAI virulence genes are regulated by global regulators of the chromosome [54].

Although the majority of the *K. oxytoca* toxin‘s biosynthesis steps can be explained by the identified PAI, detailed information about the entire synthesis pathway including modifications of precursor molecules and the product as well as the transport of the toxin are still missing. Modifications of the A and C ring of the basic ring system of PBDs are known to be essential for biologic activity and confer PBD diversity [50] (Figure 9). These modifications include glycosylation, acylation, oxidation and hydroxylation [55]. C-9 hydroxylation of anthramycin for example was shown to confer the cardiotoxic properties of this substance [56]. Such modifications can occur during NRP synthesis in cis through additional domains, or post-synthetically by associated enzymes [44]. OxyB, an operon-independent cytochrome P450 enzyme, for example, was necessary for the oxidative cyclization of vancomycin [44]. In *S. achromogenes* a constitutive dehydrogenase caused

the modification of tomaymycin to oxotomaymycin, which no longer showed biological activity [57]. Modification domains are not found within NpsA or NpsB. Modification can not only occur to NRPS substrates but also to NRPS domains and the responsible enzymes are important for successful amino acid loading to the domains [45].

The toxin gene cluster of *K. oxytoca* is smaller compared to other PBD clusters and contains fewer modifying enzymes (Figure 8). As the cytotoxic substance (333 Da) produced by the cluster is larger than tomaymycin (304 Da) or anthramycin (315 Da), additional modifying enzymes must be encoded elsewhere on the *K. oxytoca* genome.

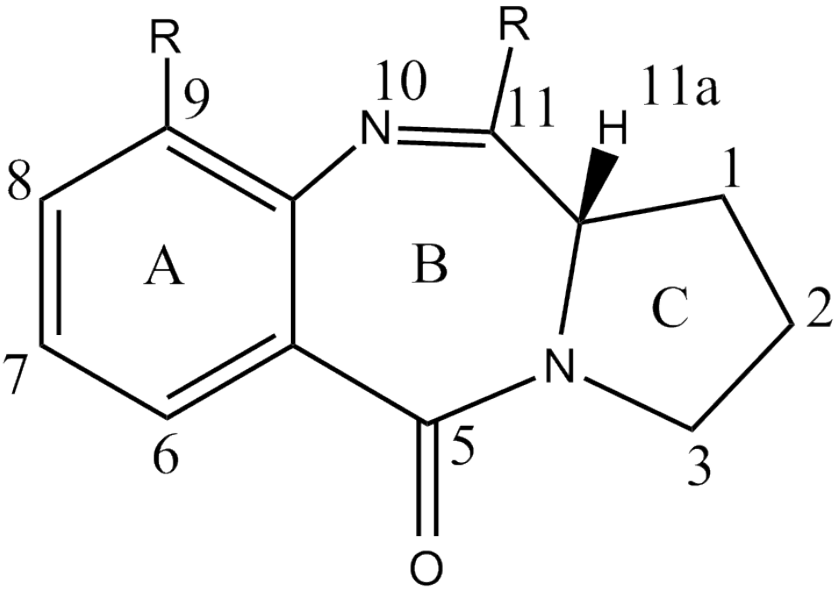

Figure 9: Basic tricyclic ring system of PBDs.
The common structure to all PBDs contains an anthranilate (A), a diazepine (B) and a hydropyrrole (C) moiety. Figure according to [49].

Although in some PBD clusters like the anthramycin cluster genes with annotated transporter function were identified, no clear mechanism for the transport of PBDs is known. The transporter gene in the anthramycin cluster shows homology to proteins of the major facilitator superfamily (MFS) [49]. Such an MFS is also encoded on the K. oxytoca gene cluster and might be implicated in drug export.

In silico predictions of genes (using programs like NRPSsp [58]) involved in these functions are difficult to make, especially because of the diversity of substrates including non-proteinogenic amino acids. Only a few of the substrates have been experimentally linked to their NRPSs. Thus, the rational search for candidate genes would be a tedious process. I concluded that continuation of the established transposon mutagenesis is the best tool to find promising genes for the still missing functions.

1.3.3. The chemical nature of the *K. oxytoca* cytotoxin

Many early publications about a cytotoxic substance found in *K. oxytoca* focus on its chemical properties [12, 13]. In the 1980s, a pentacyclic PBD-like secondary metabolite was isolated from *K. oxytoca* cultures. The structure of the purified substance was called tilivalline [59]. It exhibited cytotoxic properties against mammalian cells and no DNA binding was observed for a 11-β-cyano tilivalline analogue [60]. Tilivalline was isolated from a *K. oxytoca* isolate which was archived at the Statens Serum Institute but at this time point cannot be unambiguously re-identified. Earlier studies done in the Zechner group focusing on the chemical nature of the toxin discovered that the substance was stable and still exhibits its cytotoxic phenotype in the cell-free supernatant for up to 7 days storage time at room temperature. When stored at -20°C, cytotoxicity could still be measured after 2 months of storage. Furthermore, the cytotoxic effect could only be disrupted after heating to 100°C for 30 minutes. Alkaline conditions (pH 12) did not abolish the cytotoxic effect whereas treatment with HCl (pH 2) did [61]. Size exclusion chromatography with lyophilized supernatant confirmed the fact of a substance of low molecular weight. More recent attempts to purify the cytotoxin were based on reports for purification of PBDs like sibiromycin [62]. *n*-butanol extraction of the *K. oxytoca* AHC-6 supernatant followed by preparative high performance liquid chromatography (HPLC) yielded a white solid substance which still exhibited the cytotoxic phenotype. It was further investigated by mass spectrometry (MS) and NMR-spectroscopy. These analyses suggested the existence of a pentacyclic, PDB-motif containing molecule with a molecular formula of $C_{20}H_{19}N_3O_2$ and a molecular weight of 333 Da. Thus, a different substance than the one identified in the Minami laboratory [13]. The cytotoxicity of the purified 333 Da substance could be reconfirmed in the cell culture assay [46].

2. Aims of this study

This study was aimed at finding a genotypical correlation between cytotoxin-producing *K. oxytoca* strains. We hypothesized that the toxin synthesis genes identified on the PAI should be detectable in all toxin-positive *K. oxytoca* strains if this is the general mechanism for production of the cytotoxic PBD. A PCR screen for PAI specific genes was used to see if all toxigenic isolates carry the toxin biosynthesis genes.

Furthermore, the established transposon mutagenesis approach was continued to extend the knowledge of the underlying genetics of *K. oxytoca* cytotoxicity. We expected to identify genes involved in toxin secretion from the bacterial cell as well as genes causing modifications of precursors of the cytotoxin, or leading to post-synthetic modification of the cytotoxic substance itself. Loss of cytotoxicity mutants will be submitted to in depth analysis of the underlying mechanisms. Gene homology search will be used to discover the probable function of the affected gene in the cytotoxic phenotype. Additionally, potenial transport-affecting mutants will be identified by screening for intracellularly retained cytotoxic substance or precursor molecules by HPLC/MS. This technique will also allow for the detection of modified substances in case the transposon mutant is affected in a gene causing modifications during PBD synthesis. As probable modifications change the polarity and mass of a substance, comparison of wild type *K. oxytoca* and transposon mutant HPLC/MS-spectra will then help in identifying the differences in produced substances.

3. Materials & Methods

3.1. Media, buffers, solutions and chemicals

Unless otherwise indicated all media, buffers and solutions were prepared with ddH_2O. Sterilization was achieved by autoclaving at 121°C for 20 minutes.

Table 2: Media, buffers, solutions and chemicals used in this study.

cell culture medium	Minimum Essential Medium alpha + GlutaMAX™ (Invitrogen, Lofer, Austria) + 10% fetal bovine serum (Invitrogen) + 100 µg/ml penicillin + 100 µg/ml streptomycin
CASO medium	30 g/l CASO Bouillon (Roth, Karlsruhe, Germany)
CASO agar plates	40 g/l CASO Agar (Roth)
LB agar plates	10 g tryptone 5 g yeast extract 5 g NaCl 16 g Agar-Agar
MTT reagent solution	3-(4,5-Dimethyl-2- thiazolyl)-2,5-diphenyl-2H-tetrazolium bromide (Sigma-Aldrich, Missouri, USA) 5 mg/ml PBS (Invitrogen)
MTT lysis solution	1:25 (vol/vol) mixture of 96 % acetic acid and 2-propanol
TAE buffer (1x) (pH 7.2)	4 mM Tris-Acetate 136.1 g/l sodium acetate 19 g/l EDTA
0.5 M EDTA (pH 8)	186 g/l Ethylenediaminetetraacetic disodium salt * 2H_2O
3 M sodium acetate (pH 5.2)	408 g/l CH_3COONa
DNA loading dye 10x	0.1 ml 20 % SDS 5.7 ml 87 % glycerol 4.2 ml 1x TAE buffer 5 mg Bromphenole Blue 5 mg Xylene Cyanole
Ethidium bromide	10 mg/ml
Lämmli buffer	solution 1 1,1 g SDS 0,42 g EDTA 0,17 g $Na_2H_2PO_4$*H_2O 1,1 ml β-mercaptoethanol pH 7.2 adjustment ad 10 ml ddH2O solution 2 20 mg bromphenol blue 10 ml 50% gylcerol mix equal amounts of solutions 1 and 2
SDS running buffer (10x) (pH 8.3)	30,2 g Tris 188 g glycine

CAPS transfer buffer (2 l) (pH 11)	4,43 g 3-(cyclohexylamino)-1-propanesulfonic acid 200 ml methanol pH adjustment with NaOH keep away from light
1 M Tris (pH 7.5)	121.1 g Tris pH adjustment with HCl
Tris buffered saline (TBS)	20 ml 1 M Tris pH 7.5 30 ml 5 M NaCl
TBS/Tween/Triton (TTT)	20 ml 1 M Tris pH 7.5 30 ml 5 M NaCl 2 ml Triton X-100 0,5 ml Tween 20
Coomassie staining solution	50 g 5% aluminium sulfate 100 ml 10% ethanol 0,2 g 0,02% Coomassie Blue G-250 23,4 ml 2% o-phosphoric acid
lysozyme stock	125 mg/ml; store at -20°C
SDS gel solution A	50 ml 1 M Tris/HCl pH 6.8 4 ml 10% SDS 46 ml H_2O
SDS gel solution B	75 ml 2 M Tris/HCl pH 8.8 4 ml 10% SDS 21 ml H_2O

3.2. Bacterial strains and eukaryotic cell lines

3.2.1. Bacterial strains

Main bacterial strains used in this study are listed in Table 3. *Klebsiella* sp. isolate collection is listed in Table 7 (Appendix). All clinical isolates were obtained from patients treated at the Medical University of Graz and other hospitals, as well as from healthy individuals.

Table 3: Bacterial strains used in this study.
Amp^R , ampicillin resistance phenotype; Km^R kanamycin resistance phenotype;

Strain	Relevant genotype	Reference
E. coli DH5α	endA1 recA1 gyrA96 thi-l hsdR17 supE44 λ− relA1 deoR _(lacZYAargF)- U169 ϕ80dlacZ_(M15)	[80]
E. coli BW20767	RP4–2-Tc::Mu-1 kan::Tn7 integrant leu- 63::IS10 recA1 zbf-5 creB510 hsdR17 endA1 thi uidA (ΔMluI)::pir+	[88]
E. coli K12 MG1655	F- lambda- ilvG- rfb-50 rph-1	[87]
K. oxytoca AHC-6 (wildtype)	Amp^R	clinical AAHC stool isolate (Medical University Clinic Graz)
K. oxytoca ATCC 13182 (ATCC)	Amp^R	DSM 5175
K. oxytoca AHC-6 Δ*npsA*	Amp^R	[46]
K. oxytoca AHC-6 *yncE*::Tn5	Amp^R , Km^R	this study

3.2.2. Eukaryotic cell lines

The eukaryotic cell line HEp-2 was used for all cell culture application of this study.

3.2.3. Growth conditions

All bacterial strains were grown in CASO medium at 37°C under aerobic conditions and constant shaking (180 rpm). Strains were also grown on CASO agar plates at 37°C under aerobic conditions. Bacterial strains containing plasmids were grown with appropriate antibiotic selection. The following antibiotic concentrations were used:

ampicillin	100 µg/ml
chloramphenicol	10 µg/ml and 30 µg/ml
kanamycin	50 µg/ml

Eukaryotic cell lines in this study were grown in cell culture medium (Table 2). Cell cultures were incubated at 37°C with 5% CO_2 and 95% humidity. Cells were freshly seeded every 48 hours following supplier‘s recommendations.

3.3. Plasmids and oligonucleotides

Storage information for plasmids and oligonucleotides is available at K:/User/AG_ZechnerE/05_3erProtokolle_DIPLOMARBEITEN_DISSERTATIONEN/DIPLOMARBEITEN/Herzog Kathrin 2012.

Table 4: Plasmids used and constructed in this study.
Km^R,kanamycin resistance phenotype; Cm^R, chloramphenicol resistance phenotype; Tc^R , tetracycline resistance phenotype

Plasmid	Description	Reference
pRL27	Km^R, *tnp*, *oriT*, *ori*R6K	[40]
pACYC184	Cm^R, Tc^R	[79]
plasp873A	Km^R *ori*R6K mutant 873	this study
plasp873B	Km^R *ori*R6K mutant 873	this study
plasp1145A	Km^R *ori*R6K mutant 1145	this study
plasp1145B	Km^R *ori*R6K mutant 1145	this study
pACYC184YncE	Cm^R	this study
pACYC184YncEHis	Cm^R	this study

Table 5: Oligonucleotides used in this study.

* indicates the position is given relative to the open reading frame

#	Oligo-nucleotides	Sequence 5‘-3‘	Position	Template
1	S1	AGAGTTTGATCCTGGCTCAG	8-27	*E.coli* AYJ01695
2	S2	GGACTACCAGGGTATCTAAT	806-787	*E.coli* AYJ01695
3	nrp_sonde_fwd	GGCGGGAACCAGCTGCAAAT	6280-6299	plasp89 [42]
4	nrp_sonde_rev	TTGCTTTGCAACAGTTCGCG	6550-6569	plasp89 [42]
5	KpnI_tomAup_fwd	GCTAAGGTACCCTAATTCACTTTTGACCAGG	-545-(-)525 *	*npsA* (*K. oxytoca* AHC-6)
6	XhoI_tomAup_rev	GCTTACTCGAGTCACACGCATAAAATCTTCT	-47-(-)27 *	*npsA* (*K. oxytoca* AHC-6)
7	ori6k_rev	CACAGGAACACTTAACGGCT	1810-1829	pRL27
8	claude_fwd	AGCAACACCTTCTTCACGAG	3433-3452	pRL27
9	BamHI_YncE_fwd	CCCGGATCCTAAATCAAAGGGAGTCGTC	(-)15-1 *	*yncE* (*K. oxytoca* AHC-6)
10	SalI_YncE_rev	CCGTCGACTCACAGCGCGATGCGGA	1046-1059 *	*yncE* (*K. oxytoca* AHC-6)
11	SalI_YncEHis_rev	CCGTCGACCTAATGATGGTGATGGTGGTGCAGCGCGATGCGGATAAC	1046-1059 *	*yncE* (*K. oxytoca* AHC-6)
12	Ecoli_YncE_fwd	GCATTTACGTCATCTGTTTTCATC	3-26 *	*yncE (E.coli* K12 MG1655)
13	Ecoli_YncE_rev	CTGTTTAGTGGATTTTTGTTTCAC	994-1017 *	*yncE (E.coli* K12 MG1655)
14	GAPDH_fwd	GTTGAAGTGAAAGACGGTCATCTG	172-195 *	*GAPDH* (*K. oxytoca* AHC-6)
15	GAPDH_rev	AAGTTGTCGTTCAGAGCGATACC	892-914 *	*GAPDH* (*K. oxytoca* AHC-6)
16	yncD_fwd	GGGACTACAGGTGCTAAACC	225-244 *	*yncD* (*K. oxytoca* AHC-6)
17	yncD_rev	CATTCGTCATAGCTCAGGCC	760-779 *	*yncD* (*K. oxytoca* AHC-6)
18	yncE_end_fwd	TGGTAAGAGCTACAAGGTGGTC	900-921 *	*yncE* (*K. oxytoca* AHC-6)
19	OMLP_fwd	GAACATTGATGGTCGTTTGCG	8-27 *	*OMLP* (*K. oxytoca* AHC-6)
20	OMLP_rev	ATTATCTTCCACCAGCTGAGC	199-219 *	*OMLP* (*K. oxytoca* AHC-6)
21	pehX_fwd	CTGACTCGCGTTTATTTTCC	(-)100-(-)80 *	*pehX* (*K. oxytoca* AHC-6)
22	pehX_rev	GCTGCAGCGCCTGGGTATTC	534-553 *	*pehX* (*K. oxytoca* AHC-6)

3.4. DNA methods

3.4.1. Polymerase Chain Reaction

a) Colony PCR

100 µl of ddH_2O were inoculated with one single bacterial colony of an over-night grown agar plate. The suspension was heated to 100°C for 10 minutes. After a brief centrifugation step (10 sec, 13 000 rpm) the suspension was kept on ice and later used as PCR template. For all colony PCRs performed in this study *Taq* DNA polymerase (Fermentas GmbH, St. Leon-Rot, Germany) with the appropriate 10x *Taq* buffer was used. 2mM dNTP working mix was prepared using Fermentas dNTP Set (100 mM Solutions).
The colony PCR mix was prepared according to the following instructions:

ddH_2O	17.7 µl
10x Taq buffer	2.5 µl
Primer 1 (10 pM)	1.2 µl
Primer 2 (10 pM)	1.2 µl
dNTP mix (2 mM)	1.2 µl
Taq DNA polymerase (5U/µl)	0.2 µl
template DNA	1 µl
Total volume	25 µl

In case more than one primer pair was used, the volume of ddH_2O was decreased accordingly.
This protocol was also used for the *Klebsiella* isolate collection screen. (4.1)

b) PCR for cloning

DNA fragments for cloning purposes were amplified using Phusion® High-Fidelity polymerase by New England Biolabs according to manufacturer‘s recommendations. (NEB Inc., Ipswich, USA)

The thermo cycling profiles used were:

	Taq DNA polymerase	Phusion® DNA polymerase
	95°C, 3 min	98°C, 30 sec
35 x	95°C, 30 sec 60°C, 30 sec * 72°C, 1 min **	98°C, 10 sec 60°C, 30 sec * 72°C, 1 min **
	72°C, 5 min	72°C, 5 min
	4°C, ∞	4°C, ∞

*... corresponding primer annealing temperature, **... corresponding extension time

3.4.2. Chromosomal DNA preparation

Chromosomal DNA was extracted using the QIAGEN DNeasy Blood & Tissue Kit (QIAGEN, Hilden, Germany) following supplier‘s recommendations. DNA concentration was measured with the NanoDrop™ photometer or estimated with agarose gel electrophoresis (see 3.4.6)

3.4.3. Plasmid DNA preparation

Plasmid DNA extraction was achieved using the Fermentas GeneJET™ Plasmid Miniprep Kit as recommended by the manufacturer.

3.4.4. Restriction enzyme digestion

Restriction endonucleases were purchased by Fermentas or NEB and used according to the company‘s protocol.

3.4.5. Ligation

Ligation of DNA fragments was achieved using T4 DNA ligase (Fermentas) and the appropriate 10x ligation buffer. For plasmid construction, dephosphorylated vector DNA was ligated with a threefold molar excess of insert DNA and 1 U of T4 DNA ligase at 16°C overnight. As a religation control, a ligation mix was prepared in parallel without insert DNA. Before used for transformation, the ligation mix was desalted for a minimum of 1 hour by drop dialysis.

3.4.6. Agarose gel electrophoresis

Agarose gels were prepared using PeqGold Universal Agarose (peqlab, Erlangen, Germany) to a final concentration of 1% (w/v) with 1x TAE buffer and supplemented with 0.05 µg/ml ethidium bromide. 1x TAE was used as running buffer as well and gels were run at 5 - 10 V/cm. For size and concentration estimation, gel bands were compared to standard DNA ladders GeneRuler™ 1 kb DNA ladder or Lambda DNA/EcoRI+HindIII marker (Fermentas) (Figure 10).

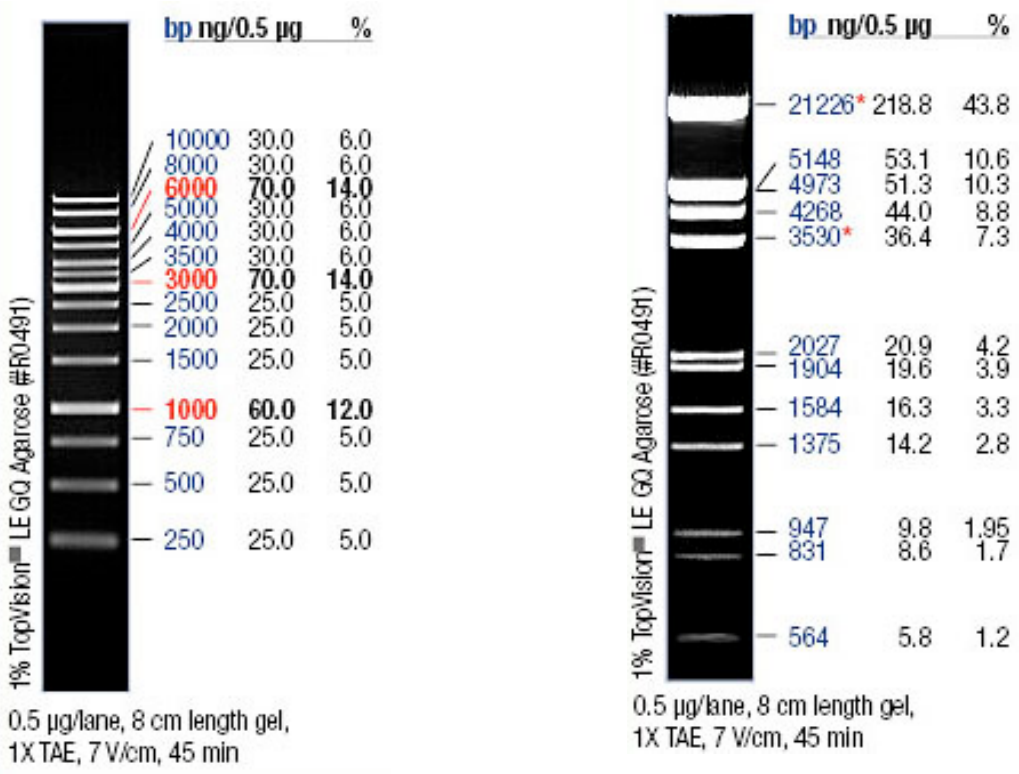

Figure 10: Standard DNA ladders used in this study.
Left: 1 kb DNA ladder; right: Lambda DNA/EcoRI+HindIII marker

3.4.7. Agarose gel extraction

The designated DNA bands were cut out from the agarose gels. DNA was extracted from the gels slices using GeneJET™ Gel Extraction Kit (Fermentas) following the manufacturer‘s instructions.

3.4.8. DNA sequencing

Sequencing was performed by Eurofins MWG Operon (Ebersberg, Germany) according to their barcode Sanger sequencing protocol. Therefore, 1.5 µl of a 10 pmol/µl primer solution was mixed with purified plasmid DNA (50 - 100 ng/µl) to a total volume of 15 µl.
The obtained sequences were analyzed using the BLAST program of the NCBI database. The blastx tool compared the six-frame conceptual translation products of the nucleotide query sequence (of both strands) against a protein sequence database. GenBank, RefSeq Nucleotides, EMBL, DDJB, and PDB sequences were browsed. The blastx program settings were left at default, meaning the BLOSUM62 matrix was used, maximal target sequence was set to 100, the expect threshold to 10, word size to 3, filter to low complexity regions and no masking was used. Details can be found in [42].
Comparative search was in parallel also performed against the *K. oxytoca* AHC-6 sequence on the RAST (Rapid Annotation using Subsystem Technology) server using the implemented BLAST tool.

3.5. Transposon mutagenesis

3.5.1. Conjugational transfer of pRL27

The donor strain *E. coli* BW20767 harboring the miniTn5 plasmid pRL27 was incubated overnight at 37°C and 180 rpm in 2 ml of CASO medium containing 50 µg/ml kanamycin. The recipient strain, *K. oxytoca* AHC-6, was incubated under the same conditions but with 100 µg/ml ampicillin. The following day 1 ml of the overnight culture (ONC) was used to inoculate 40 ml of the corresponding CASO medium. After incubation for 1 hour at 37°C the OD_{600} was measured. The donor and recipient were mixed at a ratio of 1:10, whereat the needed volume of donor culture was set to OD_{600} of 1. The mix was then centrifuged (10 min, 4 000 rpm) and the pellet was resuspended in 50 µl PBS. The following conjugation was performed by putting the mix on a sterile 0.45 µm cellulose acetate filter (Millipore, Billerica, USA). The filter was applied on a LB agar plate and incubated at 37°C overnight. The filter was then resuspended in 1 ml of PBS and this suspension was diluted up to 10^{-5}. The dilutions were plated on CASO agar plates containing 50 µg/ml kanamycin and 100 µg/ml ampicillin and incubated overnight at 37°C.

3.5.2. Plasposon rescue

Chromosomal DNA of loss of cytotoxicity mutants was extracted as described under 3.4.2 and analyzed with agarose gel electrophoresis comparing it to a Lambda DNA/EcoRI +HindIII marker (Fermentas). A minimum of 500 ng of chromosomal DNA was digested with 5 U BamHI overnight at 37 °C. Precipitation of the cut DNA fragments was performed in 2.5 volumes of 96% ethanol and 0.5 volumes of 3 M sodium acetate overnight at -20°C. The precipitate was recovered by centrifugation and washing with 70% ethanol and subsequently dissolved in ddH_2O. The fragmented DNA was then self-ligated using T4 DNA Ligase and desalted (see 3.4.5). Electro competent *E. coli* BW20767 cells were transformed with the ligation mix as described in 3.7 and plated on CASO agar plates with 50 µg/ml kanamycin. Plasposons of the obtained colonies were extracted as mentioned in 3.4.3. The plasposons were cut using SmaI or BamHI restriction enzymes and plasposon size was determined using agarose gel electrophoresis in comparison with a Lambda DNA/EcoRI+HindIII marker. Finally, plasposons were sent to Eurofins MWG Operon for sequencing.

3.5.3. Mutant storage

The generated Tn5 mutants were stored in 96 well plates with 40% glycerol at -80°C. Storage information as well as MTT assay results of each mutant is available at K:/User/ AG_ZechnerE/05_3erProtokolle_DIPLOMARBEITEN_DISSERTATIONEN/ DIPLOMARBEITEN/Herzog Kathrin 2012

3.6. Preparation of electro competent cells

Electro competent *E. coli* cells were prepared by inoculation of 200 ml CASO medium with 0.2 ml of an *E.coli* ONC. The cells were grown at 37°C until an OD_{600} of 0.5 - 0.7 was reached. Prior to centrifugation (10 min, 10 000 rpm, 4°C) the cell suspension was chilled on ice for at least 10 minutes. The pelleted cells were then resuspended in 200 ml of ice cold 10% glycerol and centrifuged again under the previous conditions. The washing step was repeated twice with 100 ml and then 10 ml ice cold 10% glycerol. Finally, the pellet was resuspended in 1 ml of 10% glycerol and 40 µl aliquots were frozen with liquid nitrogen and stored at -80°C. For electro competent *K. oxytoca* cells 200 ml CASO medium containing 0.7 mM EDTA were inoculated with 0.2 ml of a *K. oxytoca* ONC. This

culture was grown to an OD_{600} of 0.2 - 0.4. Subsequent steps were performed as described above.

3.7. Transformation

Transformation of electro competent *E. coli* cells with plasmid DNA or ligation mix was achieved by electroporation using an Eppendorf electroporator 2510 and 0.2 cm electroporation cuvettes (Eppendorf, Hamburg, Germany). Electro competent cells were thawed on ice and mixed with the appropriate amount of plasmid DNA (50 - 500 ng) or dialyzed ligation mix (5 - 30 µl) and transferred to a chilled cuvette. Electroporation was carried out at 2500 V with optimal time constants ranging between 5.2 to 5.8 ms. For regeneration cells were transferred in 900 µl pre-warmed CASO medium and incubated at 37°C for one hour to allow for the expression of the antibiotic resistance. Subsequently, dilutions were prepared and plated on CASO agar plates with the appropriate antibiotic selection and incubated overnight at 37°C.
Electro competent *K. oxytoca* cells were transformed similarly with the exception of a longer regeneration time of 2 hours.

3.8. RNA methods

In order to avoid contamination with RNases, laboratory equipment was cleaned with RNase Away (MolecularBioProducts, San Diego, USA) and RNase-free plastic ware was used.

3.8.1. RNA extraction

$5*10^8$ cells of an ONC were mixed with 2 volumes of RNAprotect Bacteria Reagent (QIAGEN) and incubated for 5 min at room temperature for immediate RNA stabilization. After centrifugation (10 min, 10 000 rpm) the supernatant was removed by gently inverting the tube. 200 µl of TE buffer containing 2 µl of lysozyme stock solution and 20 µl of Proteinase K were added. This mixture was mixed vigorously on the vortex mixer and incubated for 30 minutes at room temperature. The subsequent RNA isolation was carried out with RNeasy Mini Kit following the company‘s instructions. Isolated RNA was kept on ice and quantified by NanoDrop measurement. DNase digestion of the extracted DNA was achieved by incubation of 2 µg of RNA with Fermentas DNase I and the appropriate buffer at 37°C for 1 hour. DNase I was inactivated with 4 µl of 25 mM EDTA and incubation at 65°C for 10 min. RNA concentration was measured with NanoDrop measurement.

3.8.2. Reverse transcription

For reverse transcription of RNA into cDNA Fermentas RevertAidTM H Minus First Strand cDNA Synthesis Kit was used. 200 - 400 ng of DNase I digest were mixed with 1 µl of gene specific primer (15 pmol) and ddH2O was added up to a volume of 12 µl. This primary mix was incubated at 65°C for 5 min, shortly centrifuged and kept on ice. 4 µl of 5x buffer, 1 µl of RiboLock RNase Inhibitor, 2 µl of 10 mM dNTP mix and 1 µl of reverse transcriptase were added to a total volume of 20 µl. For RT minus control, the same mix was prepared but without adding reverse transcriptase to check for remaining DNA amounts. As an internal control a second RT mix set was prepared with GAPDH (glyceraldehyde 3-phosphate dehydrogenase) targeting primers to allow for relative expression analysis. The thermo cycling profile used was:

42°C, 60 min

70°C, 5 min

4°C, ∞

Transcribed cDNA was stored at -20°C.

3.8.3. Second strand synthesis

For second strand synthesis Taq DNA polymerase was used according to the following protocol:

ddH_2O	19,7 µl
10x Taq buffer	3 µl
Primer 1 (10 pM)	1 µl
Primer 2 (10 pM)	1 µl
dNTP mix (2 mM)	3 µl
Taq DNA polymerase (5U/µl)	0,3 µl
template cDNA	2 µl
Total volume	30 µl

	95°C, 3 min
30 x	95°C, 30 sec 58°C, 30 sec 72°C, 1:30 min
	72°C, 5 min
	4°C, ∞

Chromosomal DNA was amplified in parallel using the same primers as a positive control.

3.9. Protein methods

3.9.1. SDS Page

For sample preparation 1 ml bacterial culture (OD_{600} of 1.5) was centrifuged (5 min, 8 000 rpm) and the pellet was washed once with PBS. Following a second similar centrifugation step, 50 µl of Lämmli buffer were added to the pelleted cells and heated to 100°C for 30 min. Subsequently, 10 µl of sample were loaded on a SDS gel along with 5 µl of PageRuler™ Prestained Protein Ladder (Fermentas) in a separate gel slot. Gels were run at 16 mA per gel for about 20 min until the samples reached the separation gel. Then the current was raised to 20 mA per gel for about 40 min. Gels were then washed twice for 10 min with dH_2O. Visualization of the separated proteins was achieved by shaking the gel for 2 hours in Kang staining solution.

stacking gel		separating gel
7.5 ml	A solution B	1.25 ml
15 ml	Rotiphorese® Gel 30	650 µl
7.35 ml	ddH_2O	3,07 µl
157.5 µl	10% APS	25 µl
45 µl	TEMED	15 µl

3.9.2. Western Blot

Prior to blotting the 0.45 µm PVDF (polyvinylidene fluoride) membrane (Millipore) was activated with 100% methanol for 15 sec followed by washing for 2 min in dH_2O and 5 min in transfer buffer. The blot was assembled and the transfer was performed via tank blotting in transfer buffer for 90 min at 220 mA. The membrane was then dried for 30 min at 37°C and washed 2 times for 10 min in TBS.

Blocking of unspecific binding sites was realized by incubating the membrane in 20 ml TBS with 3% bovine serum albumin (BSA) for 1 hour at room temperature. Subsequently, the membrane was washed 2 times for 10 min in TTT and once for 10 min in TBS. The first antibody, mouse Penta-His Antibody (QIAGEN), was used in a 1:2000 dilution in TBS with 3% BSA and incubated overnight at 4°C on the membrane. The next day the membrane was washed 3 times for 10 min in TTT and once for 10 min in TBS. The goat anti-mouse IgG secondary antibody was used in a 1:10000 dilution in TBS with 10% milk powder with an incubation time of 1 hour at room temperature. The final washing steps included 3 times 10 min in TTT and once for 10 min in TBS.

Detection was achieved via enhanced chemiluminescence (ECL) on the basis of the horseradish peroxidase coupled to the secondary antibody converting luminol to 3-aminophthalate. The Amersham™ ECL detection system (GE Healthcare, Buckinghamshire, UK) was used according to manufacturer‘s recommendations.

3.10. Evaluation of cytotoxic phenotype

3.10.1. Preparation of conditioned supernatant

The strain to be tested was grown in 2 ml CASO medium (+100 µg/ml ampicillin for *K. oxytoca* AHC-6 and ATCC and + 100 µg/ml ampicillin, and 50 µg/ml kanamycin for transposon mutants) for 16 hours at 37°C and 180 rpm. 1 ml of this ONC was centrifuged (20 min, 4 000 rpm, 4 °C) and the supernatant was filtered through a sterile 0.2 µm syringe filter. The filtrate was collected in sterile tubes and used in the cell culture assay or stored at -20°C until needed.

For high throughput screening of the generated mutant library CASO medium (+100 µg/ml ampicillin and 50 µg/ml kanamycin) in a sterile 96 deep well plate was inoculated via replica plating of the frozen stocks. Cultures of *K. oxytoca* AHC-6 wildtype and ATCC were prepared in parallel. Filtered supernatant was generated via centrifugation and filtration as described above.

3.10.2. MTT assay

Eukaryotic Hep2 cells were grown to 60 - 80% confluency in cell culture medium (see Table 2) and seeded in 96 well tissue culture plates (Greiner, Kremsmünster Austria) with $1.5*10^4$ cells per 100 µl cell culture medium per well. Conditioned supernatant was diluted to 1:3, 1:9, 1:27, 1:81 and 1:243 with PBS and 50 µl of the dilution was added per well. As a negative control 50 µl PBS were added to separate wells.

After 2 days of incubation at 37°C with 5% CO_2 and 95% humidity the cell survival was examined via light microscopy. Afterwards, quantitative cell survival was determined via MTT staining. Therefore the medium was removed from each well and 200 µl pre-warmed PBS were added. Then 25 µl of MTT reagent solution were added per well and incubated for 1 - 2 hours. In this time the yellow colored MTT was reduced to a purple colored formazan by living cells. The liquid supernatant was removed and 200 µl MTT lysis solution were added to lyse the cells and set the purple formazan free. Quantification was done by measuring the OD_{595} with a microplate reader. Each sample was tested in triplicate and compared to the PBS only control which was set to 100%. Statistical analysis was done with GraphPad Prism5 (GraphPad Software, Inc., La Jolla, USA) program using the t test.

3.10.3. Microscopy

Qualitative assessment of cell viability was done with light and phase contrast microscopy using a Nikon ECLIPSE TE300 microscope.

3.11. French press cell lysis

For the following HPLC analysis of the cell lysate *K. oxytoca* cells were disrupted with French press cell lysis. For this purpose 4 l CASO medium were inoculated with 2 ml of an ONC and incubated for 16 hours at 37°C. Afterwards, cells were collected via centrifugation (30 min, 10 000 rpm) and the pellet was washed with dH_2O. This centrifugation and washing step was repeated twice and the pellet was subsequently resuspended in 35 ml PBS. Cell disruption with French® pressure cell press (SLM Aminco Instruments Inc., USA) was performed at a pressure gauge level of 10000 psi using the 40K cell. In total 4 cycles were performed to guarantee efficient lysis. During the whole process, the suspension was kept on ice.

3.12. HPLC analysis

3.12.1. Organic extraction

According to earlier studies on PBD extraction [62], the cytotoxic substance was extracted two times from the supernatant or cell lysate with *n*-butanol. For better cell lysate extraction this mixture was centrifuged at 10000 rpm for 20 min to allow optimal separation of the layers. The combined *n*-butanol layers were carefully concentrated under reduced pressure at 40°C. This process led to a crude whitish extract, which was dissolved in 1 ml of *n*-butanol. Insoluble salts were filtered off.

3.12.2. High performance liquid chromatography

Analytical reversed phase HPLC was used for separation of analytical amounts according to non-polar interactions of the extract obtained. A Poroshell column 120 (100 x 3 mm; 2.7 µm) with endcapped C18 chains from Agilent (Santa Clara, USA) was used. Eluent A consisted of H_2O with 0.01% of formic acid (pH 3 - 4), eluent B was acetonitrile. Elution appeared in a linear gradient from 2% to 100% eluent B in 8 min. The UV detector scanned a range of 200 - 400 nm. From previous studies it was known that the cytotoxic substance showed maximum absorption at 220 nm and a retention time of 4.4 min.

3.12.3. Mass spectrometry

Mass-to-charge ratios were measured with the coupled LCMS-2020 (Shimadzu, Kyoto, Japan). The analytes were ionized with electrospray ionization (ESI) followed by a quadrupol mass analysis. The scan was limited for protonated and deprotonated substances to a range of 50 - 600 amu/Da. Selective ion monitoring (SIM) was performed in parallel scanning for the masses of 334 and 356 Da, which equal the mass of the cytotoxic substance (333 Da) in the protonated form (334 Da) and a sodium adduct (356 Da).

4. Results

4.1. Screen of *Klebsiella sp.* isolate collection for occurrence of cytotoxin synthesis genes

The PAI, encoding genes involved in the development of the cytotoxic phenotype, was identified previously in the Zechner lab [42]. To evaluate whether this PAI is unique to cytotoxin producing *K. oxytoca* strains we tested a total of 100 *Klebsiella* isolates from different body sites for the occurrence of the PAI on the chromosome by PCR. The *Klebsiella* isolates used in this study are listed in Table 7 (Appendix). Previous species differentiation was done by API 20E tests, 16S rDNA sequencing and indole reaction [61].

4.1.1. Selection of adequate PAI targets

In order to cover the essential parts of the PAI with a minimal amount of targets, the two targets in Figure 11 were chosen.

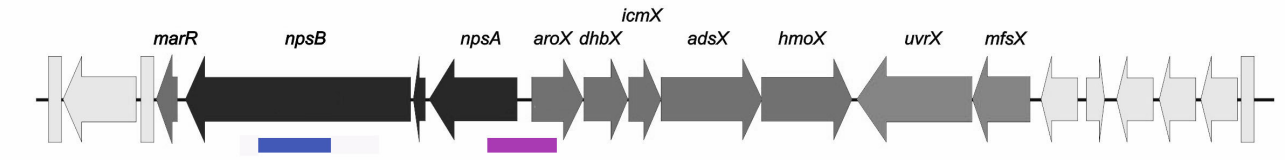

Figure 11: Pathogenicity island of *K. oxytoca* AHC-6 with PCR screen targets.
npsB target (blue)...290 bp; intergenic target (purple)...500 bp

One of them (blue) covered a 290 bp sequence stretch in the *npsB* gene, the other one (purple) was chosen to be in the intergenic region of *npsA* and *aroX* over a length of 500 bp. Amplification was achieved by using primers 3 and 4 for the *npsB* target and primers 5 and 6 (Table 5) for the intergenic target.
First, these targets allowed us to check for the existence of both NRPSs which are essential for cytotoxin production and secondly by incorporating intergenic space conservation of gene organization could be investigated.

4.1.1. *K. oxytoca* species specific target

We wanted to include a target specific for *K. oxytoca* in the PCR screen. Kovtunovych et al. proposed a PCR based discrimination of *K. oxytoca* from all other *Klebsiella* species targeting the polygalacturonase *pehX* gene [63]. However in previous studies done in the Zechner lab [61] this screen resulted in a number of false positive and false negative results. Therefore a 16S rDNA gene target was chosen as a *Klebsiella* specific target [64] using primers 1 and 2 (Table 5) resulting in a 798 bp PCR amplicon.
With the previously annotated genomic sequence of *K. oxytoca* AHC-6, it was possible to create a new primer pair for the *K. oxytoca* species specific *pehX* gene. Recently gained preliminary results suggest a successful species specific discrimination on the basis of the new *pehX* screen. None of the tested *Klebsiella* species were positive for this target except *K. oxytoca* strains.

4.1.2. A correlation between phenotype and genotype could be detected

The screen of 100 *Klebsiella* isolates for the *npsB* and intergenic target as well as the 16S rDNA target was carried out as described in 3.4.1.
The resulting PCR products were separated using agarose gel electrophoresis and their size was determined by comparison to a standard DNA ladder (GeneRuler™ 1 kb DNA ladder). While the 798 bp internal control band was expected for all isolates screened, the 290 bp and 500 bp bands were expected only to be present in *K. oxytoca* cytotoxin producing strains. An example of the resulting agarose gel electrophoresis pattern for a screen of *K. oxytoca* isolates is shown in Figure 12. Cytotoxin-producing strains were characterized by all three bands, whereas cytotoxin-negative *K. oxytoca* showed only the upper internal control band.

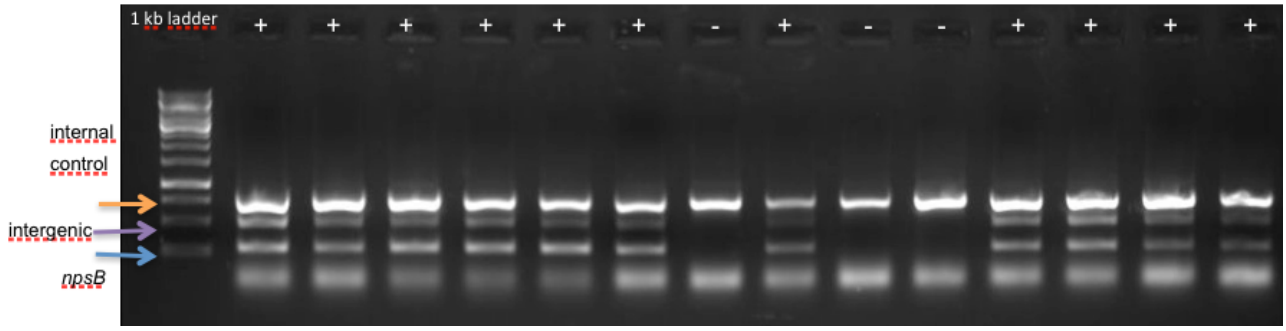

Figure 12: PCR screen amplicons of toxin producing (+) and non-toxin producing (-) *K. oxytoca* strains analyzed by agarose gel electrophoresis.
Klebsiella strains were analyzed for the presence of 2 PAI specific targets (*npsB...290bp*, intergenic...500 bp) and one internal control 16S rDNA target (798 bp). Size of bands was determined by comparison with a 1 kb standard DNA ladder.

In total out of the 46 toxin-producing *K. oxytoca* isolates all 46 carried the PAI specific PCR targets. Of the 53 non-toxin producing *K. oxytoca* strains 45 did not have the targets. Other *Klebsiella* sp. screened did not score positive for either of the PAI targets. In summary, it can be said that a 100% correlation was established between cytotoxin production and the presence of the PAI on the *K. oxytoca* genome. Conversely, 15% of non-toxin producing strains were positive for the PAI targets but showed no cytotoxic phenotype (Figure 13).

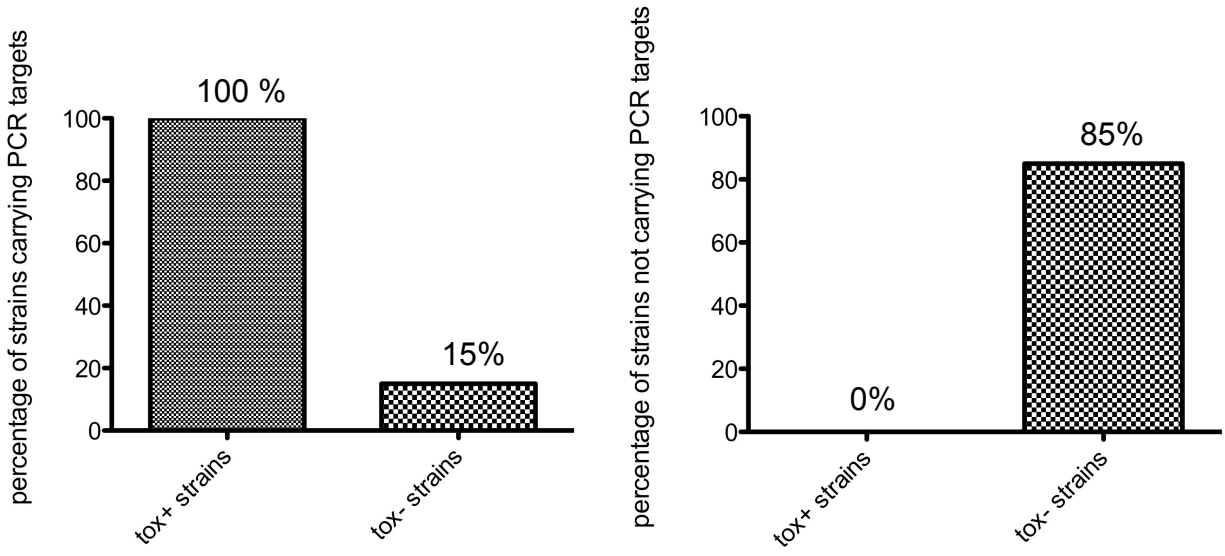

Figure 13: Distribution of PAI specific targets among *K. oxytoca* strains
Left: Percentage of *K. oxytoca* strains carrying both PAI specific targets (*npsB*, intergenic region) in relation to their cytotoxicity phenotype
Right: Percentage of *K. oxytoca* strains (tox+ and tox-) not carrying the PAI specific targets

4.2. Transposon mutagenesis continued

4.2.1. Transposon mutagenesis keeps on doing its job

The miniTn5 based mutagenesis with the pRL27 plasmid was chosen as it has already been established in the Zechner lab [42] and showed various favorable features discussed in 1.3.2. Transposition occurred in the recipient *K. oxytoca* AHC-6 after conjugational transfer of the pRL27 plasmid by the donor *E. coli* BW20767. To evaluate the efficiency of the transposon mutagenesis conjugation frequency was determined. This was done by plating the conjugation mix on selective agar plates for the discrimination of donor, recipient and transconjugant cells. The conjugation frequency was then calculated as the ratio of recombinant cfu/ml to donor cfu/ml. Mean values ranged around $6*10^{-2}$. Despite the CPS of *K. oxytoca* AHC-6, chromosomal DNA extraction yielded high enough amounts for successful plasposon rescue. Estimated plasposon sizes varied between 10 - 25 kb. Vector backbone co-integration was not seen during the plasposon sequencing. Initially, 800 Tn mutants were screened for loss of cytotoxicity with the high throughput screen (3.10). Two clones which showed the desired phenotype were subjected to closer analysis. Figure 14 shows an example of this high throughput screen. The supernatants of mutants 855 - 900 grown in CASO (+100 µg/ml ampicillin and 50 µg/ml kanamycin) were collected and filtered. HEp-2 cells in 96 well tissue plates were incubated with the supernatant according to 3.10.2. Compared to *K. oxytoca* AHC-6 wild type (orange) mutant 873 (Mut873, blue) shows no cytotoxic activity in contrast to all other mutants tested in this assay.

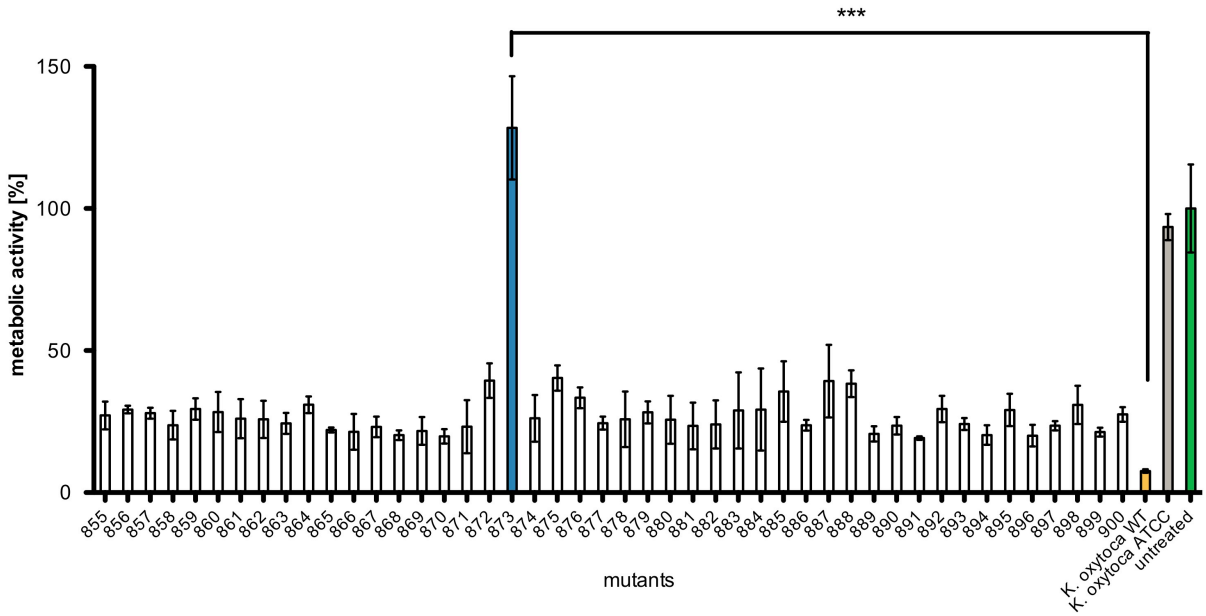

Figure 14: Representative results of the high throughput cytotoxicity cell culture assay
Percentage of metabolic activity was determined via MTT staining and represents the remaining metabolically active HEp-2 cells after treatment with 1:3 dilution of bacterial supernatant. Toxigenic *K. oxytoca* AHC-6 wild type (orange) was used as a positive control, *K. oxytoca* ATCC as a non-toxin producing control. Metabolic activity of cells treated with PBS only was set to 100%. (n = 3; $p < 0.005$)

4.2.2. Mutant 873 - an „old acquaintance“

4.2.2.1. Loss of cytotoxicity screen

In the high throughput screen Mut873 showed significant loss of cytotoxicity compared to the *K. oxytoca* AHC-6 wild type strain (Figure 14) and was therefore subjected to more detailed phenotype characterization. Supernatant of Mut873 was collected after 16 hours of incubation and diluted up to 1:81. Figure 15 shows the comparison of dilution 1:3 of Mut873 and the *K. oxytoca* AHC-6 wild type strain. The significant decrease in cytotoxicity could be confirmed.

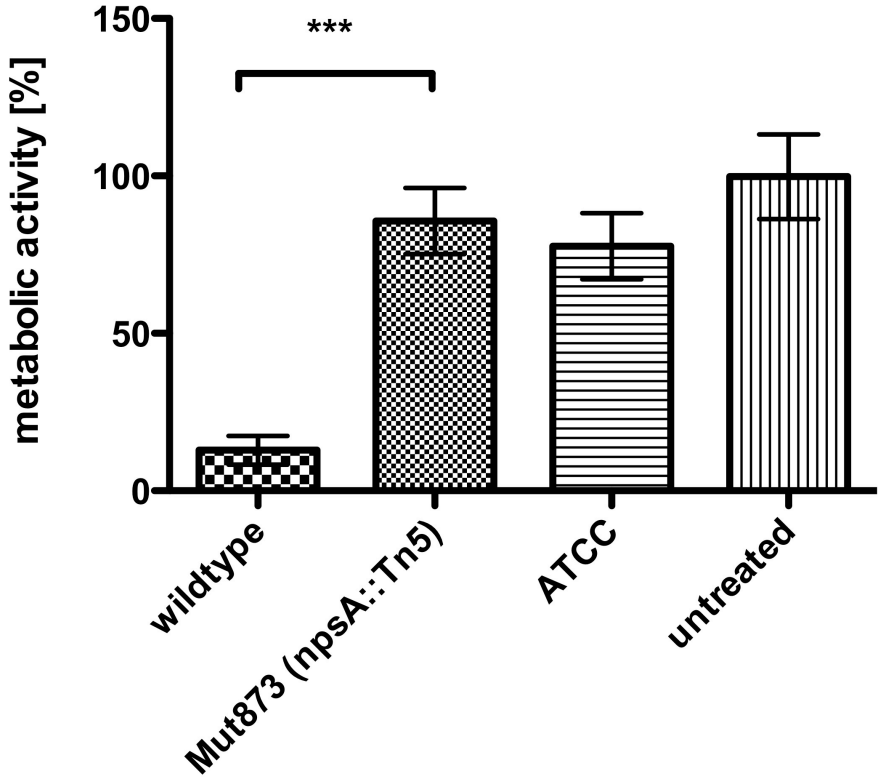

Figure 15: Cytotoxicity cell culture assay of Mut873
The relative metabolic activity of treated HEp-2 cells was analyzed in comparison to *K. oxytoca* wild type (toxigenic) and *K. oxytoca* ATCC (non-toxigenic). Bacterial supernatant was added at a 1:3 dilution. PBS treated HEp-2 cell metabolic activity was set to 100%. (n = 3; $p < 0.005$)

4.2.2.2. Two plasposons of different size could be isolated

Plasposon rescue of Mut873 was performed as described in 3.5.2 and yielded two different plasposons, plasp873A and plasp873B. Restriction digest of the plasposons with SmaI and BamHI (shown in Figure 16) revealed roughly estimated plasposon sizes of 18 and 20 kb, respectively, compared to a Lambda DNA/EcoRI+HindIII marker.

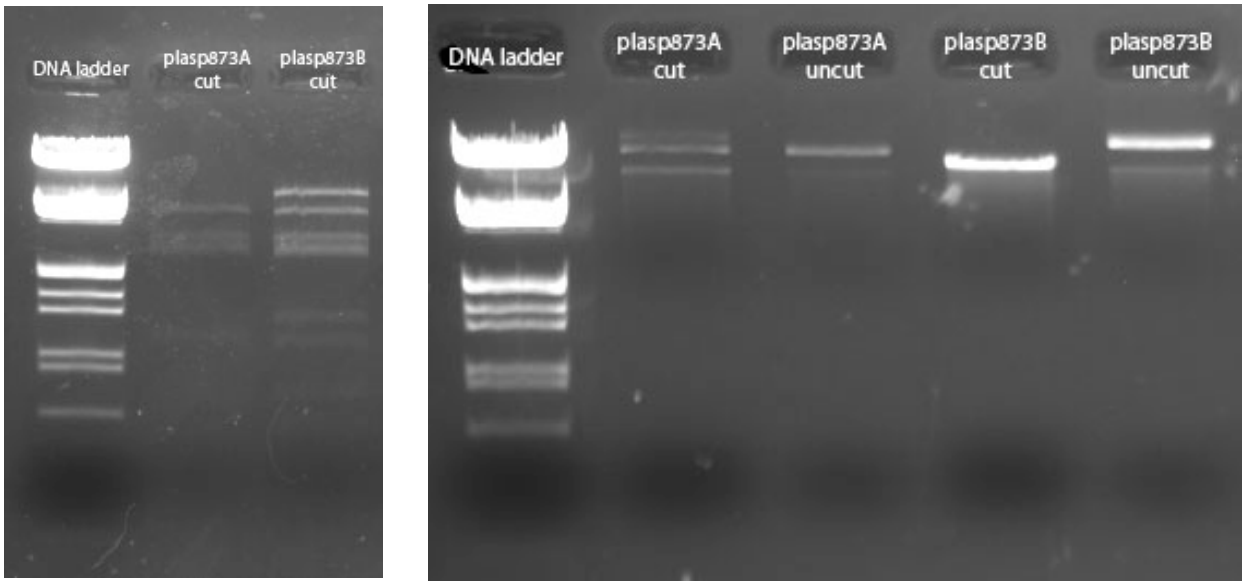

Figure 16: Plasposons of Mut873 analyzed by agarose gel electrophoresis.
Left: 10µl of isolated plasmid DNA of plasp873A and plasp873B was cut with SmaI; Right: restriction pattern after BamHI digest of plasp873A and plasp 873B, uncut plasmid DNA was loaded in equal amounts. Size estimation was achieved by comparison with a Lambda DNA/EcoRI +HindIII marker.

4.2.2.3. Sequencing and identification of the disrupted gene of Mut873

Plasp873A and plasp873B were sent to MWG for sequencing. The obtained sequence was trimmed and pRL27 sequence parts were removed and revealed identical sequences of both plasposons. The resulting 1045 bp sequence was blasted against the *K. oxytoca* AHC-6 genome on the RAST server and showed similarity to the non-ribosomal peptide synthase *npsA* of the PAI (Figure 17).

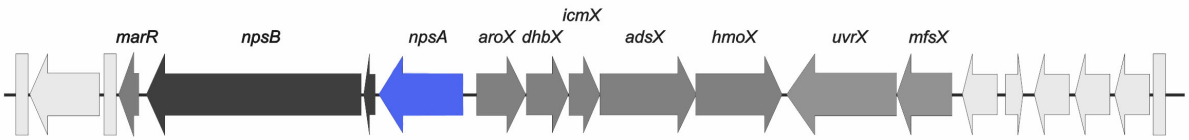

Figure 17: *K. oxytoca* toxin gene cluster depicting the position of the affected gene (*npsA*, blue) of Mut873

NpsA was already identified and characterized as an essential gene for cytotoxin production in earlier studies [42]. In this context complementation of a *npsA* knockout mutant was achieved (Figure 18) and the *npsA* gene product was identified as being essential for cytotoxin production.

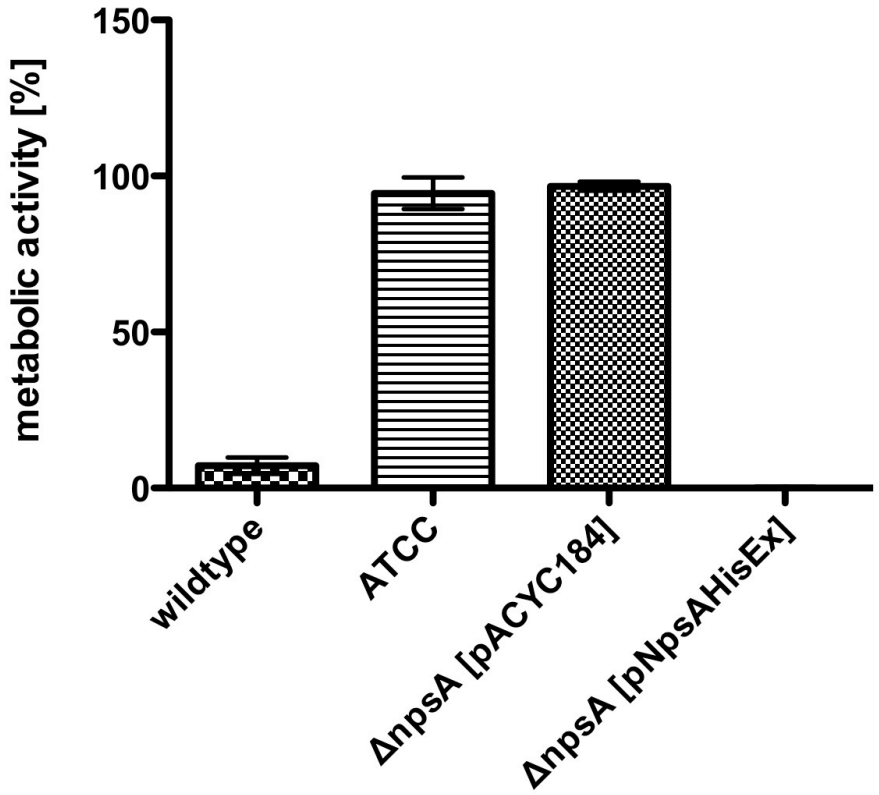

Figure 18: Cytotoxicity cell culture assay of Δ*npsA* mutant in trans complementation. Relative metabolic activity of HEp-2 cells was assessed after treatment with supernatant of *K. oxytoca* wild type, *K. oxytoca* ATCC, Δ*npsA* mutant with the vector control and Δ*npsA* mutant with the complementation vector pNpsHisEx. Metabolic activity of PBS treated HEp-2 cells was set to 100%. [46]

4.2.3. Loss of cytotoxicity mutant 1145

4.2.3.1. Loss of cytotoxicity screen

Mutant 1145 (Mut1145) also showed loss of cytotoxicity in the high throughput screen. An in-depth analysis was done similar to Mut873. Figure 19 shows the cytotoxicity screen of the 1:3 dilution of bacterial supernatant compared to *K. oxytoca* wild type and the non-toxigenic *K. oxytoca* ATCC control. A significant loss of cytotoxicity could be detected.

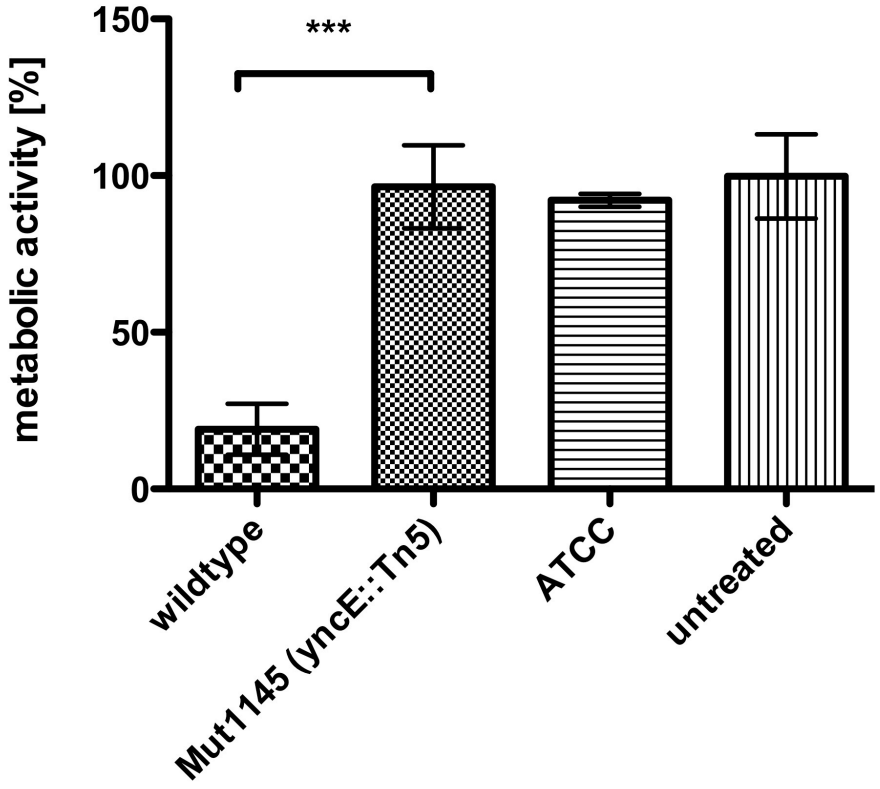

Figure 19: Cytotoxicity cell culture assay of Mut1145
The relative metabolic activity of treated HEp-2 cells was analyzed in comparison to *K. oxytoca* wild type (toxigenic) and *K. oxytoca* ATCC (non-toxigenic). Bacterial supernatant was added at a 1:3 dilution. PBS treated HEp-2 cell metabolic activity was set to 100%. (n = 3; $p < 0.005$)

4.2.3.2. Plasposon rescue of plasp1145A and plasp1145B

Chromosomal DNA extraction followed by ligation of plasposons and their subsequent amplification in an *E. coli* λpir host led to the recovery of two plasposons of different size, plasposons plasp1145A and plasp1145B. Following the restriction digest with SmaI and BamHI their sizes were estimated to be 15 kb and 14 kb, respectively (Figure 20).

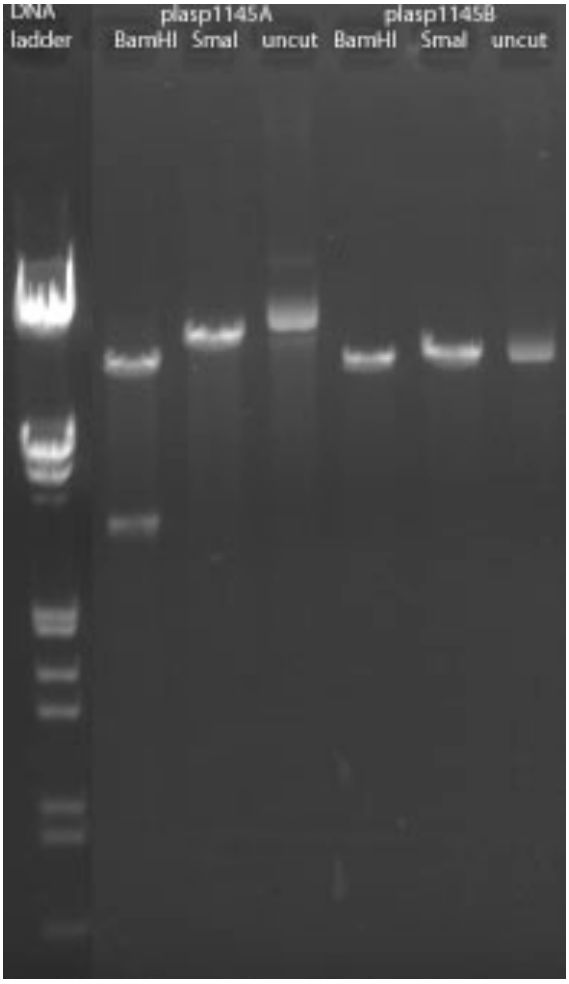

Figure 20: Plasposons of Mut1145 analyzed by agarose gel electrophoresis.
10 µl of plasp1145A and plasp1145B were cut with BamHI and SmaI, each at a time. The same amount of undigested plasmid DNA was loaded on the gel. Size estimation was achieved by comparison with Lambda DNA/EcoRI+HindIII marker. BamHI...BamHI restriction; SmaI...SmaI restriction

4.2.3.3. Loss of cytotoxicity is not due to altered growth of Mut1145

It had to be ruled out that growth deficiency was the reason for the loss of cytotoxicity of Mut1145. Therefore, a growth curve experiment was performed comparing the cfu/ml and OD_{600} of Mut1145 and *K. oxytoca* wild type. 200 ml of CASO medium were inoculated to an OD_{600} of ~0.0015 with ONCs of Mut1145 and wild type. The cultures were incubated at 37°C under constant shaking (180 rpm). At the time points 2, 4, 6, 16, 24, and 48 hours OD_{600} was measured and 1 ml of culture was diluted in CASO medium and plated on CASO agar plates. The plates were incubated overnight at 37°C and the following day cfu/ml count was analyzed. Figures 21 and 22 show the results of this growth curve experiment. No significant difference was detected when comparing the OD_{600} values of wild type and mutant strain. The cfu/ml count at time point 16 hours shows significant difference using the t test. ($p = 0.0089$, $n = 3$). This is the time point when conditioned supernatant was prepared for loss of cytotoxicity screen. The growth difference detected can be neglected as it is considered normal growth variation between bacterial cultures.

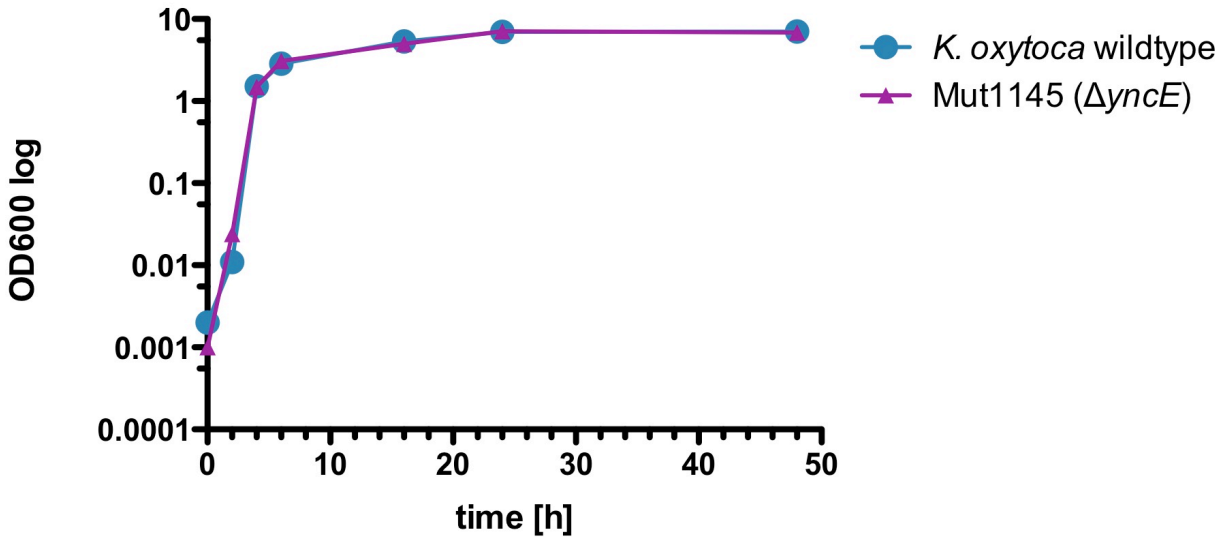

Figure 21: OD_{600} measurement of Mut1145 compared to *K. oxytoca* wildtype over 48 hours of cultivation time.
Cell density was measured photometrically at time points 2, 4, 6, 16, 24 and 48 hours after inoculation.

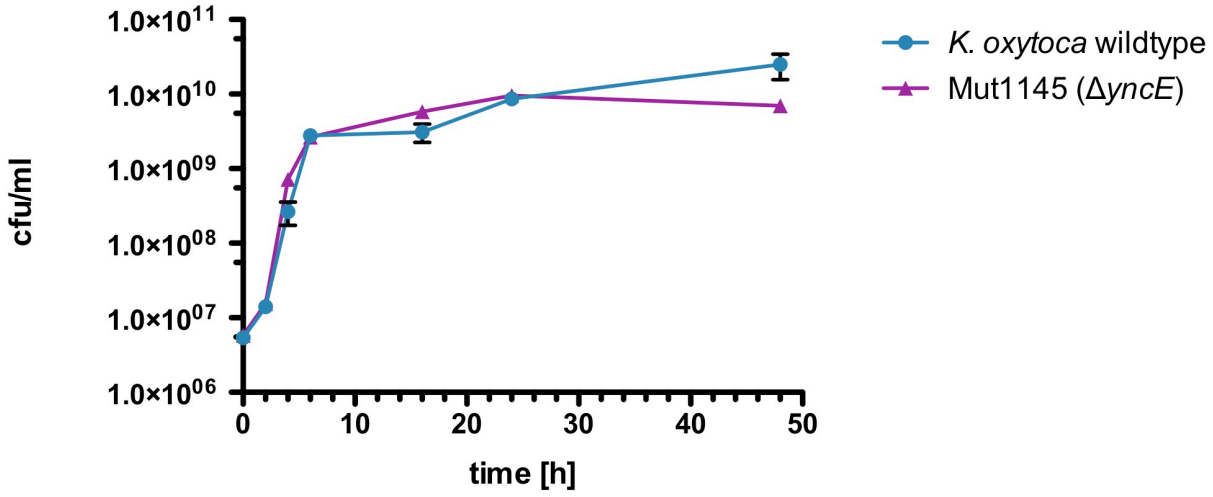

Figure 22: Cfu/ml measurement of Mut1145 compared to *K. oxytoca* wildtype over 48 hours of cultivation time.
Bacterial growth was evaluated via colony counts on agar plates from samples of time points 2, 4, 6, 16, 24 and 48 hours after inoculation. (n = 3)

4.2.3.4. *yncE* is affected in Mut1145

Sequencing results of plasp1145A and plasp1145B revealed identical affected genome sequences. After trimming and vector removal, a 1647 bp sequence was obtained and subjected to homology search. The hit with the highest similarity in the *K. oxytoca* AHC-6 genome identified a 1062 bp hypothetical protein. This sequence was then subjected to BLAST homology search (3.4.8) and led to the identification of the *yncE* gene product of *K. pneumoniae* (accession number YP_001335569.1; Max score: 582; E value: 0.0; Max ident: 90%). In *K. oxytoca* AHC-6 the surrounding up- and downstream sequence contains the TonB-dependent *yncD* precursor (2112 bp) and also encodes a putative outer membrane (OM) lipoprotein (222 bp) as shown in Figure 23.

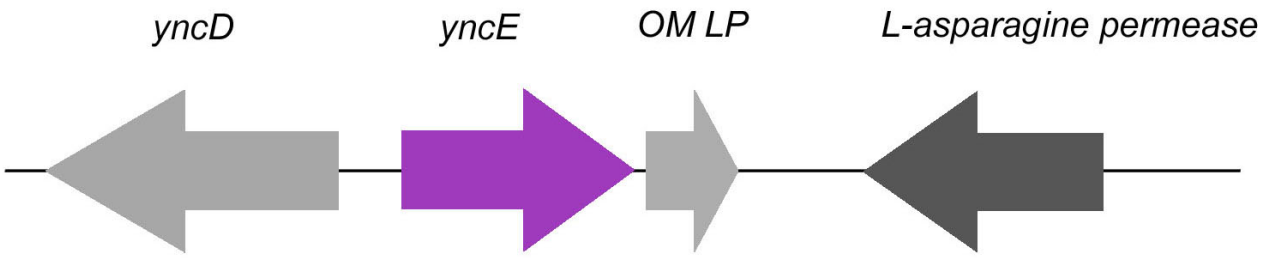

Figure 23: Gene map depicting the affected gene of Mut1145 (*yncE*, purple) and adjacent genes.
6.5 kb of *K. oxytoca* AHC-6 sequence is shown. OM LP... outer membrane lipoprotein

4.2.3.5. Comparative HPLC/MS analysis of cell lysates

Little is known about *yncE* function in *Klebsiella*. The only data about the gene function was available for *E. coli yncE,* which also showed high homology in the BLAST search (accession number NP_415969.1; Max score: 528; E value: 0.0; Max ident: 80%). A multiple sequence alignment of the gene sequences of the *yncE* homologues of *K. oxytoca, K. pneumoniae* and *E. coli* is shown in Figure 34 in the appendix. The *E. coli* homologue is thought to play a role in iron transport by interacting with *yncD*, a TonB-dependent OM receptor [65]. As the *yncE* homologue in *K. oxytoca* AHC-6 is located next to *yncD* on the genome, a similar function in *K. oxytoca* was assumed. A putative role for *yncE* in not only iron transport but also cytotoxin transport was hypothesized. Therefore, we were interested whether the cytotoxin or its precursors could be detected intracellularly. To answer this question cell lysates and supernatants of *K. oxytoca* wild type, *K. oxytoca ΔnpsA,* and *K. oxytoca* Mut1145 were subjected to *n*-butanol extraction as described in 3.11 and 3.12. HPLC-MS analysis was applied to detect the cytotoxin or its precursors in the extract.

First, the cell lysate of *K. oxytoca* wild type was analyzed. HPLC analysis revealed a eluate at 4.4 min retention time, the same as for the cytotoxic substance in the supernatant. In the MS spectrum of this peak, the mass-to-charge ratios 334 Da and 372 Da were detectable which equal the mass of the cytotoxic substance (333 Da) plus a proton [$M+H^+$] or a potassium [$M+K^+$].

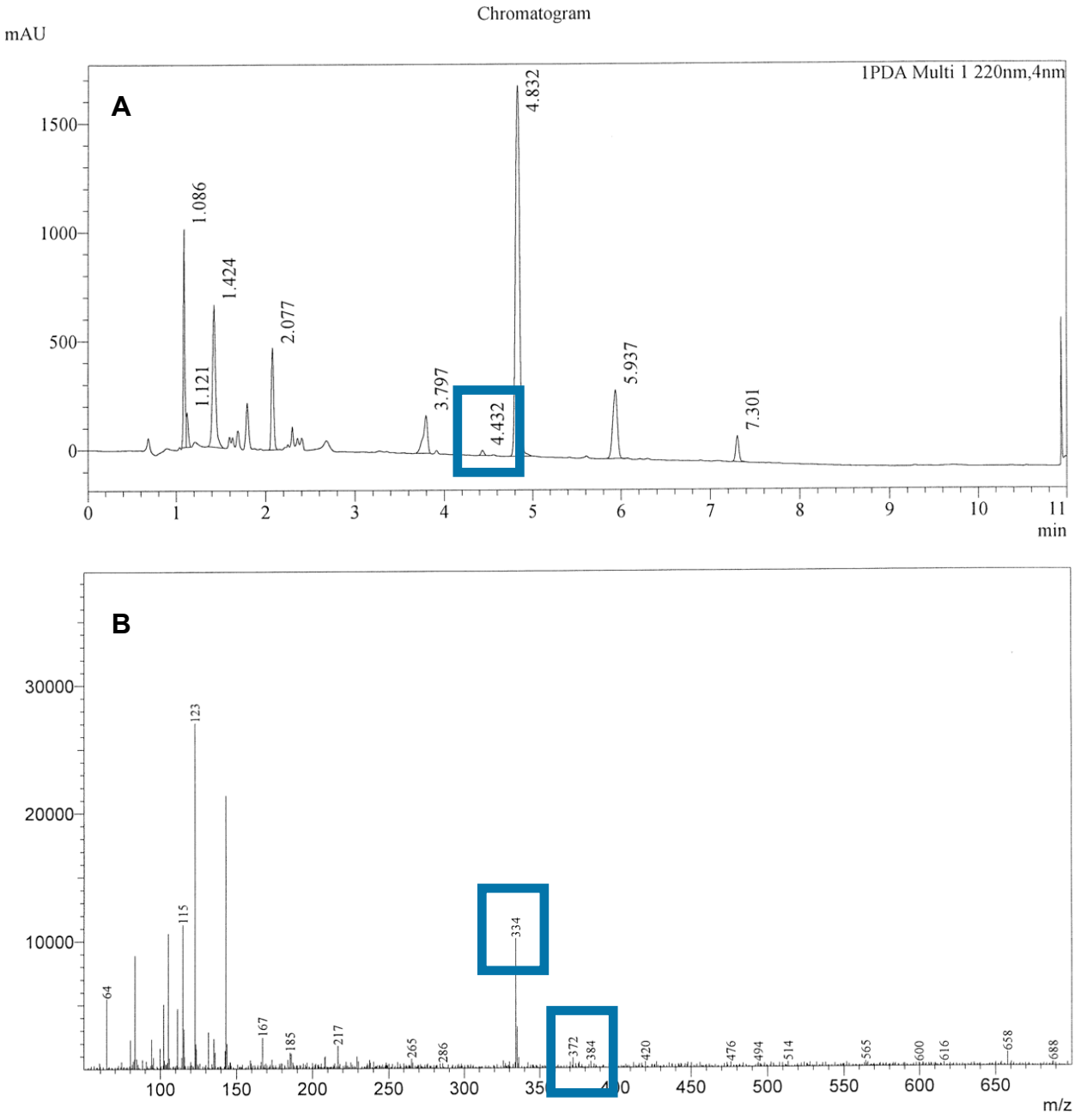

Figure 24: HPLC-MS results of *K. oxytoca* AHC-6 cell lysate *n*-butanol extract.
A: UV chromatogram (220 nm) of the HPLC analysis as a function of intensity over time. The highlighted peak at 4.4 min retention time is characteristic for the *K. oxytoca* cytotoxin.
B: Mass spectrum of the eluate of 4.4 min retention time. Spectrum shows peak intensity as a function of mass to charge ratio. Peaks at 334 Da and 372 Da resemble the cytotoxic substance (333 Da) $+H^+$ and the substance $+K^+$ respectively.

In the cell lysate of the *ΔnpsA* mutant (Figure 25) no peak at 4.4 min retention time could be measured which means that the cytotoxic substance is not produced and could not be detected intracellularly in a cytotoxin synthesis mutant.

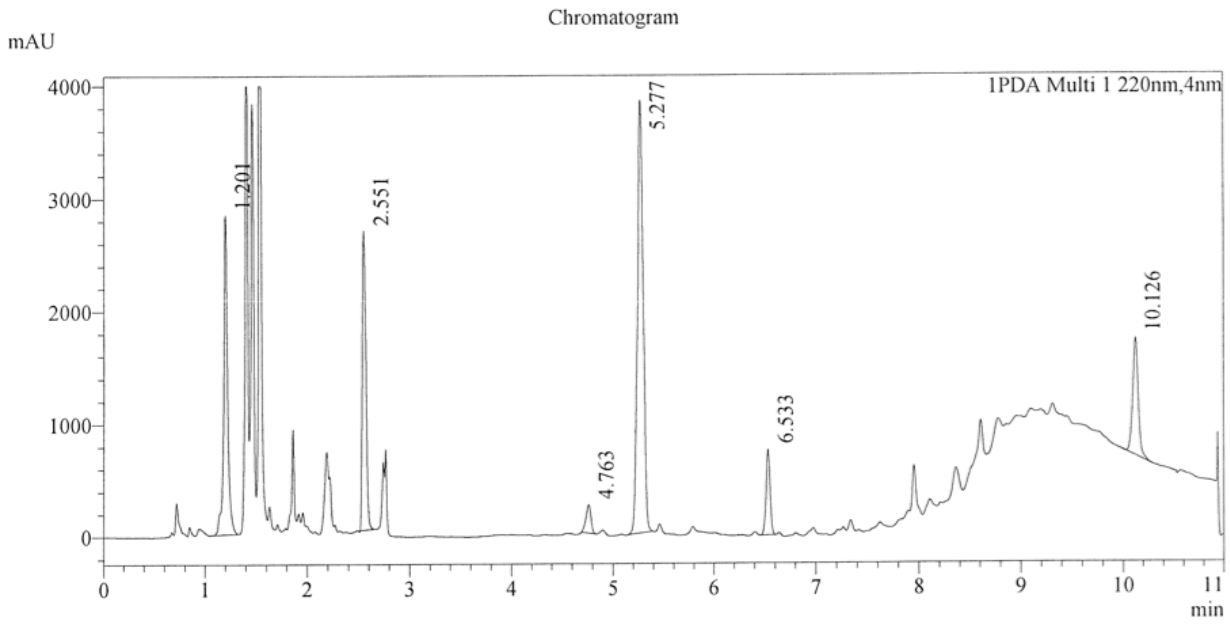

Figure 25: HPLC result of *K. oxytoca ΔnpsA* mutant cell lysate *n*-butanol extract.
UV chromatogramm (220 nm) of the HPLC analysis as a function of intensity over time. No toxin characteristic peak (4.4 min retention time) could be detected.

Supernatant of Mut1145 was subjected to the same analysis (Figure 26). Analog to the cytotoxicity screen, no cytotoxic substance was secreted and therefore could not be detected at 4.4 min retention time.

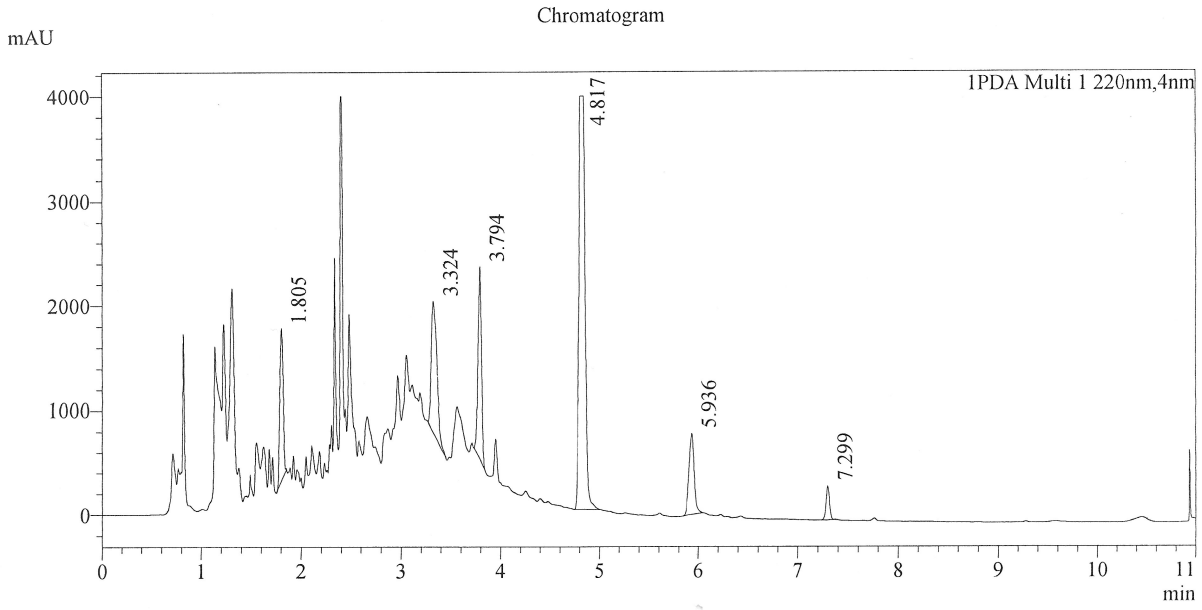

Figure 26: HPLC result of *K. oxytoca* Mut1145 supernatant butanol extract.
UV chromatogramm (220 nm) of the HPLC analysis as a function of intensity over time. No toxin characteristic peak (4.4 min retention time) could be detected.

In the Mut1145 cell lysate the HPLC chromatogram shows a clear peak at 4.4 min retention time. This would mean that a substance of similar polarity is detectable. The mass spectrum of this peak however reveals mass peaks at 444 [M+H$^+$], 466 [M+Na$^+$] and 482 [M+K$^+$] indicating the presence of a substance of 443 Da, 110 Da larger than the cytotoxic substance detectable in the supernatant and cell lysate of *K. oxytoca* wild type.

Analysis of the extract on preparative HPLC could show that the polarity of the 333 Da cytotoxic substance and the 443 Da substance in Mut1145 were not identical, as the retention time of the 443 Da substance was little increased compared to the retention time of the cytotoxic substance.

Further characterization of the 110 Da larger substance would require purification via preparative HPLC. So far, the amounts in the cell lysate were too little to obtain high enough yields of the substance.

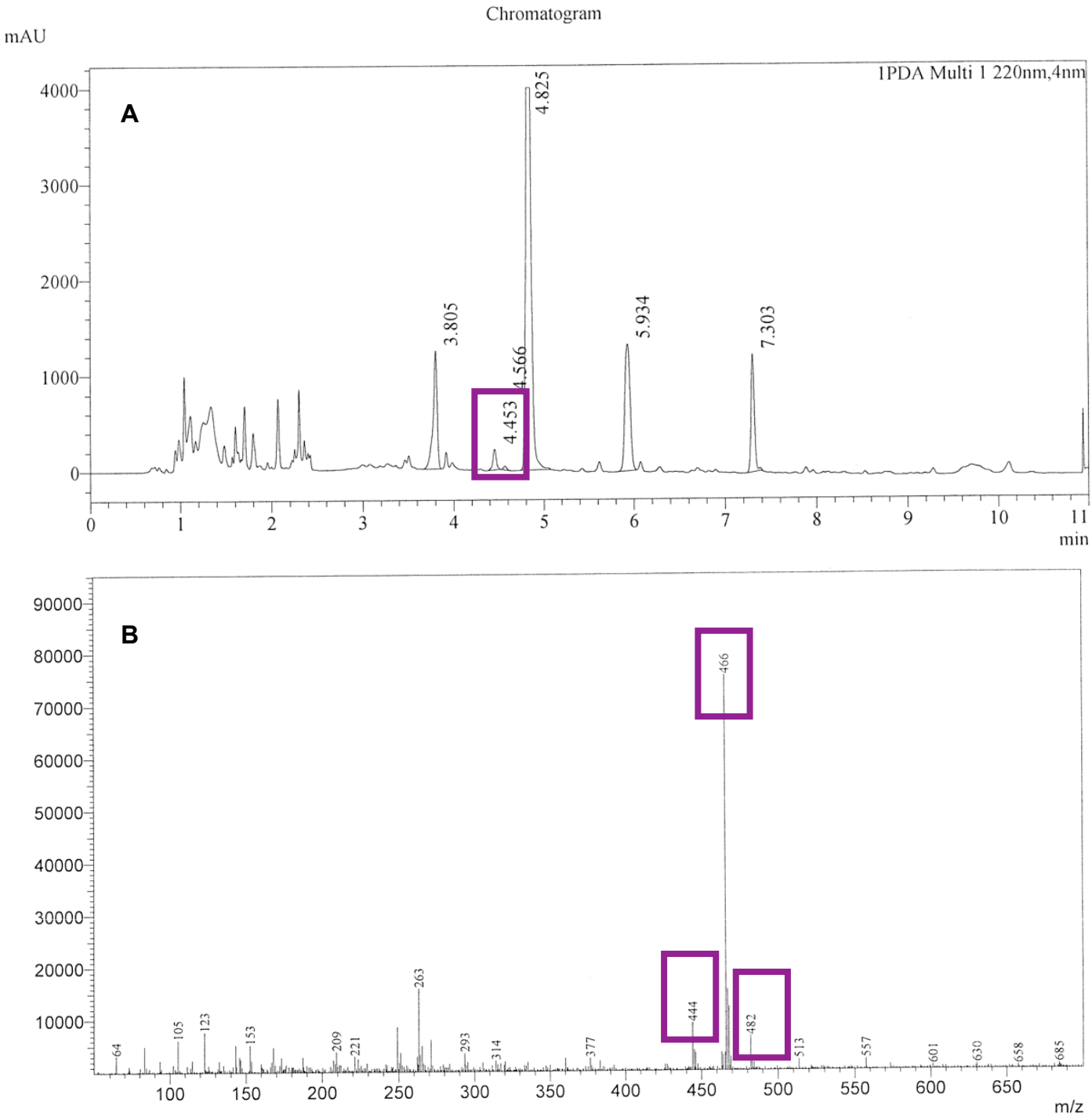

Figure 27: HPLC-MS results of *K. oxytoca* Mut1145 cell lysate *n*-butanol extract.
A: UV chromatogram (220 nm) of the HPLC analysis as a function of intensity over time. The highlighted peak at 4.4 min retention time is characteristic for the *K. oxytoca* cytotoxin and identified a substance of similar polarity in the extract.
B: Mass spectrum of the eluate at 4.4 min retention time. Spectrum shows peak intensity as a function of mass to charge ratio. Peaks at 444 Da, 466 and 482 Da resemble a substance of 443 Da $+H^+$, $+Na^+$ or $+K^+$ respectively.

4.2.3.6. MTT assay of cell lysates

To evaluate whether cytotoxicity could also be seen for the intracellular substances, we performed a cytotoxicity screen of the cell lysates of *K. oxytoca* wild type and *K. oxytoca ΔnpsA*. Cell lysates were prepared like conditioned supernatant (3.10.1) and HEp-2 cells were incubated with dilutions of 1:9, 1:27 and 1:81. In the MTT assay all samples exhibited cytotoxic properties, likely due to LPS components in the cell lysate. No information regarding the specific cytotoxicity due to the toxin could be gained from this assay.

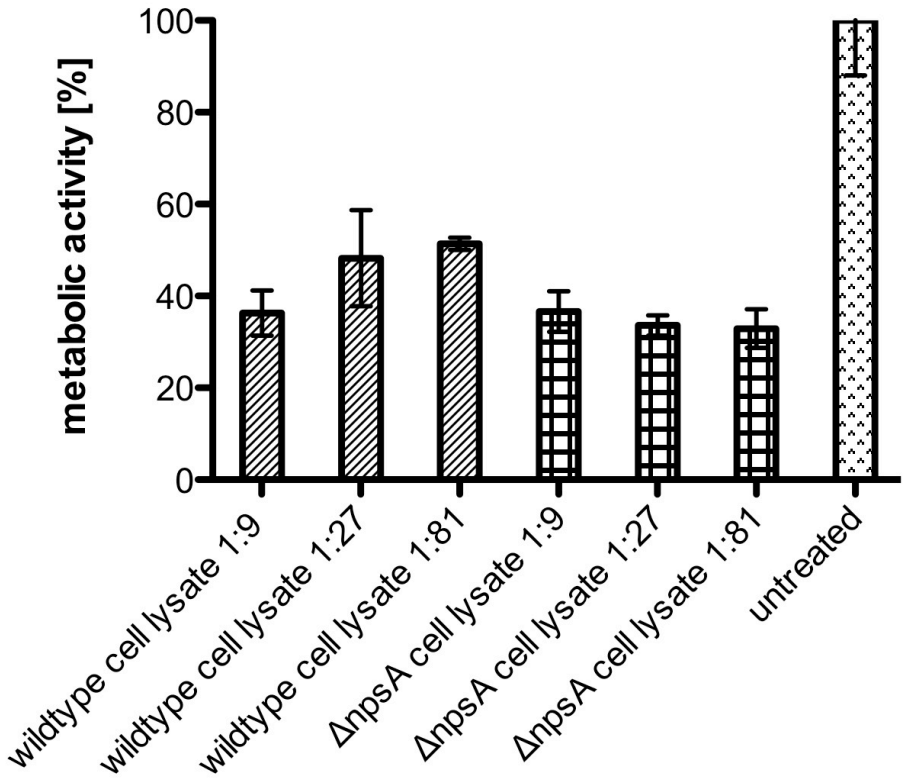

Figure 28: Cytotoxicity cell culture assay of *K. oxytoca* cell lysates.
The relative metabolic activity of treated HEp-2 cells was analyzed in comparison to *K. oxytoca* wild type (toxigenic) and *K. oxytoca* ATCC (non-toxigenic). Filtered bacterial cell lysates were added at dilutions 1:9, 1:27 and 1:81. PBS treated HEp-2 cell metabolic activity was set to 100%. (n = 3)

4.2.3.7. In trans complementation of the *yncE* mutation

Complementation of the *yncE* mutation was attempted by providing the *yncE* wild type sequence in trans on a pACYC184 plasmid. Therefore, *yncE* was amplified from the *K. oxytoca* AHC-6 chromosome with primers 9 and 10 for pACYC184YncE construct, and primers 9 and 11 for a similar His-tagged construct. The inserts were then cut with BamHI and SalI and ligated into a correspondingly prepared vector. The constructs were amplified in *E.coli* DH5α and subsequently *K. oxytoca* Mut1145 were transformed with the complementation vectors. The tetracycline resistance cassette of pACYC184 was destroyed by the insertion of the YncEHis fragment, therefore transformants were selected based on their chloramphenicol resistance. pACYC184 is a low copy vector with about 15 copies per cell [66]. For complementation purposes, no amplification of the vector was carried out and the expression of the insert under the control of the *tetA* promoter was not induced.

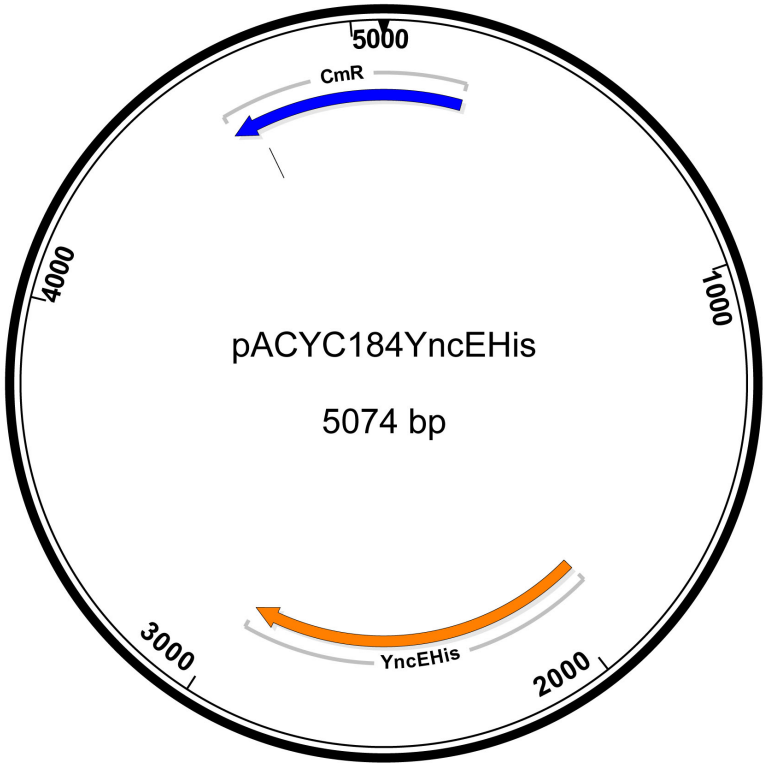

Figure 29: Plasmid map of complementation vector pACYC184YncEHis.
YncEHis insert was cloned into the plasmid via BamHI and SalI restriction sites thereby destroying the tetracyclin resistance cassette. CmR, chloramphenicol resistance marker.

The constructed strains were then checked in the cell culture assay for regained cytotoxicity. Cultures were incubated for 24 hours at 37°C and samples were collected in between at 16 hours and at the end of incubation time. Supernatant preparation and MTT assay were carried out as usual. Dilutions 1:3, 1:9, 1:27, 1:81, and 1:243 were tested. Figure 30 shows the comparison of 1:3 dilutions of *K. oxytoca* wild type, non-toxigenic *K. oxytoca* ATCC, *K. oxytoca* Mut1145 (*ΔyncE*), *K. oxytoca ΔyncE* pACYC184, *K. oxytoca ΔyncE* pACYC184YncE and *K. oxytoca ΔyncE* pACYC184YncEHis. Mut1145 with the complementation vector shows no cytotoxic phenotype meaning that no complementation was achieved.

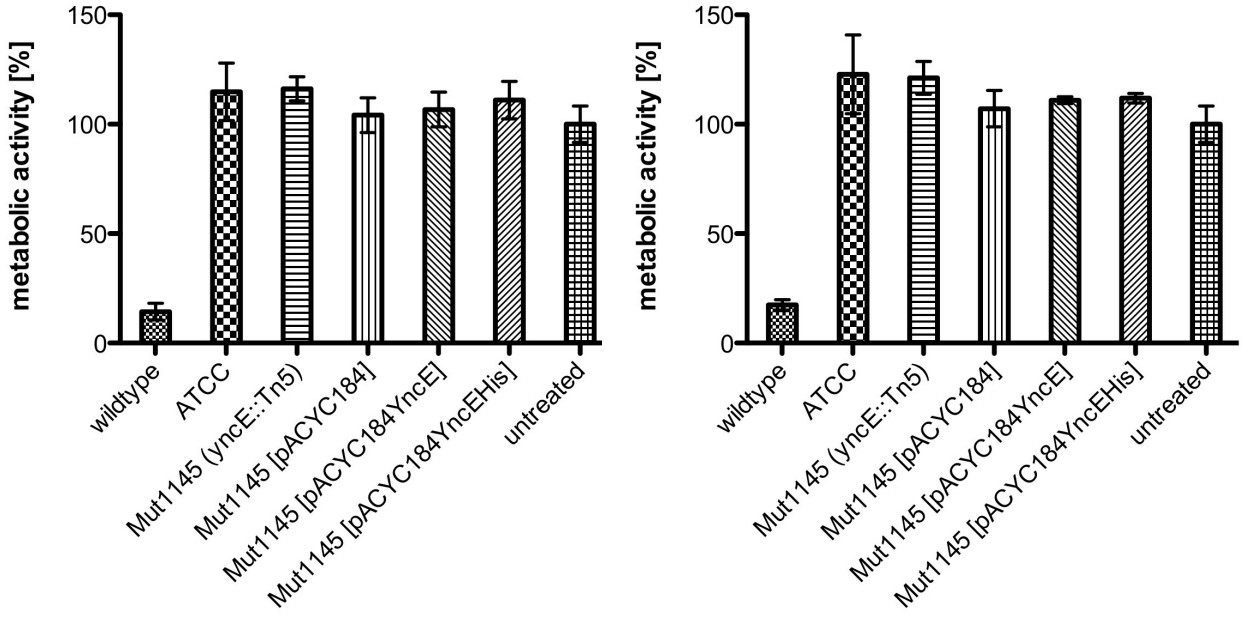

Figure 30: Cytotoxicity cell culture assay to test complementation of *K. oxytoca* Mut1145. Left: Supernatant after 16 hours of bacterial growth; Right: Supernatant after 24 hours of bacterial growth. The relative metabolic activity of treated HEp-2 cells was analyzed in comparison to *K. oxytoca* wildtype (toxigenic) and *K. oxytoca* ATCC (non-toxigenic). Supernatant was added at a 1:3 dilution. PBS treated HEp-2 cell metabolic activity was set to 100%. (n = 3)

To check whether the failed complementation was due to lack of expression of yncE from the complementation vector a Western Blot was performed. Samples for expression analysis were taken after 16 hours of incubation and prepared according to 3.9. As an experimental control NadRHis protein extract was run in parallel on the SDS gel. Protein bands were compared to a protein ladder for size estimation. The molecular weight for YncE was calculated to be approximately 38 kDa. Figure 31 shows an overlay of the resulting SDS gel and Western Blot. In the lane of Mut1145 with the YncEHis-construct complementation vector a band at ~35 kDa corresponding to the expected size of YncEHis is visible. Missing expression of YncE from the complementation plasmid could therefore not be the reason for unsuccessful complementation of the *yncE* mutation.

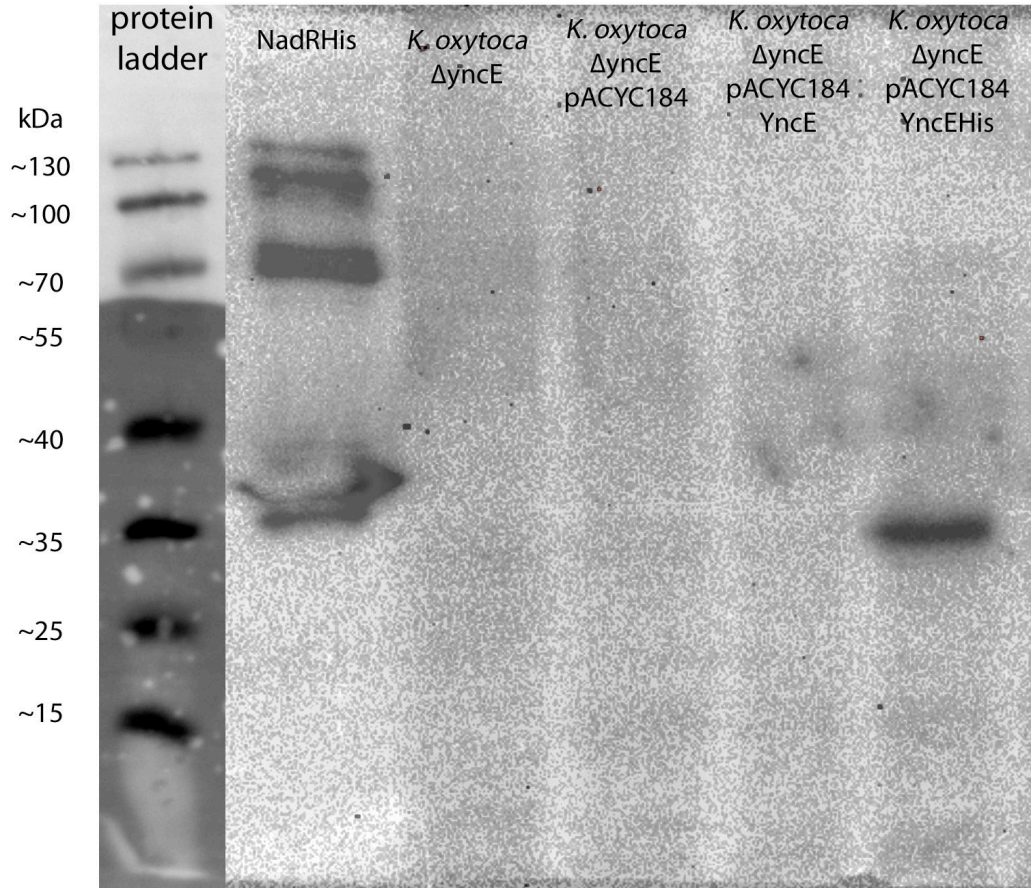

Figure 31: Overlay of SDS gel and Western Blot for detection of YncEHis from complementation vector pACYC184YncEHis.
Protein samples were taken after 16 hours of bacterial growth. Same amounts of protein (normalized by OD_{600}) were loaded in each lane on the SDS gel. After tank blotting proteins were visualized by anti-His-antibody and a secondary HRP-conjugated antibody followed by ECL detection. Size estimation was achieved by comparison to PageRuler Prestained Protein Ladder.

4.2.3.8. RT-PCR to check the expression of *yncE* and its neighbors

In *E. coli, yncE* is regulated by the Fe^{2+}-Fur complex and is de-repressed under iron restriction [38]. If the role of the *yncE* of *K. oxytoca* is similar to its *E. coli* homologue, its expression would be repressed under the conditions used for mutagenesis. We used RT-PCR to evaluate the expression of *yncE* in *K. oxytoca* under non-restrictive conditions to see if the expression profile resembles the one in *E. coli*.

4.2.3.8.1. Choosing the right targets

To check the expression of *yncE* itself, primers at the start and end of the coding sequence (CDS) were chosen (primers 9 and 10, Figure 32). As we also wanted to investigate the possibility of *yncE* and the putative outer membrane lipoprotein (OM LP) forming an operon, we created primers checking the expression of *OM LP* and a polycistronic mRNA (primers 19 and 20, and 18 and 20 respectively). Furthermore, the expression of *yncD* was checked as it is an important interaction protein of *yncE* in *E.coli* and probable regulatory elements could be located in the *yncE* CDS (primers 16 and 17).

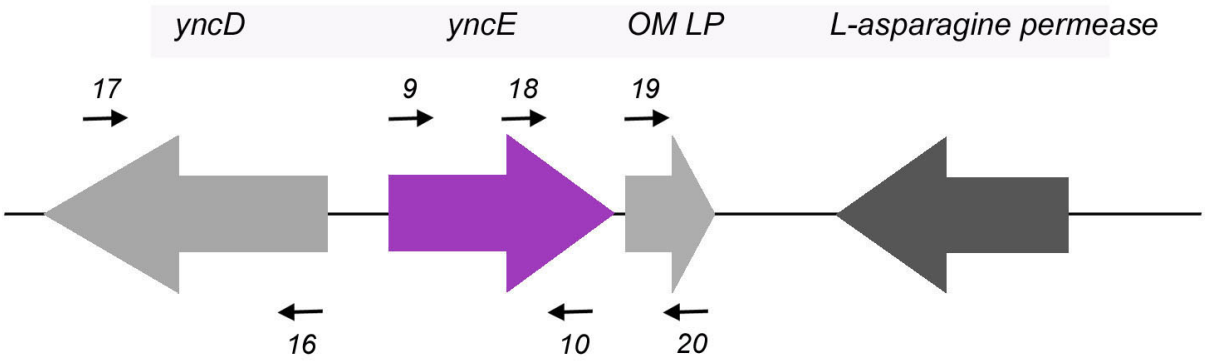

Figure 32: *yncE* genomic region with primers used in RT-PCR.
Primers according to Table 5

4.2.3.8.2. *yncE* is not expressed under replete conditions

RT-PCR was performed as described in 3.8. In short, *E. coli* MG1655, *K. oxytoca* AHC-6, and *K. oxytoca* Mut1145 were cultured in CASO medium and total RNA was extracted. After DNase I digestion, RNA was transcribed in cDNA using gene specific primers. *GAPDH* was used as an internal control. Table 6 summarizes the RT-PCR results. *E. coli*

yncE was not expressed under iron repletion. The same was true for *K. oxytoca* wild type *yncE* and understandably for the mutated form of Mut1145. Expression of *yncD* was not influenced by the *yncE* mutation as transcripts were generated in both *K. oxytoca* wild type and Mut1145. The downstream encoded *OM LP* was also expressed in both conditions and an operon structure of *yncE* and *OM LP* can be ruled out as no polycistronic mRNA was detected.

Table 6: Summary of expression analysis of *yncE* and adjacent genes by RT-PCR in *E. coli, K. oxytoca* wild type, and *K. oxytoca* Mut1145 (Δ*yncE*).
+...gene expressed; -...gene not expressed; n/a...expression not determined; (n = 3)

	yncE	*yncD*	*OM LP*	*yncE + OM LP*
***E. coli* MG1655**	-	n/a	n/a	n/a
***K. oxytoca* wildtype**	-	+	+	-
K. oxytoca* Δ*yncE	-	+	+	-

5. Discussion

5.1. Genotype allows prediction of cytotoxic phenotype

The PCR screen for PAI specific targets performed in this study resulted in a 100% correlation between occurrence of the targets on the *K. oxytoca* genome and exhibition of a cytotoxic phenotype. 15% of *K. oxytoca* strains scored positive for both targets but were negative in the cell culture assay. As the PCR screen did not cover the whole PAI but just representative targets, other parts could be missing in these strains. PAIs in general are more likely to be affected by point or deletion mutations so an event, in which this genetic loss happened to the discussed 15% of toxin-negative strains, is possible. In case, the PAI indeed confers growth advantages to the strains producing its encoded toxin, strains who are not in need of this fitness advantage can take the liberty to lose this phenotype. This could be case in a setting where two *K. oxytoca* strains colonize the same niche and the toxin production of one strain can rescue the other non-toxigenic one. Apart from possible mutation events, the PAI genes leading to the cytotoxic phenotype could also be turned off in these strains. Whether regulation of cytotoxin biosynthesis happens on transcriptional or on translational level and which signals trigger the turning-on and -off is not clear yet. Just like for other PBD gene clusters [67], regulation of the biosynthesis pathway is unclear. Sibiromycin and anthramycin gene clusters contain genes like *sibA* (a homologue to ORF25 in *S. refuineus*) and *sibX*, which show sequence similarity to transcriptional regulators. Thus biosynthesis regulation may take place on this level [56]. Animal models which address the question of the role of the cytotoxin are in progress but it is likely that toxin biosynthesis is a critical step in *K. oxytoca* virulence. Therefore the regulation of this pathway needs to be elucidated.

The screen for PAI specific targets could establish the link between genotype and phenotype as it is now clear that the biosynthesis genes are essential for ability to produce the cytotoxin. In the 15% of strains possessing the targets but not showing cytotoxicity in cell culture, the screen should be expanded to identify eventually missing PAI genes and narrow down the possibilities for the detected discrepancy between genotype and phenotype.

5.1.1. Speculating about a possible diagnostic PCR

The detected 100% correlation in toxin-positive strains between genotype and phenotype will be the basis for the development of a diagnostic multiplex PCR. The detection of species specific or virulence genes in clinical specimens like stool or sputum by PCR has been performed for various human pathogens like *Vibrio cholerae* [68], *Salmonella* [69], *E. coli* strains producing verotoxin or shiga-like toxins (SLT) [70, 71] and *C. difficile* [2]. These studies described various ways of DNA extraction from stool samples which would be the first crucial step for a *K. oxytoca* diagnostic PCR. For *Salmonella* for example, a two step protocol was described, starting with a 6 hours enrichment culture followed DNA extraction and PCR screen [69]. A similar protocol was used for *E. coli* SLT gene detection [71]. It was seen that an initial enrichment step enhanced the sensitivity of the PCR screen by increasing the amount of starting material and furthermore by dilution of inhibitors for *Taq* polymerase. Especially in fecal samples bile salts and bilirubin can lower the assay performance. This problem could be overcome by diluting the sample material e.g. in enrichment culture or by purification of the nucleic acids with fiber powder [72]. For the actual DNA extraction out of stool two main methods were used. The centrifugation method involved consecutive centrifugation steps with increasing speed yielding a pure bacterial pellet. The heat-lysis method was based on incubation of the resuspended specimen with lysozyme and Proteinase K followed by phenol-chloroform extraction [73]. More recent studies also showed DNA extraction with automated systems [74] and specialized kits are already available for purchase. All methods are possible for *K. oxytoca* PCR detection and need to be tested for optimal DNA yield. An enrichment step before DNA extraction should also be considered as in the described studies detection limits were as low as 200 bacteria per reaction mixture. This enrichment could be performed, for example, in CASO medium containing ampicillin to lower the background of microbiota. Additionally, this step would achieve a dilution of inhibitory substances. Use of a specific PCR protocol, called booster PCR, was shown to lower the detection limit to about 10 *E. coli* cells in the sample [75]. This protocol should be tested during establishment of the *K. oxytoca* PCR screen and evaluated against regular *Taq* DNA polymerase PCR. For *C. difficile,* nucleic acid amplification testing (NAAT) is becoming more prominent as commercially available tests have proven to be highly specific for *tcdB* and *tcdA* targets [2]. In general, NAAT is considered a promising clinical technique as it allows fast detection of microorganisms which is especially important for fastidious pathogens like *Mycobacterium tuberculosis.* Furthermore, rapid identification of the pathogen implies

better outcome for the patient and could also minimize inpatient stays thereby lowering number of patients at risk of nosocomial infections. The potential output of the *K. oxytoca* PCR screen needs to be discussed regarding their interpretation and consequential diagnoses. One of the biggest problems of a diagnostic PCR screen is the case of a negative result for the targets as this could be caused, in addition to the actual absence of the targets, also by methodic problems like insufficient starting material or high concentrations of inhibitory substances. Although the method can be optimized to work for the majority of samples, concentration variations in biological samples are common and can allow false negative results. On the other hand, false positive results are less likely to occur once a *K. oxytoca* species specific target is found. Additionally, the screen done in this study showed that no other *Klebsiella* spp was positive for either of the PAI targets. That indicates that a positive result for the PCR targets really identifies toxin-producing *K. oxytoca* in the patient‘s stool. The diagnostic PCR can be therefore applied in patients presenting with AAHC characteristic symptoms to clarify the presence of *K. oxytoca* in the stool. Furthermore, it can be used to help in the risk assessment of healthy carriers. Knowledge of the presence of toxin-producing *K. oxytoca* in their intestinal flora is useful when prescribing antibiotics. By avoiding penicillin antibiotics, the patients can be spared the likely side effect of development of an AAHC.

5.1.2. The quest for *K. oxytoca* species specific targets

The availability of a *K. oxytoca* species specific target is one of the requirements for the development of a diagnostic multiplex PCR making use of the correlation found between occurence of PAI genes and cytotoxin production. In the PCR screen performed in this study, an internal control targeting the 16S rDNA of *Klebsiella* was used and yielded positive results for all *Klebsiella* species tested. Classification of the tested strains as *Klebsiella* spp was done in earlier studies in the Zechner lab [61] mainly based on 16S rDNA sequencing, API 20E testing and indole reaction results. *K. oxytoca* can be distinguished from *K. pneumoniae* by the ability to produce indole from tryptophan, a reaction catalyzed by tryptophanase. However, about 9% of clinical isolates of indole-positive *Klebsiella* sp. belong to *K. planticola* species [76]. Studies have shown that differentiation between *K. oxytoca* and *K. planticola* could be achieved by the utilization of melezitose and the fail to utilize 3-hydroxybutyrate by *K. oxytoca*. These carbon substrate assimilation tests however are not standard in diagnostic laboratories. A discrimination of indole-positive *Klebsiella* was also attempted by a PCR screen for the ß-lactamase

bla$_{OXY-1}$ and *bla*$_{OXY-2}$ gene. It was shown that all *K. oxytoca* strains were positive for either of the targets while *K. planitocola* contained neither gene [77, 78]. As this method was only used to distinguish indole-positive *Klebsiella* sp. it required preliminary work and the *bla*$_{OXY-1}$ and *bla*$_{OXY-2}$ genes can not be used as *K. oxytoca* species specific targets without prior biochemical tests. Many other genes like *gyrA* and *parC* have been used to try to distinguish *K. oxytoca* but have failed due to insufficient specificity [79]. In 2003, a study suggested the identification of *K. oxytoca* using a PCR screen for the polygalacturonase *pehX* gene [63]. *K. oxytoca* differs from the rest of the *Klebsiella* sp. by its capability to degrade pectate. The polygalacturonase cleaves a polygalacturonic chain of demethoxylated pectin and is probably used by *K. oxytoca* in the environment to penetrate into the root tissue of plants [80]. The PCR screen of the study in 2003 resulted in the amplification of a 344 bp sequence of the *pehX* gene in all *K. oxytoca* strains tested and was negative for other *Klebsiella* sp. as well as for pectolytic *Erwinia* sp. strains. A recent study done in the Zechner lab [61] used the same primers (PEH-C and PEH-D) as suggested by the study of Kovtunovych [63] to identify *K. oxytoca*. Contrary to the earlier published study, we obtained inconsistent results for 10% of the 143 screened *Klebsiella* strains, either false positive or false negative signals. Template sequence for the primers used was the *pehX* gene sequence of *K. oxytoca* VN13 (accession number: AY065648). A BLAST homology search against the *K. oxytoca* AHC-6 genome revealed 89% identity of the two *pehX* genes. Primers PEH-C and PEH-D show mismatches of 2 bases when compared to *K. oxytoca* AHC-6 which might have led to possible false negative results.

For this study new *pehX* primers were created (primers 21 and 22 in Table 5), binding in regions of 100% homology between the *pehX* of *K. oxytoca* VN13 and *K. oxytoca* AHC-6. In a preliminary screen all *K. oxytoca* strains tested were postitive for the 653 bp amplicon while other *Klebsiella* species strains tested negative. This screen has yet to be extended to a larger number of strains and repeated to get significant data.

5.2. Proof for the potential of transposon mutagenesis

The miniTn5 based mutagenesis used in this study proved again to be a fast and powerful tool to detect genes involved in a certain phenotype. The single steps leading to the identification of loss of cytotoxicity mutants in *K. oxytoca* have been established earlier in the Zechner lab [42]. In the present study it could be reconfirmed that efficient conjugational transfer of the transposon vector pRL27 was achieved as conjugation frequencies were comparable to the ones obtained before. Also, chromosomal DNA extraction and plasposon rescue could generate sufficient DNA yield to guarantee for reliable gene sequencing. With the *K. oxytoca* AHC-6 genome at hand, identification of affected genes in the mutants could be done faster. BLAST homology search was only needed to identify the function of the second Tn mutant (Mut1145) generated in the study as the *npsA* gene affected in Mut873 was already characterized.

5.2.1. The *K. oxytoca* toxin gene cluster as a horizontally acquired PAI

Altogether up to now, this transposon mutagenesis approach yielded 6 loss of cytotoxicity mutants. 3 of them hit genes in the 20 kb toxin gene cluster of *K. oxytoca* which only makes up 0.3 % of the genome. Thus, the probability of random transposon integration into the same small portion of the genome is fairly small (0,00 00 7334%).

This added to the evidence of the identified toxin gene cluster being a PAI which is a hotspot for transposon mutagenesis. PAIs are known to show higher rates of mutations indicating a higher intrinsic genetic instability [54]. The tRNAs which are often flanking PAIs and are also found at the borders of the toxin gene cluster in *K. oxytoca* are thought to facilitate those mutational events [54]. Among the mutational events, loss of parts or the whole PAI is also commonly seen. In the case of *K. oxytoca,* loss of the whole island can be observed when comparing the AHC-6 genome to the *K. oxytoca* KCTC1686 genome. The recently published whole genome sequence of KCTC1686 (GenBank ID: CP003218.1) supported our assumption of the PAI of *K. oxytoca* AHC-6 as a horizontally acquired genetic element. We compared the tRNAs and the core genome sequences flanking the toxin gene cluster by BLAST search.Interestingly, in the KCTC 1686 strain the toxin gene cluster is missing but another genomic island of about 70 kb was inserted between the same asparagine tRNAs encoding for example parts of a type IV secretion

system or the MazEF toxin-antitoxin operon. In *K. pneumoniae* strains the sequence between asparagine tRNAs is known to be taken by genomic islands encoding secretion systems and sometimes virulence factors like yersiniabactin [81]. The high homology and similar GC content of the NRPSs genes with *Streptomyces* spp genes and the fact that both, *K. oxytoca* and *Streptomyces,* are soil bacteria could give a hint for the genetic origin of the PAI. The probable spontaneous loss of the PAI could be detected in the PCR screen done in this study. A follow-up isolate of the toxigenic *K. oxytoca* AHC-6 strain, used as wild type strain throughout this study, scored negatively in the cytotoxicity cell culture assay. Pulsed field gel electrophoresis analysis performed earlier in the Zechner lab showed identical fingerprints for the two isolates [61]. In the PCR screen, the follow-up isolate AHC 6-2 did not show any of the PAI specific amplicons indicating a spontaneous loss of the PAI within the same *K. oxytoca* isolate, a mechanism which is common for PAIs as an adaption to the environment.

5.2.2. *yncE* and its disguised role for *K. oxytoca* cytotoxicity

5.2.2.1. What *E. coli* tells us

The identification of the *yncE* homologue as the affected gene of Mut1145 posed the question of the *yncE* gene function in general. Information was only available for the *E. coli* homologue (79% homology according to blastx search) and placed *yncE* in the context of iron regulation and transport. Structural analysis performed with YncE identified seven YVTN ß-propeller motifs [65]. Proteins containing these motifs are solely implicated in alcohol catabolism. A global study done on iron-dependent genes in *E. coli* revealed a putative new iron-uptake pathway consisting of the divergently arranged genes *yncD*, a probable TonB-dependent OM receptor and *yncE*, which is thought to be a periplasmic oxidase [38]. The proposed iron transport pathway via YncE/YncD is shown in Figure 33. YncD serves as an OM transporter requiring energy in the form of proton motive force which is transduced to the OM via the TonB-ExbB-ExbD complex [82]. Once the siderophore with bound Fe^{3+} is transported into the periplasm, further steps require a periplasmic binding protein which is likely to be the function of YncE. Sec-dependent secretion of YncE into the periplasm has been shown [83]. After transport across the inner membrane, Fe^{3+} is reduced to Fe^{2+} which serves as a regulator for many signaling processes.

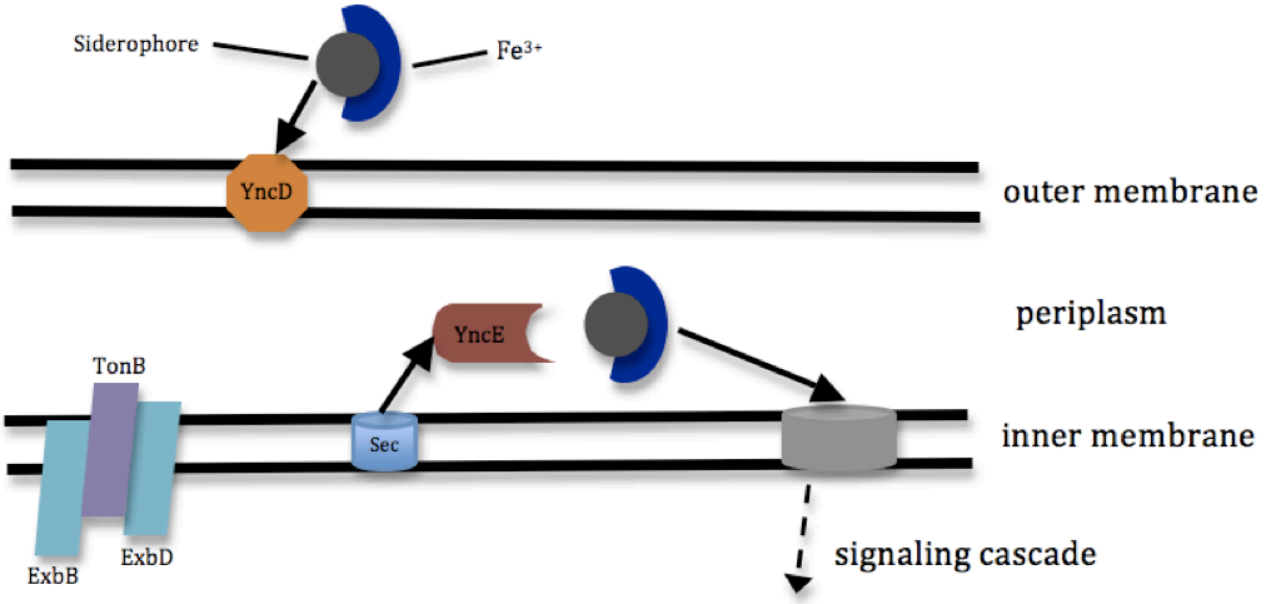

Figure 33: Illustration of the possible iron-uptake pathway of YncE
Figure based on [82]

Both genes, *yncD* and *yncE*, are regulated by the Fur protein. Under iron-replete conditions a dimer of Fur in complex with Fe^{2+} binds to a consensus DNA sequence leading to the prevention of gene transcription. Fur has been found to not only regulate genes involved in iron transport but also metabolic pathways and virulence genes like the SLT [39]. In *Klebsiella pneumoniae,* Fur regulation includes CPS genes [37]. For *E. coli yncE,* 18-fold repression is shown under iron replete conditions. The Fur box, the DNA binding site of the Fur dimer, was initially thought to be a 19 bp consensus sequence (5‘-GATAATGATAATCATTATC-3‘) found up to 200 bp upstream of Fur regulated genes [84]. This sequence was not found in a scanned sequence of up to 500 bases of the *yncE* gene in *K. oxytoca,* contradicting the hypothesis of a Fur regulation similar to *E. coli yncE*. Other studies have shown that also overlapping binding sites are recognized by Fur and that even indirect regulation via Fur is possible [84, 85]. For *Klebsiella pneumoniae,* it was recently shown that Fur shows flexibility with respect to its recognition site. Fur boxes with only 13 out of the 19 Fur box consensus bases have been detected [37]. This again renders possible the presence of such a modified Fur box upstream of *yncE* in *K. oxytoca*. In fact, a 19-bp-sequence motif found 106 bases upstream of the *yncE* CDS is identical in 13 of the 19 Fur box consensus bases. Therefore, regulation of *yncE* by Fur is likely.

5.2.2.2. What could *yncE* do in *K. oxytoca*?

After identification of *yncE* to be the affected gene in the loss of cytotoxicity mutant Mut1145, two possible roles for *K. oxytoca* cytotoxicity were hypothesized. Either *yncE* was implicated in the toxin transport, being located periplasmatically and also involved in the transport of iron, or *yncE* was involved in the regulation of toxin production, for example by being part of a signal transduction cascade which controls the transcription of genes essential for toxin biosynthesis. From previous studies done in the Zechner lab we knew that iron starvation did not alter the cytotoxic phenotype of *K. oxytoca* AHC-6 [61], therefore a decrease of intracellular iron due to the *yncE* mutation could be excluded as the reason for loss of cytotoxicity.

The possible transport function was investigated by looking for the toxin or toxin precursors intracellularly. HPLC/MS analyses done in this study could detect the cytotoxic substance in *K. oxytoca* AHC-6 wildtype by identifying a substance which elutes at 4.4 min from the HPLC column just like the cytotoxic substance from the *K. oxytoca* supernatant. The intracellular substance also showed identical mass-to-charge ratio peaks at 334 Da and 372 Da. For the *yncE* mutant, no cytotoxic substance was present in the supernatant which corresponds with the loss of cytotoxicity result of the cell culture assay. The HPLC chromatogram of the cell lysate of Mut1145 showed a peak at the mentioned retention time of 4.4 min. Given that HPLC separation is achieved according to polarity of the substances, we could infer that a substance of analog polarity is located intracellularly in Mut1145. The mass spectrum of this eluate revealed peaks which indicate the presence of a 443 Da substance. Thus, Mut1145 produced a 110 Da larger substance of similar polarity that could not be found in the wildtype strain. Preparative HPLC which allowed more precise information about the polarity, showed a slight difference between the two substances of different mass. If the 443 Da substance is a derivate of the cytotoxic substance, the polarity difference is explainable by the modification that also causes the mass difference of 110 Da. As we do not know how the toxin is modified inside the cell, prediction of the identity of the 110 Da modification is difficult. High-resolution mass spectrometry could help in the elucidation of this question by providing a molecular formula in which the known formula of the cytotoxic substance could be fit in. Keeping in mind the roles of *yncE* in *E. coli*, the modification of the substance could either be directly accomplished by YncE for example involving alcoholic residues or *yncE* could be involved in a signal transduction cascade leading to the modification of the cytotoxin. Unfortunately,

purification of small amounts of the 443 Da substance via preparative HPLC failed, so far making further structural analyses impossible.

We were also interested in the role of YncE as a regulator of cytotoxin biosynthesis. As the complementation of the mutation in trans did not work although YncEHis was expressed from the complementation vector, we started to investigate the expression pattern of *yncE* itself and the possibility of a polar effect of the mutation. *yncE* in *E. coli* is derepressed under iron depletion. If *K. oxytoca yncE* has a similar function and regulation, it should not be expressed under repletion conditions. RT-PCR analysis was performed comparing the expression patterns of *yncE* and the neighbouring genes *yncD* and the outer membrane lipoprotein. As the gene organization of *OM LP* and *yncE* would allow for an operon structure and the *yncE* mutation could then have a polar effect, the existence of a polycistronic mRNA was also checked. The RT-PCR results showed that *yncE* in *K. oxytoca* was not expressed under iron repletion similarly to its *E. coli* homologue. In contrast, the *OM LP* was transcribed in all conditions. It appears that *OM LP* is transcribed independently of *yncE*.. Also, *yncD* was expressed under the given conditions. Taken together, the mutation in *yncE* did not affect the neighboring genes ruling out a polar effect. Therefore, the loss of cytotoxicity is unlikely to be due to the missing *yncE* gene product, but has a more complex background. It could be that because of the integration of the transposon cassette, a sterical change in the DNA was induced, causing the modified phenotype. It could also be that the transcript of *yncE* serves as a noncoding RNA (ncRNA) which acts in cis or in trans as a regulator of expression of genes necessary for toxin synthesis. The insertion of the cassette in the *yncE* CDS could have disrupted this ncRNA and a complementation in trans in these cases is often not possible. Lastly, the complementation could have also failed due to a copy problem, as the amount of YncE expressed from the vector might have been too high for physiological conditions. The most important step to elucidate the *yncE* function would be therefore to create a deletion mutant of yncE, allowing to clarify the role of the cassette insertion in the mutated phenotype. Complementation could then also be reattempted with a vector encoding *yncE* under its own promotor to guarantee physiological amounts in the cell. Furthermore, the regulatory role of *yncE* on toxin biosynthesis could be elucidated by checking the expression of genes of the toxin gene cluster with RT-PCR in the wild type versus the mutant background.

As the alignment of the consensus sequence of the Fur box with the upstream regions of *yncE* revealed a putative Fur box with low identity (13 of 19 positions), expression regulation of *yncE* by iron was suspected. We tried to analyze the expression of *yncE*

under different iron concentrations, but the results under iron depletion were inconsistent also with respect to the internal controls used (data not shown). Further work needs to be done to elucidate the role of iron limitation in *yncE* expression in *K. oxytoca.*

A recent study [86] demonstrated that *yncD,* which is an in vivo-induced antigen, has an essential role in *Salmonella* survival inside the murine host. As (the divergently transcribed) YncD works together with YncE in the iron uptake pathway, an influence of YncE on *Salmonella* virulence was implied. The nature of the virulence pathway has not been elucidated yet. Importantly however, the link between the YncD/E system and virulence was made, which could also be seen in *K. oxytoca* Mut1145.

With the current state of knowledge no clear function for *yncE* in the process of toxin production or transport can be identified and further analyses need to be done to address this question.

6. Conclusion

In this study the characterization of the molecular basis for *K. oxytoca* cytotoxin production was extended. The correlation between the presence of the identified PAI on the genome of a toxigenic *K. oxytoca* isolate and cytotoxin production was studied with a PCR screen targeting PAI specific genes. All cytotoxin-producing isolates tested were positive for both targets, resulting in a 100% correlation between genotype and phenotype. By contrast, neither of the targets was detectable in 85% of toxin-negative *K. oxytoca* strains. No other *Klebsiella* spp tested positive for either of the targets. The results are the basis for a possible diagnostic multiplex PCR screen that could also help in the risk assessment of healthy carriers. A requirement for the diagnostic screen is a *K. oxytoca* species specific target. The *pehX* polygalacturonase gene is a promising candidate and is currently under investigation.

As the genes encoded in the toxin gene cluster of *K. oxytoca* do not provide sufficient information about toxin secretion or modification of the cytotoxic substance or its precursors, transposon mutagenesis was continued in this study. A total of 6 loss of cytotoxicity mutants have been obtained. One of the mutants of this study affected a NRPS gene on the PAI, strengthening the idea of the PAI as a horizontally acquired genetic element which shows a higher degree of genetic instability compared to the core genome. The second loss of cytotoxicity mutation affected a gene homologous to the *yncE* gene of *E. coli* that is involved in TonB-dependent iron uptake and repressed under iron repletion. RT-PCR results showed a similar expression pattern for *yncE* of *K. oxytoca* and ruled out a polar effect of the mutation. HPLC/MS analyses detected a 110 Da larger substance than the cytotoxin in the *yncE* mutant which is of similar polarity, suggesting a modified version of the cytotoxin. High resolution mass spectrometry needs to be done to identify this substance. As also the complementation of *yncE* in trans failed, the role for *yncE* in loss of cytotoxicity is still open. As the next step a deletion mutant should be created and expression pattern of the PAI genes in the mutant background need to be investigated.

7. References

1. Hogenauer, C., et al., *Mechanisms and management of antibiotic-associated diarrhea.* Clin Infect Dis, 1998. **27**(4): p. 702-10.

2. Karen C, C. and B. John G, *Biology ofClostridium difficile: Implications for Epidemiology and Diagnosis.* Annual Review of Microbiology, 2011. **65**(1): p. 501-521.

3. Davies, Abigail H., et al., *Super toxins from a super bug: structure and function ofClostridium difficiletoxins.* Biochemical Journal, 2011. **436**(3): p. 517-526.

4. Kelly, C.P., C. Pothoulakis, and J.T. LaMont, *Clostridium difficile colitis.* N Engl J Med, 1994. **330**(4): p. 257-62.

5. Bartlett, J.G., *Clostridium difficile-associated Enteric Disease.* Curr Infect Dis Rep, 2002. **4**(6): p. 477-483.

6. Toffler, R.B., E.G. Pingoud, and M.I. Burrell, *Acute colitis related to penicillin and penicillin derivatives.* Lancet, 1978. **2**(8092 Pt 1): p. 707-9.

7. Hogenauer, C., et al., *Klebsiella oxytoca as a causative organism of antibiotic-associated hemorrhagic colitis.* N Engl J Med, 2006. **355**(23): p. 2418-26.

8. Zollner-Schwetz, I., et al., *Role of Klebsiella oxytoca in antibiotic-associated diarrhea.* Clin Infect Dis, 2008. **47**(9): p. e74-8.

9. Beaugerie, L., et al., *Klebsiella oxytoca as an agent of antibiotic-associated hemorrhagic colitis.* Clin Gastroenterol Hepatol, 2003. **1**(5): p. 370-6.

10. Sakurai, Y., et al., *Acute right-sided hemorrhagic colitis associated with oral administration of ampicillin.* Dig Dis Sci, 1979. **24**(12): p. 910-5.

11. Minami, J., et al., *Enterotoxic activity of Klebsiella oxytoca cytotoxin in rabbit intestinal loops.* Infect Immun, 1994. **62**(1): p. 172-7.

12. Minami, J., et al., *Production of a unique cytotoxin by Klebsiella oxytoca.* Microb Pathog, 1989. **7**(3): p. 203-11.

13. Minami, J., et al., *Biological activities and chemical composition of a cytotoxin of Klebsiella oxytoca.* J Gen Microbiol, 1992. **138**(9): p. 1921-7.

14. Higaki, M., et al., *Cytotoxic component(s) of Klebsiella oxytoca on HEp-2 cells.* Microbiol Immunol, 1990. **34**(2): p. 147-51.

15. Joainig, M.M., et al., *Cytotoxic Effects of Klebsiella oxytoca Strains Isolated from Patients with Antibiotic-Associated Hemorrhagic Colitis or Other Diseases Caused by Infections and from Healthy Subjects.* Journal of Clinical Microbiology, 2010. **48**(3): p. 817-824.

16. Madigan, M.T., *Brock biology of microorganisms*. 13th ed2012, San Francisco: Benjamin Cummings. xxviii, 1043, 77 p.

17. Kayser, F.H., *Medical microbiology*2005, Stuttgart ; New York, NY: Georg Thieme Verlag. xxvi, 698 p.

18. Podschun, R. and U. Ullmann, *Klebsiella spp. as nosocomial pathogens: epidemiology, taxonomy, typing methods, and pathogenicity factors.* Clin Microbiol Rev, 1998. **11**(4): p. 589-603.

19. Selden, R., et al., *Nosocomial klebsiella infections: intestinal colonization as a reservoir.* Ann Intern Med, 1971. **74**(5): p. 657-64.

20. Johnson, J.G. and S. Clegg, *Role of MrkJ, a Phosphodiesterase, in Type 3 Fimbrial Expression and Biofilm Formation in Klebsiella pneumoniae.* Journal of Bacteriology, 2010. **192**(15): p. 3944-3950.

21. Hart, C.A., *Klebsiellae and neonates.* J Hosp Infect, 1993. **23**(2): p. 83-6.

22. Tullus, K., et al., *Nationwide spread of Klebsiella oxytoca K55 in Swedish neonatal special care wards.* APMIS, 1992. **100**(11): p. 1008-14.

23. Gupta, A., *Hospital-acquired infections in the neonatal intensive care unit--Klebsiella pneumoniae.* Semin Perinatol, 2002. **26**(5): p. 340-5.

24. Smith, J.M. and S.T. Chambers, *Klebsiella oxytoca revealing decreased susceptibility to extended spectrum beta-lactams.* J Antimicrob Chemother, 1995. **36**(1): p. 265-7.

25. Livermore, D.M., *beta-Lactamases in laboratory and clinical resistance.* Clin Microbiol Rev, 1995. **8**(4): p. 557-84.

26. Podschun, R., I. Penner, and U. Ullmann, *Interaction of Klebsiella capsule type 7 with human polymorphonuclear leucocytes.* Microb Pathog, 1992. **13**(5): p. 371-9.

27. Ofek, I., et al., *Nonopsonic phagocytosis of microorganisms.* Annu Rev Microbiol, 1995. **49**: p. 239-76.

28. Schembri, M.A., et al., *Capsule and fimbria interaction in Klebsiella pneumoniae.* Infect Immun, 2005. **73**(8): p. 4626-33.

29. Babu, J.P., et al., *Interaction of a 60-kilodalton D-mannose-containing salivary glycoprotein with type 1 fimbriae of Escherichia coli.* Infect Immun, 1986. **54**(1): p. 104-8.

30. Sebghati, T.A., et al., *Characterization of the type 3 fimbrial adhesins of Klebsiella strains.* Infect Immun, 1998. **66**(6): p. 2887-94.

31. Schurtz, T.A., et al., *The type 3 fimbrial adhesin gene (mrkD) of Klebsiella species is not conserved among all fimbriate strains.* Infect Immun, 1994. **62**(10): p. 4186-91.

32. Ong, C.-l.Y., et al., *Molecular analysis of type 3 fimbrial genes from Escherichia coli, Klebsiella and Citrobacter species.* BMC Microbiology, 2010. **10**(1): p. 183.

33. Benge, G.R., *Bactericidal activity of human serum against strains of Klebsiella from different sources.* J Med Microbiol, 1988. **27**(1): p. 11-5.

34. Merino, S., et al., *Mechanisms of Klebsiella pneumoniae resistance to complement-mediated killing.* Infect Immun, 1992. **60**(6): p. 2529-35.

35. Lawlor, M.S., C. O'Connor, and V.L. Miller, *Yersiniabactin Is a Virulence Factor for Klebsiella pneumoniae during Pulmonary Infection.* Infection and Immunity, 2007. **75**(3): p. 1463-1472.

36. Podschun, R., A. Fischer, and U. Ullmann, *Siderophore production of Klebsiella species isolated from different sources.* Zentralbl Bakteriol, 1992. **276**(4): p. 481-6.

37. Lin, C.T., et al., *Fur regulation of the capsular polysaccharide biosynthesis and iron-acquisition systems in Klebsiella pneumoniae CG43.* Microbiology, 2010. **157**(2): p. 419-429.

38. McHugh, J.P., *Global Iron-dependent Gene Regulation in Escherichia coli: A NEW MECHANISM FOR IRON HOMEOSTASIS.* Journal of Biological Chemistry, 2003. **278**(32): p. 29478-29486.

39. Calderwood, S.B. and J.J. Mekalanos, *Iron regulation of Shiga-like toxin expression in Escherichia coli is mediated by the fur locus.* J Bacteriol, 1987. **169**(10): p. 4759-64.

40. de Lorenzo, V. and K.N. Timmis, *Analysis and construction of stable phenotypes in gram-negative bacteria with Tn5- and Tn10-derived minitransposons.* Methods Enzymol, 1994. **235**: p. 386-405.

41. Larsen, R.A., et al., *Genetic analysis of pigment biosynthesis in Xanthobacter autotrophicus Py2 using a new, highly efficient transposon mutagenesis system that is functional in a wide variety of bacteria.* Arch Microbiol, 2002. **178**(3): p. 193-201.

42. Schneditz, G.T., *Genetic Analysis of Klebsiella oxytoca Cytotoxin Production.* Master Thesis, 2010. **1**.

43. Schwarzer, D., R. Finking, and M.A. Marahiel, *Nonribosomal peptides: from genes to products.* Nat Prod Rep, 2003. **20**(3): p. 275-87.

44. Marahiel, M.A., *Working outside the protein-synthesis rules: insights into non-ribosomal peptide synthesis.* J Pept Sci, 2009. **15**(12): p. 799-807.

45. Marahiel, M.A., T. Stachelhaus, and H.D. Mootz, *Modular Peptide Synthetases Involved in Nonribosomal Peptide Synthesis.* Chem Rev, 1997. **97**(7): p. 2651-2674.

46. Schneditz, G.T., unpublished data, 2012.

47. Arima, K., et al., *Studies on tomaymycin, a new antibiotic. I. Isolation and properties of tomaymycin.* J Antibiot (Tokyo), 1972. **25**(8): p. 437-44.

48. Nishioka, Y., et al., *Mode of action of tomaymycin.* J Antibiot (Tokyo), 1972. **25**(11): p. 660-7.

49. Gerratana, B., *Biosynthesis, synthesis, and biological activities of pyrrolobenzodiazepines.* Medicinal Research Reviews, 2010: p. n/a-n/a.

50. Thurston, D.E., et al., *Effect of A-ring modifications on the DNA-binding behavior and cytotoxicity of pyrrolo[2,1-c][1,4]benzodiazepines.* J Med Chem, 1999. **42**(11): p. 1951-64.

51. Knapp, S., et al., *Large, unstable inserts in the chromosome affect virulence properties of uropathogenic Escherichia coli O6 strain 536.* J Bacteriol, 1986. **168**(1): p. 22-30.

52. Groisman, E.A. and H. Ochman, *Pathogenicity islands: bacterial evolution in quantum leaps.* Cell, 1996. **87**(5): p. 791-4.

53. Hacker, J. and E. Carniel, *Ecological fitness, genomic islands and bacterial pathogenicity. A Darwinian view of the evolution of microbes.* EMBO Rep, 2001. **2**(5): p. 376-81.

54. Schmidt, H. and M. Hensel, *Pathogenicity Islands in Bacterial Pathogenesis.* Clinical Microbiology Reviews, 2004. **17**(1): p. 14-56.

55. Walsh, C.T., *The chemical versatility of natural-product assembly lines.* Acc Chem Res, 2008. **41**(1): p. 4-10.

56. Li, W., et al., *Biosynthesis of Sibiromycin, a Potent Antitumor Antibiotic.* Applied and Environmental Microbiology, 2009. **75**(9): p. 2869-2878.

57. Hurley, L.H., *Pyrrolo(1,4)benzodiazepine antitumor antibiotics. Comparative aspects of anthramycin, tomaymycin and sibiromycin.* J Antibiot (Tokyo), 1977. **30**(5): p. 349-70.

58. Prieto, C., et al., *NRPSsp: non-ribosomal peptide synthase substrate predictor.* Bioinformatics, 2012. **28**(3): p. 426-7.

59. Mohr, N. and H. Budzikiewicz, *Tilivalline, a new pyrrolo[2, 1-c][1,4] benzodiazepine metabolite from klebsiella.* Tetrahedron, 1982. **38**(1): p. 147-152.

60. Kohda, K., et al., *Wide difference between the cytotoxicity of the 11-alpha-and 11-beta-cyano analogues of tilivalline and their epimeric conversion.* Biochem Pharmacol, 1995. **49**(8): p. 1063-8.

61. Joainig, M.M., *Molecular Characterization of Klebsiella oxytoca.* Dissertation, 2010. **1**.

62. Hurley, L.H., et al., *Pyrrolo[1,4]benzodiazepine antibiotics. Biosynthesis of the antitumor antibiotic sibiromycin by Streptosporangium sibiricum.* Biochemistry, 1979. **18**(19): p. 4225-9.

63. Kovtunovych, G., et al., *Identification of Klebsiella oxytoca using a specific PCR assay targeting the polygalacturonase pehX gene.* Res Microbiol, 2003. **154**(8): p. 587-92.

64. Boye, K. and D.S. Hansen, *Sequencing of 16S rDNA of Klebsiella: taxonomic relations within the genus and to other Enterobacteriaceae.* Int J Med Microbiol, 2003. **292**(7-8): p. 495-503.

65. Baba-Dikwa, A., et al., *Overproduction, purification and preliminary X-ray diffraction analysis of YncE, an iron-regulated Sec-dependent periplasmic protein fromEscherichia coli.* Acta Crystallographica Section F Structural Biology and Crystallization Communications, 2008. **64**(10): p. 966-969.

66. Sambrook, J. and D.W. Russell, *Molecular cloning : a laboratory manual*. 3rd ed2001, Cold Spring Harbor, N.Y.: Cold Spring Harbor Laboratory Press.

67. Li, W., et al., *Cloning and Characterization of the Biosynthetic Gene Cluster for Tomaymycin, an SJG-136 Monomeric Analog.* Applied and Environmental Microbiology, 2009. **75**(9): p. 2958-2963.

68. Albert, M.J., et al., *Rapid detection of Vibrio cholerae O139 Bengal from stool specimens by PCR.* J Clin Microbiol, 1997. **35**(6): p. 1633-5.

69. Chiu, C.H. and J.T. Ou, *Rapid identification of Salmonella serovars in feces by specific detection of virulence genes, invA and spvC, by an enrichment broth culture-multiplex PCR combination assay.* J Clin Microbiol, 1996. **34**(10): p. 2619-22.

70. Ramotar, K., et al., *Direct detection of verotoxin-producing Escherichia coli in stool samples by PCR.* J Clin Microbiol, 1995. **33**(3): p. 519-24.

71. Paton, A.W., et al., *Direct detection of Escherichia coli Shiga-like toxin genes in primary fecal cultures by polymerase chain reaction.* J Clin Microbiol, 1993. **31**(11): p. 3063-7.

72. Wilde, J., J. Eiden, and R. Yolken, *Removal of inhibitory substances from human fecal specimens for detection of group A rotaviruses by reverse transcriptase and polymerase chain reactions.* J Clin Microbiol, 1990. **28**(6): p. 1300-7.

73. Brian, M.J., et al., *Polymerase chain reaction for diagnosis of enterohemorrhagic Escherichia coli infection and hemolytic-uremic syndrome.* J Clin Microbiol, 1992. **30**(7): p. 1801-6.

74. Wolf, H., et al., *Diagnosis of pediatric pulmonary tuberculosis by stool PCR.* Am J Trop Med Hyg, 2008. **79**(6): p. 893-8.

75. Saulnier, P. and A. Andremont, *Detection of genes in feces by booster polymerase chain reaction.* J Clin Microbiol, 1992. **30**(8): p. 2080-3.

76. Monnet, D. and J. Freney, *Method for differentiating Klebsiella planticola and Klebsiella terrigena from other Klebsiella species.* J Clin Microbiol, 1994. **32**(4): p. 1121-2.

77. Fournier, B., et al., *Chromosomal beta-lactamase genes of Klebsiella oxytoca are divided into two main groups, blaOXY-1 and blaOXY-2.* Antimicrob Agents Chemother, 1996. **40**(2): p. 454-9.

78. Liu, Y., B.J. Mee, and L. Mulgrave, *Identification of clinical isolates of indole-positive Klebsiella spp., including Klebsiella planticola, and a genetic and molecular analysis of their beta-lactamases.* J Clin Microbiol, 1997. **35**(9): p. 2365-9.

79. Brisse, S. and J. Verhoef, *Phylogenetic diversity of Klebsiella pneumoniae and Klebsiella oxytoca clinical isolates revealed by randomly amplified polymorphic DNA, gyrA and parC genes sequencing and automated ribotyping.* Int J Syst Evol Microbiol, 2001. **51**(Pt 3): p. 915-24.

80. Kovtunovych, G., O. Lar, and N. Kozyrovska, *Cloning and structural analysis of the Klebsiella oxytoca VN13 peh gene.* Biopolymers and cell 2000. **16**(5): p. 356-363.

81. Bach, S., A. de Almeida, and E. Carniel, *The Yersinia high-pathogenicity island is present in different members of the family Enterobacteriaceae.* FEMS Microbiol Lett, 2000. **183**(2): p. 289-94.

82. Noinaj, N., et al., *TonB-Dependent Transporters: Regulation, Structure, and Function.* Annual Review of Microbiology, 2010. **64**(1): p. 43-60.

83. Baars, L., et al., *Defining the role of the Escherichia coli chaperone SecB using comparative proteomics.* J Biol Chem, 2006. **281**(15): p. 10024-34.

84. Lavrrar, J.L. and M.A. McIntosh, *Architecture of a Fur Binding Site: a Comparative Analysis.* Journal of Bacteriology, 2003. **185**(7): p. 2194-2202.

85. Chen, Z., et al., *Discovery of Fur binding site clusters in Escherichia coli by information theory models.* Nucleic Acids Research, 2007. **35**(20): p. 6762-6777.

86. Xiong, K., et al., *Deletion of yncD gene in Salmonella enterica ssp. enterica serovar Typhi leads to attenuation in mouse model.* FEMS Microbiol Lett, 2012. **328**(1): p. 70-7.

87. Neidhardt, F.C. and R. Curtiss, *Escherichia coli and Salmonella : cellular and molecular biology*. 2nd ed1996, Washington, D.C.: ASM Press.

88. Metcalf, W.W., et al., *Conditionally replicative and conjugative plasmids carrying lacZ alpha for cloning, mutagenesis, and allele replacement in bacteria.* Plasmid, 1996. **35**(1): p. 1-13.

89. Rose, R.E., *The nucleotide sequence of pACYC184.* Nucleic Acids Res, 1988. **16**(1): p. 355.

90. Woodcock, D.M., et al., *Quantitative evaluation of Escherichia coli host strains for tolerance to cytosine methylation in plasmid and phage recombinants.* Nucleic Acids Res, 1989. **17**(9): p. 3469-78.

8. Appendix

Table 7: *Klebsiella* spp. isolates used in this study

AAC, antibiotic associated colitis; AAHC, antibiotic associated hemorrhagic colitis; COPD, chronic obstructive pulmonary disease; CRSBI, catheter-related bloodstream infections; CSSTI, Complicated Skin and Soft Tissue Infection; DFS, diabetic foot syndrome; IBD, iinflammatory bowel disease; UTI, urinary tract infection

results of the cytotoxicity assay are indicated as + for toxin-producer and - for toxin-negative strains; PCR screen results show a + for presence of the target and - for absence

					PCR Screen		
Isolate collection #	**Species**	**Isolation Site**	**Diagnosis**	**Cytotoxic effect**	***npsB* target**	**integenic target**	**synonym**
1	*K. oxytoca*	stool	AAHC	+	+	+	
2	*K. oxytoca*	stool	AAHC	+	+	+	
3	*K. oxytoca*	laboratory strain		-	-	-	
4	*K. oxytoca*	laboratory strain		-	-	-	
5	*K. oxytoca*	stool	AAHC	~	+	+	
10	*K. oxytoca*	skin wound swab	DFS	+	+	+	
11	*K. oxytoca*	urine	complicated UTI	-	-	-	
12	*K. oxytoca*	respiratory culture	exacerbated COPD	-	-	-	

					PCR Screen		
Isolate collection #	**Species**	**Isolation Site**	**Diagnosis**	**Cytotoxic effect**	***npsB* target**	**integenic target**	**synonym**
15	*K. oxytoca*	skin wound swab	DFS	-	+	+	
16	*K. oxytoca*	respiratory culture	bronchiectasis	-	-	-	
17	*K. oxytoca*	stool	AAHC	-	-	-	
26	*K. oxytoca*	blood	CRBSI	+	+	+	
29	*K. oxytoca*	respiratory culture	pneumonia	+	+	+	
33	*K. oxytoca*	skin wound swab	CSSTI	-	-	-	
34	*K. oxytoca*	stool	AAHC	+	+	+	AHC-6
35	*K. oxytoca*	stool	diarrhea	-	-	-	
37	*K. oxytoca*	stool	asymptomatic carrier	+	+	+	
38	*K. oxytoca*	mucosal wound swab	conjunctivitis	-	+	+	
39	*K. oxytoca*	respiratory culture	pneumonia	-	-	-	
41	*K. oxytoca*	stool	diarrhea	-	-	-	
45	*K. oxytoca*	stool	remission	-	-	-	AHC-6-2
47	K. *ornitholytica*	stool	IBD	-	-	-	

					PCR Screen		
Isolate collection #	**Species**	**Isolation Site**	**Diagnosis**	**Cytotoxic effect**	***npsB* target**	**integenic target**	**synonym**
50	*K. oxytoca*	stool	diarrhea	-	-	-	
51	K. *ornitholytica*	stool	diarrhea	-	-	-	
56	*K. oxytoca*	stool	AAHC	+	+	+	
71	*K. oxytoca*	blood	CRBSI	+	+	+	
73	*K. oxytoca*	stool	asymptomatic carrier	-	-	-	
75	*K. oxytoca*	skin wound swab	DFS	-	-	-	
76	*K. oxytoca*	stool	AAHC	-	-	-	
77	*K. oxytoca*	stool	remission	+	+	+	
78	*K. oxytoca*	stool	IBD	-	-	-	
80	*K. oxytoca*	stool	AAC	+	+	+	
81	*K. oxytoca*	stool	asymptomatic carrier	+	+	+	
82	*K. oxytoca*	stool	IBD	-	-	-	
83	*K. oxytoca*	stool	AAC	+	+	+	
84	*K. oxytoca*	stool	AAC	-	-	-	

					PCR Screen		
Isolate collection #	**Species**	**Isolation Site**	**Diagnosis**	**Cytotoxic effect**	***npsB* target**	**integenic target**	**synonym**
85	K. *ornitholytica*	stool	hemorrhagic colitis	-	-	-	
88	*K. planticola*	stool	AAC	-	-	-	
91	*K. oxytoca*	stool	hemorrhagic colitis	+	+	+	
92	*K. oxytoca*	stool	IBD	-	-	-	
94	*K. pneumoniae*	stool	AAC	-	-	-	
96	*K. oxytoca*	stool	AAC	+	+	+	
103	*K. oxytoca*	stool	asymptomatic carrier	-	-	-	
105	*K. oxytoca*	skin wound swab	DFS	+	+	+	
106	*K. oxytoca*	mucosal wound swab	ulcus cruris	+	+	+	
107	*K. oxytoca*	skin wound swab	DFS	+	+	+	
109	*K. oxytoca*	skin wound swab	dermatitis	-	-	-	
111	*K. oxytoca*	stool	asymptomatic carrier	+	+	+	
112	*K. oxytoca*	stool	asymptomatic carrier	-	-	-	
113	*K. oxytoca*	stool	asymptomatic carrier	-	+	+	

					PCR Screen		
Isolate collection #	**Species**	**Isolation Site**	**Diagnosis**	**Cytotoxic effect**	***npsB* target**	**integenic target**	**synonym**
114	*K. oxytoca*	stool	AAC	-	+	+	
116	*K. oxytoca*	stool	AAHC	-	-	-	
117	*K. terrigena*	stool	AAC	-	-	-	
118	*K. oxytoca*	stool	AAHC	+	+	+	
119	*K. oxytoca*	stool	AAHC	+	+	+	
120	*K. oxytoca*	stool	AAC	-	-	-	
121	*K. oxytoca*	stool	AAC	-	-	-	
122	*K. oxytoca*	stool	follow-up colitis	+	+	+	
123	*K. oxytoca*	stool	follow-up colitis	+	+	+	
125	*K. oxytoca*	stool	AAHC	+	+	+	
128	*K. oxytoca*	stool	IBD	+	+	+	
131	*K. oxytoca*	stool	asymptomatic carrier	-	-	-	
133	*K. terrigena*	stool	diarrhea/AAD	-	-	-	
135	*K. pneumoniae*	stool	asymptomatic carrier	-	-		

					PCR Screen		
Isolate collection #	**Species**	**Isolation Site**	**Diagnosis**	**Cytotoxic effect**	***npsB* target**	**integenic target**	**synonym**
140	*K. oxytoca*	stool	diarrhea	+	+	+	
149	*K. terrigena*	stool	asymptomatic carrier	-	-	-	
162	*K. pneumoniae*	stool	diarrhea/AAD		-	-	
177	*K. oxytoca*	urine	UTI	-	+	+	
178	*K. oxytoca*	urine	UTI	-	+	+	
179	*K. oxytoca*	urine	UTI	-	-	-	
180	*K. oxytoca*	stool	AAHC	-	-	-	
180-g	*K. oxytoca*	stool	AAHC	-	+	+	
180-k	*K. oxytoca*	stool	AAHC	-	+	+	
180-1	*K. oxytoca*	stool	AAHC	+	+	+	
180-2	*K. oxytoca*	stool	AAHC	+	+	+	
184	*K. oxytoca*	blood	bacteremia-peritonitis	-	-	-	
185	*K. oxytoca*	blood	bacteremia-cholangitis	+	+	+	
186	*K. oxytoca*	blood	bacteremia-pneumonia	-	-	-	

					PCR Screen		
Isolate collection #	**Species**	**Isolation Site**	**Diagnosis**	**Cytotoxic effect**	***npsB* target**	**integenic target**	**synonym**
188	*K. oxytoca*	stool	AAHC	+	+	+	
189	*K. oxytoca*	stool	AAHC	-	-	-	
193	*K. oxytoca*	stool	asymptomatic carrier	+	+	+	
194	*K. oxytoca*	stool	asymptomatic carrier	-	-	-	
195	*K. oxytoca*	stool	asymptomatic carrier	+	+	+	
195-H	*K. oxytoca*	urine	UTI	-	-	-	
196	K. *ornitholytica*	stool	diarrhea	-	-	-	
197	*K. oxytoca*	stool	asymptomatic carrier	-	-	-	
198	*K. oxytoca*	stool	asymptomatic carrier	-	-	-	
199	*K. oxytoca*	stool	AAHC	+	+	+	
202	*K. oxytoca*	blood	bacteremia-CRBSI	-	-	-	
203	*K. oxytoca*	laboratory strain		+	+	+	
204	*K. oxytoca*	stool	AAHC	+	+	+	
205	*K. oxytoca*	stool	AAHC	+	+	+	

					PCR Screen		
Isolate collection #	**Species**	**Isolation Site**	**Diagnosis**	**Cytotoxic effect**	***npsB* target**	**integenic target**	**synonym**
206	*K. oxytoca*	stool	AAHC	-	-	-	
213	*K. oxytoca*	stool	IBD	+	+	+	
215	*K. oxytoca*	stool	IBD	+	+	+	
221	*K. oxytoca*	stool	IBD	+	+	+	
222	*K. oxytoca*	stool	AAHC	+	+	+	
223	*K. oxytoca*	stool	diarrhea/colitis	-	-	-	
226	*K. pneumoniae*	laboratory strain		-	-	-	
227	*K. oxytoca*	stool	AAHC	+	+	+	
228	*K. oxytoca*	urine		+	+	+	
230	*K. oxytoca*	blood	bacteremia-vasculitis	-	-	-	
231	*K. oxytoca*	respiratory culture	pneumonia	-	-	-	
232	*K. oxytoca*	blood	AAHC	+	+	+	
233	*K. oxytoca*	stool	AAC	-	-	-	
234	*K. oxytoca*	stool	diarrhea/colitis	+	+	+	

					PCR Screen		
Isolate collection #	**Species**	**Isolation Site**	**Diagnosis**	**Cytotoxic effect**	***npsB* target**	**integenic target**	**synonym**
235	*K. oxytoca*	stool	IBD	+	+	+	

Figure 34: Sequence alignment of *K. oxytoca yncE, K. pneumoniae yncE* and *E. coli yncE* shown in descending order.
Alignment was done using the ClustalW2 tool of the European Bioinformatics Institute Home Page

```
fig|571.8.peg.4006              ATGTCATTACGTCATCTGTCCGCGCCGCGTCTGCGCCGTTCACTGTTGTT 50
gi|238892256_c2835627-2834566   ATGTCATTACGTCATTTTGCCGCGCCGCGACTGCGCCATTCACTGCTCGT 50
gi|49175990_1521331-1522392     ATGCATTTACGTCATCTGTTTTCATCGCGCCTGCGTGGTTCATTACTGTT 50
                                ***   ********* *     *  **** *****   **** *  *  *

fig|571.8.peg.4006              AACTTCATTACT-GCTGGCGGGGAGC-TTTAGCGCCCATGCGGCGGAAGA 98
gi|238892256_c2835627-2834566   CACTTCTCTGCT-GCTGGCAGGCAGC-TTTAGCGCCCACGCCGCGGAAGA 98
gi|49175990_1521331-1522392     AGGTTCATTGCTTGTTGTT--TCATCATTCAGTACGCAGGCCGCAGAAGA 98
                                   ***  * ** * **      * * ** **  * ** ** ** *****

fig|571.8.peg.4006              AATGCTGCGCAAAGCCGTCGGCAAGGGCGCATACGAAATGGCCTATAGCC 148
gi|238892256_c2835627-2834566   GATGCTGCGCAAGGCCGTCGGAAAAGGGGCCTACGAAATGGCCTACAGCC 148
gi|49175990_1521331-1522392     AATGCTGCGTAAAGCGGTAGGTAAAGGTGCCTACGAAATGGCTTATAGCC 148
                                 ******** ** ** ** ** ** ** ** ********** ** ****

fig|571.8.peg.4006              AGCAGGAGAACGCGCTGTGGGTGGCCACATCGCAAAGCCGTTCGCTGGAT 198
gi|238892256_c2835627-2834566   AGCAGGAGAATGCGCTGTGGGTCGCCACATCACAGAGTCGTTCGCTGGAC 198
gi|49175990_1521331-1522392     AGCAAGAAAACGCGCTGTGGCTCGCCACTTCGCAAAGCCGCAAACTGGAT 198
                                **** ** ** ********* * ***** ** ** ** **    *****

fig|571.8.peg.4006              AAAGGCGGCATCGTTTATCGTCTCGATCCGACGACCCTCGAAGTAACCCA 248
gi|238892256_c2835627-2834566   AAAGGCGGGGTGGTTTACCGTCTTGACCCCACCACCCTCGACGTGACGCA 248
gi|49175990_1521331-1522392     AAAGGTGGCGTGGTTTATCGTCTTGATCCGGTCACTCTGGAAGTGACGCA 248
                                ***** **  * ***** ***** ** **    ** ** ** ** ** **

fig|571.8.peg.4006              GATCATTCATAACGACCTGAAACCCTTCGGCGCGACGATCAATAACGCCA 298
gi|238892256_c2835627-2834566   GATTATTCACAACGATCTGAAGCCGTTCGGCGCCACTATCAACCATGCCA 298
gi|49175990_1521331-1522392     GGCGATCCATAACGATCTCAAGCCGTTTGGTGCCACCATCAATAACACGA 298
                                *   ** ** ***** ** ** ** ** ** ** ** *****  *  * *

fig|571.8.peg.4006              CCCAGACCCTGTGGTTTGGCAACACTACCGACAGCACCGTCACTGCCATT 348
gi|238892256_c2835627-2834566   CCGGCACGCTGTGGTTTGGCAATACCGTCGACAGCACTGTCACCGCTATT 348
gi|49175990_1521331-1522392     CTCAGACGTTGTGGTTTGGTAACACCGTAAACAGCGCGGTCACGGCGATA 348
                                *    **  ********** ** **     ***** * ***** ** **

fig|571.8.peg.4006              GATGCTAAAACCGGTAAGGTAAAAGGGCGTCTGGTGCTCGACGCTCGTCA 398
gi|238892256_c2835627-2834566   GACGCCAAAACCGGCGCCGTGAAGGGGCGCCTGGTGCTGGACGAGCGTCA 398
gi|49175990_1521331-1522392     GATGCCAAAACGGGCGAAGTGAAAGGCCGTCTGGTGCTGGATGATCGTAA 398
                                ** ** ***** **    ** ** ** ** ******** ** *  *** *

fig|571.8.peg.4006              GCGCAGCGAAACCGTGCGCCCGCTGGCGCCGCGCGAGCTGGCGGTCAATG 448
gi|238892256_c2835627-2834566   GCGCAGCGAAACCGTGCGCCCGCTGCAGCCGCGCGAGCTGGCGGTCAATG 448
gi|49175990_1521331-1522392     GCGCACGGAAGAGGTGCGCCCGCTGCAACCGCGTGAGCTGGTAGCTGACG 448
                                *****  ***   ************   ***** *******  *   * *

fig|571.8.peg.4006              AGAAAACCAATACCGTCTACATCACCGGCCTGGGTAAAGAGAGCGTGATT 498
gi|238892256_c2835627-2834566   AGCAGACCAACACGGTCTACATTACCGGTCTGGGCAAAGAGAGCGTGATT 498
gi|49175990_1521331-1522392     ATGCCACGAACACCGTTTACATCAGTGGTATTGGTAAAGAGAGCGTGATT 498
                                *    ** ** ** ** ***** *  **  * ** ***************

fig|571.8.peg.4006              TGGGTTGTGGATGGCGACAAGCTGACGCTGAAAGACACTATCGCTAATAC 548
gi|238892256_c2835627-2834566   TGGGTGGTAGATGGCGCGACCCTGAAGCTGAAAACGACCATTACCGGCAC 548
gi|49175990_1521331-1522392     TGGGTCGTTGATGGCGGGAATATCAAACTGAAAACCGCCATCCAGAACAC 548
                                ***** ** *******  *   * *  ******    * **       **

fig|571.8.peg.4006              CGGCGCAATGGCGACCGGCCTGGCGGTGGAC-GCAGAAGCGAACCGCATC 597
gi|238892256_c2835627-2834566   CGGGGCAATGGCGACGGGTCTGGCGATCGAT-CCGCAGGCTAAGCGTCTG 597
gi|49175990_1521331-1522392     CGGTAAAATGAGTACCGGTCTGGCGCTGGATAGCGAAGGC-AAACGTCTT 597
                                ***   ****   ** ** ****** * **   *  * ** ** **  *
```

```
fig|571.8.peg.4006                TATACCACCAACGCCGACGGCGAGCTGGTGACTATCGACAGTACCAGCAA 647
gi|238892256_c2835627-2834566     TATACCACCAACGCCGATGGCGAACTGCTGACCATCGACAGCGAGAGCAA 647
gi|49175990_1521331-1522392       TACACCACTAACGCTGACGGCGAATTGATTACCATCGACACCGCCGACAA 647
                                  ** ***** ***** ** *****  ** * ** *******       ***

fig|571.8.peg.4006                TAAGATCCTCTCGCGCAAGAAGTTGCAGGATGATGGCAAAGAGCACTTCT 697
gi|238892256_c2835627-2834566     CACGATTGCGTCGCGCAAAAAATTGCAGGATGACGGCAAAGCGCATTTCT 697
gi|49175990_1521331-1522392       TAAAATCCTCAGCCGTAAAAAGCTGCTGGATGACGGCAAAGAGCACTTCT 697
                                   *  **       ** ** **  *** ****** ******* *** ****

fig|571.8.peg.4006                ATCTGAATCTCAGCCTTGATAGCGCCGGTCATCGCGCCTTTATCACCGAC 747
gi|238892256_c2835627-2834566     ATCTTAACCTGAGTCTCGATACCGCCGGCCATCGTGCCTTTATTACCGAC 747
gi|49175990_1521331-1522392       TTATCAACATTAGCCTTGATACCGCCAGGCAGCGTGCATTTATCACCGAT 747
                                   * * **  * ** ** **** **** * ** ** ** ***** *****

fig|571.8.peg.4006                AGTAAACAGCCG--GAAGTGCTGGTGGTCGATATTCGCGATGGCAAAGTG 795
gi|238892256_c2835627-2834566     AGCAAGCAGCCG--GAAGTGCTGGTGGTCGATACCCGCGACGGCAAGGTG 795
gi|49175990_1521331-1522392       TCTAA--AGCCGCAGAAGTGTTAGTGGTCGATACCCGTAATGGCAATATT 795
                                     **  *****  ****** * **********  **  * *****  *

fig|571.8.peg.4006                CTGGAGAAAATCGCCGCGCCGGAGTCCCTGGCCGTTCTGTTTAACCCGAC 845
gi|238892256_c2835627-2834566     CTGGAGAAAATCGCCACGCCGGAGTCGCTGGCGGTGCTGTTTAACCCGGC 845
gi|49175990_1521331-1522392       CTGGCGAAGGTTGCGGCACCGGAATCACTGGCTGTGCTGTTTAACCCCGC 845
                                  **** ***  * **  * ***** ** ***** ** **********  *

fig|571.8.peg.4006                GCGCAATGAAGCCTACGTGACGCACCGCAAAGCCGGGGAAGTGAGCGTGA 895
gi|238892256_c2835627-2834566     GCGCAACGAAGCCTATGTGACGCATCGTAAGGCCGGGGAAGTCAGCGTTA 895
gi|49175990_1521331-1522392       GCGTAATGAAGCCTACGTAACGCATCGTCAGGCAGGTAAAGTCAGTGTGA 895
                                  *** ** ******** ** ***** **  * ** **  **** ** ** *

fig|571.8.peg.4006                TCGATGGTAAGAGCTACAAGGTGGTCAAAACTTTCAAAACCCCTACTCAC 945
gi|238892256_c2835627-2834566     TCGACGGCAAGAGCTACAAGGTGGTGAAGACCTTTAAAACGCCGACTCAC 945
gi|49175990_1521331-1522392       TTGACGCGAAAAGCTATAAAGTGGTGAAAACGTTCGATACGCCGACTCAT 945
                                  * ** *  ** ***** ** ***** ** ** **  * ** ** *****

fig|571.8.peg.4006                CCGAACAGCCTGATGCTTTCCGCCGATGGCAAAACGCTGTACGTTAGCGT 995
gi|238892256_c2835627-2834566     CCCAACAGCCTGGCGCTCTCCGAGGACGGCAAAACGCTGTACGTTAGCGT 995
gi|49175990_1521331-1522392       CCAAACAGCCTGGCGCTGTCTGCCGATGGCAAAACGCTGTATGTCAGTGT 995
                                  ** *********  *** ** *  ** ************** ** ** **

fig|571.8.peg.4006                GAAGCAGGAATCGACGCGTCAGAAAGAGGCGACCCAGCCGGATGACGTTA
1045
gi|238892256_c2835627-2834566     GAAACAGGCTTCCAGCCGTGAGAAAGAAGCCACCGCGCCGGACGATGTGA
1045
gi|49175990_1521331-1522392       GAAACAAAAATCCACTAAACAGCAGGAAGCTACCCAGCCAGACGATGTGA
1045
                                  *** **    ** *      ** * ** ** ***  *** ** ** ** *

fig|571.8.peg.4006                TCCGCATCGCGCTGTGA 1062
gi|238892256_c2835627-2834566     TCCGCATCGCCCTGTAA 1062
gi|49175990_1521331-1522392       TTCGTATTGCGCTGTAA 1062
                                  * ** ** ** **** *
```